Springs of the southeastern Great Artesian Basin: Hydrogeology, environmental tracers and flow direction

By

Jessica Ellen Thompson

Thesis
Submitted to Flinders University
for the degree of

Masters of Science (Groundwater Hydrology)

College of Science and Engineering
23 October 2023

TABLE OF CONTENTS

LIST OF FIGURES

LIST OF TABLES

EXECUTIVE SUMMARY

The Great Artesian Basin (GAB) is the largest artesian, fresh groundwater resource in the world, and the GAB springs are one of the rarest landforms types in Australia. The springs are the lifeblood of unique endemic flora and fauna, hold significant cultural values to Indigenous people, and are connected with aquifers that are drawn upon by local pastoral stations. Characterisation of the artesian springs and identifying their source aquifers in the southeast area of the GAB was hindered by a shortage of data, which limits understanding of the hydrogeological setting.

The first objective was to investigate hydrochemical and environmental tracer characteristics of the GAB springs and Cadna-Owie and Hooray sandstone and equivalents aquifer (abbreviated to C-H sandstone in this thesis). The second objective was to develop a potentiometric surface for the C-H sandstone aquifer and interpret flow direction. And the third objective was to develop an improved conceptual model of the regional spring setting and groundwater flow, as it was recognised that the current model does not adequately describe the system.

The development of a hydrogeological conceptual model aimed to provide the science that will ultimately underpin effective groundwater management.

This study was based on field investigations using environmental tracers of artesian springs and proximate bores and the collation of other existing hydrochemistry data sets and hydrogeological information. The study findings showed that water emanating from the GAB springs was up to 30,000 years old, are generally fresh (EC up to 1,500 µS/cm) and overall has a similar hydrogeochemical fingerprint to the C-H sandstone aquifer. Added complexities have been deciphered, with the mixing of aquifers, localised GAB recharge systems and the discharge springs are proximate to either faults or the GAB boundary.

The study findings also showed that complex hydrogeology and structural features such as faults influence groundwater flow directions and the spring expressions at the surface. The conceptual hydrogeological model of the springs across the southeastern GAB developed coupled with the key baseline data provided from the study provides valuable information that needs to be incorporated into future management and hydrogeochemical assessments of the GAB groundwater and springs. Outcomes from this study demonstrate the fundamental need for integrating new knowledge from field investigations with existing datasets to help constrain complex hydrogeological conceptual models. Additionally, this study makes the case that a multi-tracer approach from springs and proximate bores together with geological information provides a hydrogeological toolbox to investigate complex groundwater systems with multi-layered aquifer systems.

DECLARATION

I certify that this thesis does not incorporate without acknowledgment any material previously submitted for a degree or diploma in any university; and that to the best of my knowledge and belief, it does not contain any material previously published or written by another person except where due reference is made in the text.

Signed.

Date 17 March 2023

ACKNOWLEDGEMENTS

I would like to acknowledge the Government of New South Wales Department of Planning, Industry and Environment for the opportunity to lead the Great Artesian Basin spring hydrogeological and ecological survey in 2018 and 2019, and for providing study support for this thesis. The work undertaken in this thesis would not have been possible without this opportunity. I would also like to acknowledge the Australian Government's Murray-Darling Basin Authority for continued study support and flexible work arrangements while I have maintained full-time employment while undertaking this thesis as a part-time student.

I wholeheartedly thank my supervisors, Eddie Banks, Margaret Shanafield and Dylan Irvine, for all their support and guidance. I sincerely appreciate their passion, knowledge and enthusiasm for hydrochemistry and hydrogeology and value their friendship. It was a pleasure working with them and I will be eternally grateful for their patience and generosity.

I would also like to thank my other collaborators, specifically Huade Guan and Okka Batelaan, for their time teaching me new scientific methods and their contributions to scientific ideas.

In addition, I would like to thank those involved in the field surveys, particularly Graeme Armstrong and Shayne O'Sullivan of NSW National Parks and Wildlife Service, Uncle George of Walgett's Dharriwaa Elders, as well as the many landholders across western New South Wales who each generously shared their knowledge and allowed me to access their lands to survey springs and bores investigated in this study.

To my many friends and family, you should know that your support and encouragement were worth more than I can express on paper. Thank you.

1. INTRODUCTION

Groundwater is the world's largest freshwater resource and is an increasingly important water supply source globally (de Graaf et al., 2019; Richey et al., 2015). Fresh groundwater is critically important for irrigated agriculture and hence global food security (de Graaf et al., 2019). Artesian groundwater naturally emerges through fractured rock or sediment at the ground surface as a spring, which can be a major source of water, especially in arid ecosystems (National Ground Water Association, 2023b). Springs sustain groundwater-dependent ecosystems and have been the focus of human civilisation for thousands of years (Negus, 2020; Yang, Liu, Tang, Peeters, & Ye, 2022; Keegan-Treloar et al., 2022). Springs have longstanding spiritual and ecological significance to many communities and environments across the world and are the starting point of life in some of the world's indigenous communities (Cantonati et al., 2021). Springs also provide the primary source of drinking water for millions of people worldwide and supply water to industries such as agriculture, bottled water, and tourism sites (i.e. geothermal baths) (Currell & Katz, 2022). Sadly, numerous studies have documented the detrimental impacts on springs and their aquifers (Katz & Currell, 2022). These impacts include unsustainable groundwater pumping that exceeds aquifer recharge, leading to a decline in groundwater levels, and aquifer storage and impacts to connected waterbodies such as springs (de Graaf et al., 2019; Fu et al., 2019; Richey et al., 2015).

Such anthropogenic stressors have caused groundwater discharge to springs to decline, leaving many of the world's springs on a trajectory of impairment, rendered inactive or irreparably lost (Mudd, 2000; Powell et al., 2015; Wang et al., 2022). Projections for groundwater pumping will lead to 40-80% of the world's catchments below the minimum environmental flow limits required to maintain ecosystem functions by 2050 (de Graaf et al., 2019). The impacts of global climate change, such as increasing evapotranspiration rates, also add to the vulnerability of available water at spring expressions. Therefore, it is important to develop a better understanding and knowledge of the hydrogeophysical processes that drive spring flow so their source water can be managed more sustainably.

One of the world's largest and most iconic groundwater basins is the Great Artesian Basin (GAB), which covers ~22% of the Australian continent (1.7 million km^2) (National Water Commission, 2013). The GAB holds a vast volume of groundwater, estimated at around 65,900 million megalitres, which is equivalent to 130,000 Sydney Harbour storages, or about nine years of Amazon River (the world's highest-flowing river) total discharge (Geoscience Australia, 2023a; Ordens et al., 2020). Springs emanating from the GAB create permanent wetlands in arid Australia, away from major river systems, which hold significant Indigenous cultural values (Arthington et al., 2020; Moggridge, 2020). They were also heavily utilised by pastoralists until the advent of water bore drilling to expand pastoralism from the 1880s to the present day (Fensham at al., 2021). GAB groundwater is of meteoric origin with residence times that range from modern in the recharge areas to over 1 million years in the central basin (Mahara et al., 2009; Sandiford et al., 2019). GAB groundwater is thought to be well protected from the impacts of climate change, except in the small proportion that corresponds to recharge areas (Ordens et al., 2020). As such, it is a strategic water resource that offers a buffer against the expected future increase in severe droughts. On the other hand, GAB groundwater is mostly non-renewable on planning time scales, and the future climate in the GAB region is projected to be warmer and drier, which poses serious challenges for groundwater resources management including on spring discharges (Currell & Katz, 2022; Fu et al., 2019).

In a 2010 state-of-the-science report on spring protection in the United States by the (National Research Council, 2010), understanding surface water expressions and groundwater connectivity is a major knowledge gap and there is a high level of data uncertainty. Hydrochemical diversity in spring discharge and groundwater is caused by a myriad of different controlling processes which have been recognised in many spring investigations across the world (Priestley et al., 2019; Wang et al., 2022). Springs are underlain by geological structures that are often highly variable and complex, which can make it difficult to solve questions about the hydrogeological setting (Suckow et al., 2019; Wang et al., 2022). As a result, springs often exist in a multilayer aquifer system and can have inter-aquifer connectivity (Moya et al., 2016; Pandey et al., 2019; Wolaver, Priestley, Crossey, Karlstrom, & Love, 2019). The source for springs may be an outcrop formation, shallow aquifer, or it may be a deeper formation from which artesian groundwater discharges to the surface via structural elements such as faults and fractures, or a combination (Ransley et al., 2015). GAB springs may receive flow from multiple sources, including a combination of local and regional groundwater systems, as well as surface-water flows (Flook et al., 2020). Mixing of source waters complicates the hydrogeochemical assessment of spring water sources where the water shows a distribution of different apparent groundwater ages (Suckow et al., 2019).

Environmental tracers have had wide use in assessing the hydrogeochemistry of springs and groundwater systems, and it has been realised that tracers may give contradicting results if assessing individual environment tracers at face value, particularly for settings with a mixture of water sources at spring expressions (Suckow et al., 2019). To decifer the hydrogeochemistry of the water at such spring expressions and improvement of spring and associated aquifer system understanding, many spring investigations assess information obtained from different tracers together with other hydrogeological evidence such as conceptual models (Commonwealth of Australia, 2014b; Fensham et al., 2021), the potentiometric surface (S. C. Priestley et al., 2019), hydrostratigraphy (Miles, White, & Scholz, 2012), and comparison with bores, seawater or meteoric end-members (Taylor et al., 2015; Golders, 2021; Thompson, 2019).

Since the early 1900s, the GAB has been the subject of scientific investigations and management programs (Kent, Pandey, Turner, Dickinson, & Jamieson, 2019; Ordens et al., 2020). However, despite the importance of springs as a water resource, surveys of GAB springs are a relatively recent activity with increased interest (mainly about the groundwater dependant ecosystems) in Australia only since the late 1980s (Habermehl, 1980; Negus, 2020). The last 10 years have seen a large increase in available data, which corresponds to a shift in focus to the regional GAB with increasing mining extraction (i.e. coal seam gas (CSG)) (CSIRO, 2018; Sreekanth et al., 2019; Viljoen, Pinder, Mukherjee, & Herbert et al., 2020). Groundwater management initiatives such as the $300 million federal government-funded GAB Sustainability Initiative (GABSI) program and Cap and Pipe the Bores Program (Brake et al., 2020; NSW Department of Planning Industry and Environment, 2019) were designed to protect endangered spring-dependent ecosystems that rely on sufficient artesian pressure to survive and to ensure a reliable and efficient supply of good quality water for properties across north west NSW. The Australian Government has also commissioned keystone projects for basin-wide investigations, including the *National Research Flagships: Great Artesian Basin Water Resource Assessment* (Miles et al., 2012) to assess groundwater development impacts on GAB springs, and the *Hydrogeological Atlas of the Great Artesian Basin* (Ransley et al., 2015) which is a compilation of key hydrogeological and hydrochemical aspects of the GAB. The Independent Expert Scientific Committeewas commissioned for the *Bioregional Assessment* in 2018 and the *Ecological and hydrogeological survey of the Great Artesian Basin Springs* in (Commonwealth of Australia, 2014b). The National Water Commission also funded a project allocating water and maintaining springs in the western margin of the GAB. The Allocating Water and Maintaining Springs in the Great Artesian Basin (AWMSGAB) project completed in 2013 for the National Water Commission investigated complex surface and groundwater interactions and GAB springs characteristics on the western margins of the GAB. This $6.25 million project substantially updated understanding of GAB's geology, ecology and hydrology. The most recent body of work is the *Assessing the Status of Groundwater in the Great Artesian Basin* in 2019-2022 through Geoscience Australia (Wallace & Ransley, 2022), however, this was not available for review in this report. These reports help to form the baseline understanding of the GAB hydrogeology, however, the body of work for the *Ecological and hydrogeological survey of the Great Artesian Basin Springs* (Commonwealth of Australia, 2014b) was the only project that presented hydrochemistry parameters (physio-chemical parameters, major ion chemistry, minor elements chemistry and occasional isotope chemistry) for selected springs.

These large industry and government investments have led to an improved scientific understanding of the GAB's hydrogeology and were the basis for a special issue *Hydrogeology Journal - Advances in hydrogeologic understanding of Australia's Great Artesian Basin* publication (International Association of Hydrogeologists Australia, 2020). The journal comprised 26 manuscript articles that disseminated the most recent GAB science on the topics which include compartmentalisation and connectivity, aquifer flows (pathways, spring discharge rates and heterogeneity), numerical modelling, and springs and GDEs. Only four articles focus on the springs, which presented data for the northern and western GAB, however, there was none in the southeastern GAB (Flook et al., 2020; Keppel er al., 2019; S. C. Priestley et al., 2019; Wolaver et al., 2019).

Published work from local scale projects shows substantial GAB spring hydrogeochemical work has been done in the western GAB region (Andrew L Herczeg & Love, 2007; Matic, Costelloe, & Western, 2020; S. C. Priestley et al., 2019; Wolaver et al., 2019) and northern GAB region (Baublys, Hamilton, Hofmann, & Golding, 2019; Hayes et al., 2019; Jones et al., 2019; Moya et al., 2016; Perez, Ponder, Colgan, Clark, & Lydeard, 2005). However, only a single desktop study has considered the hydrogeochemistry of springs in the southeastern GAB. A recent desktop assessment by Golders (2021) (commissioned by the NSW Department of Industry and Environment) used major ions and isotopes to attempt to classify springs, however, the source of water for many springs is reported as 'ambiguous' and the conclusion states that "springs have predominantly been found to be of uncertain or mixed origin sources". This study did not incorporate other available hydrochemical data, such as from the *Ecological and hydrogeological survey of the Great Artesian Basin Springs* (Commonwealth of Australia, 2014b). The report also recommended that a "more specialist interpretation of the isotopic data might resolve, at least semi-quantitatively, the relative proportions of GAB water and modern water". Therefore, investigations are necessary to assess the hydrochemical data and understand the water sources associated with the GAB spring complexes.

1.1 Aims and objectives

Until field investigations and ground-truthing surveys were undertaken in this study in 2018-19, springs in the southeastern area of the GAB lacked hydrochemistry and multi-tracer science to characterise and constrain the water source setting. Multi-tracer hydrochemistry analysis done on GAB bores also lacked broadly across the region and was required for constraining any hydrochemistry data from GAB springs. There was also a lack of published comprehensive datasets and hydrological assessments for the south-eastern GAB.

To address this knowledge gap, field investigations were conducted to collect environmental tracers of artesian springs and proximate bores and integrate them with existing hydrochemistry datasets and hydrogeological information. The objectives of this study are to:

1. Investigate the hydrochemical and environmental tracer characteristics of the GAB springs and the main GAB aquifer.
2. Create a potentiometric surface for the main aquifer unit, which is the Cadna-Owie and Hooray sandstone, and interpret the flow direction.
3. Develop an improved hydrogeological conceptual model of the regional spring setting and groundwater flow in the southeastern GAB.

The development of a hydrogeological conceptual model aims to provide science-based evidence that will ultimately underpin effective groundwater management for the region.

2. STUDY AREA

The GAB includes semi-arid and arid parts of eastern Australia and underlies about 22% (1.7×10^6 km^2) of the Australian continent. The study area is located largely in the southern Surat Basin and the western section of the study area includes the south-central Eromanga geological basin of the GAB, including the Bourke and Bogan Supergroups (Figure 1). A "Supergroup" is defined as a major regional cluster of spring complexes with some consistent hydrogeological characteristics and geographic proximity (Fensham, Ponder, 2010a; Habermehl, 1982). One spring site, Bingewilpa, is located outside the Supergroups' boundaries. The artesian springs provided the only constant water source between the Darling River (NSW) and the remaining pools in ephemeral streams in southern Queensland (Powell et al., 2015).

Figure removed due to copyright restriction.

Figure 1. Location map showing the study area of the springs of the southeastern Great Artesian Basin, including major GAB geological structural fault lines (Geoscience Australia, 2013)**. Inset map: Study area within the GAB.**

2.1 Field activities – study site

The spring sites (Figure 1) surveyed during the field investigations were sampled in Round 1 between 6-23 March 2018, Round 2 between 8-26 October 2018 and Round 3 between 9-25 July 2019. During the surveys, there were several rainfall events just before and during the field survey program (Figure 2). In Round 1, there was 11.2 mm of rain recorded the day before sampling, 11.0 mm the week before Round 2 as well as a 26 mm rain event, and a 15.8 mm rain event at the start of Round 3. Rainfall and subsequent throughflow or runoff are different water types compared to the Hooray sandstone groundwater. The mixing of these two water types at spring expressions can add complexity to the spring water chemistry. One rainfall sample was obtained in the middle of the study area (Figure 1) in October 2018.

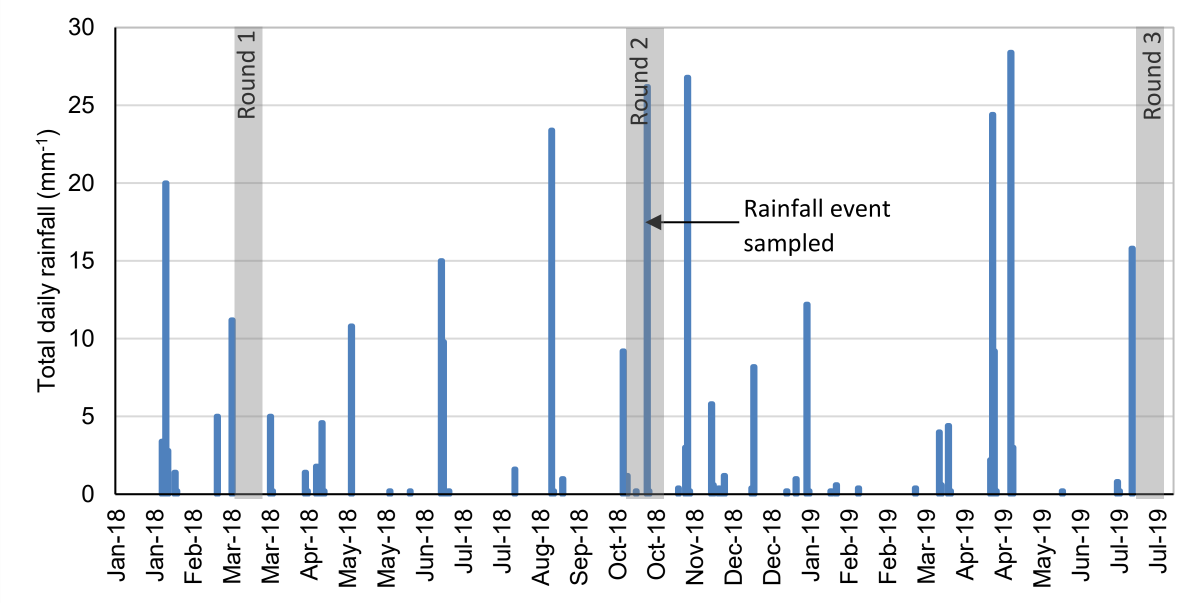

Figure 2. Histogram of total daily rainfall (blue) and sampling events (grey).

Chart notes: Bureau of Meteorology climate data station at Bourke NSW, station number 48245. Sampling event dates were 6-23 March 2018 for Round 1, 8-26 October 2018 for Round 2 and 9-25 July 2019 for Round 3.

2.2 Geology and Hydrogeology

The GAB is a complex, multi-layered aquifer system composed of interconnected geological basins. These beds were laid down by continental erosion of higher ground during the Triassic, Jurassic, and early Cretaceous periods. During this time much of inland Australia was covered by the Eromanga Sea and a layer of intervening marine sedimentary rock formed a confining layer, trapping water in the sandstone aquifer.

The aquifers within the study area are predominantly sandstones, confined by aquitards of both fluvial and marine siltstones, mudstones, and shale (New South Wales Government, 2020). Figure 3 shows the stratigraphic sequence of the geological basins in the study area (Ransley and Smerdon, 2012) and Figure 4 shows the GAB hydrostratigraphic units that form the GAB (Ransley et al., 2015). The full sequence of hydrological and geological basins for the GAB is presented in Appendix A –These hydrogeological cross-sections are based on the information on the bores' elevation of the base of hydrostratigraphic unit surfaces (Ransley et al., 2015).

The major geological basin in the study area is the Eromanga Basin, Surat Basin and Coonamble Embayment (from west to east as shown in Figure 3). The main geological units that form the major artesian source aquifer in the Eromanga Basin are the Cadna-Owie Formation and Hooray Sandstone. For the Surat Basin, the equivalent main geological units in the study area are the Mooga Sandstone, Pilliga Sandstone, and Hooray Sandstone. These are referred to collectively as the Cadna-Owie and Hooray Sandstone and equivalents aquifer (abbreviated to C-H sandstone in this thesis) and is a significant, productive GAB aquifer (Geoscience Australia, 2023b). The Hooray Sandstone aquifer is unconfined to the eastern margin, therefore groundwater recharges this unit, an area of relatively high rainfall averaging 600 mm yr^{-1}. As groundwater flows towards the west, this aquifer becomes confined as it underlays the Rolling Downs Group aquitard.

The Mooga Sandstone aquifers, whilst still geographically extensive are not as high yielding as the Pilliga and Hooray Sandstones (New South Wales Government, 2020). The Rolling Downs Group is a confining layer over the deeper C-H sandstone aquifer unit and consists of very thick aquitards of mudstones, siltstones, and shale. The upper part of the Rolling Downs Group also contains minor semi-confined aquifers (Miles et al., 2012).

Another significant GAB aquifer in the study area is the Hutton Sandstone. This GAB aquifer is separated from the C-H sandstone aquifer by a confining clay aquitard (Powell et al., 2015; Smerdon, Ransley, Radke, & Kellett, 2012). The extent of the Hutton Sandstone is restricted to the eastern margins of the study area and there are no known faults enabling hydraulic connection to the shallower units.

The entirety of these units is up to 3,000 metres thick and forms a large synclinal structure, uplifted, and exposed along its eastern margin when the Great Dividing Range formed (Geoscience Australia, 2013). This caused the Basin to tilt to the southwest, driving the artesian conditions and regional flows toward the south and west (Geoscience Australia, 2013; Habermehl, 2019; Herczeg, Torgersen, Chivas, & Habermehl, 1991).

While the simple conceptualisation of groundwater flow from east to southwest within the major aquifers associated with the major lithostratigraphic units may apply in a large part of the GAB, it falls short of describing some of the complexity in the southern GAB associated with structural features such as faults and outcropping of some of the stratigraphic units. Structural disruptions exist within the GAB sequence through major faulted displacements and polygonal faulting with displacements ranging up to 400 metres. The central Eromanga

Basin has experienced the greatest structural overprint from both faulting and folding (Radke & Ransley, 2019). The existence of these structural features is likely to significantly impact groundwater through-flow within the GAB and may enhance vertical flow and interconnectivity across the major aquifers of the basin (Geoscience Australia, 2013).

The hydrogeological settings assume that Rolling Downs Group aquitard sediments generally provide an effective confining layer (Fensham et al., 2021) and this is supported by empirical data suggesting vertical groundwater flow is less than 10−5 metres per year (Hasegawa et al., 2016).

Figure removed due to copyright restriction.

Figure 3. The C-H sandstone aquifer in the study area with respect to the other major stratigraphic units across the GAB (Ransley & Smerdon, 2012a).

Several studies have noted that tectonics has impacted the groundwater flow directions within the GAB aquifers (Sandiford et al., 2019; Smerdon et al., 2012). The C-H sandstone aquifer regional vertical transmissivity and lateral flow are likely to be impeded by faulting

(Geoscience Australia, 2013), and are expected to enhance upward leakage to discharge spring expressions in parts of the study area.

Polygonal faulting is pervasive within the Rolling Downs Group sequence of the Eromanga Basin. Here, intra-formational polygonal faulting extends throughout the entire Rolling Downs Group aquitard and up through to the surface. Although displacements by polygonal faulting are relatively small, the pervasiveness of this phenomenon is considered to significantly increase vertical permeability which introduces inter-aquifer connectivity across the Rolling Downs Group aquitard (Ransley & Smerdon, 2012).

(Ransley & Smerdon, 2012) also mention that the Eulo Ridge and its subsurface extension to the southwest into NSW are close to being a watertable divide that separates the Surat and Eromanga Basins. However, while the Eulo Ridge acts to impede groundwater flow between the Surat and Eromanga basins in the deeper GAB aquifers, the potentiometric surface of the shallower C-H sandstone aquifer indicates convergence of south-westerly groundwater flow to the south of the Eulo Ridge. This could play a significant role in separating the hydrochemical signatures of artesian spring groups sampled in the southeastern GAB. Discharge springs also exist along the margins of the GAB, near Palaeozoic intrusions and associated faults, which breach the confining unit of the Rolling Downs Group aquitard (Powell et al., 2015).

Figure removed due to copyright restriction.

Figure 4. A three-dimensional hydrogeological conceptualisation of the Great Artesian Basin (Ransley & Smerdon, 2012)

2.3 Springs

The artesian springs are a function of the underlying geology and aquifers in these basins. The springs' surface expressions emanate through the surficial Paleogene to Neogene sandstone. Underlying this unit is the Rolling Downs Group clay aquitard. Underneath this aquitard is the major GAB aquifer unit, the C-H sandstone aquifer, which is hypothesised to be feeding the GAB springs.

Regional groundwater flow is towards the southern and south-western margins. Although lateral groundwater movement dominates, vertical upward leakage is considered important, particularly for discharge spring expressions (Ransley & Smerdon, 2012). An essential condition for the occurrence of springs is that the hydraulic head within the source aquifer (i.e., the aquifer providing water to the springs, hypothesised in this study to be the C-H sandstone) must be sufficient for water to discharge to the surface (Keegan-Treloar et al., 2022). In confined aquifers, no major flow is expected through the confining unit unless preferential pathways (e.g., faults or fractures) are present. The discharge springs occur under a range of conditions (Figure 5) including where (Habermehl, 1982; Fensham, Ponder, 2010a):

- water-bearing sediments approach the ground surface near the margins of the GAB,
- water flows through faults or unconformities in the overlying sediments, and
- a conduit is provided at the contact between the confining sediments and the outcropping of bedrock (e.g., granites).

Apart from the springs, natural permanent surface water is restricted to the south, east, and northern extremes of the study area. The Darling River is a permanent water supply, downstream from Brewarrina. The Warrego River supports numerous permanent waterholes; although the stream dissipates into anabranches south of Cunnamulla. Cuttaburra Creek diverts flood waters from the Warrego River and forms just two permanent waterholes. The Paroo River contains just three permanent waterholes between Eulo and Hungerford. During floods, the Warrego and Culgoa may flow and join the Darling River, while Cuttaburra Creek and the Paroo River terminate in extensive floodplains and ephemeral lakes (Powell et al., 2015).

While the connectivity of groundwater sources to spring vents is understood in general terms (Figure 5), the details of the hydrology at individual spring locations are poorly understood. In some cases, even the identity of the aquifer supplying groundwater to a spring is not known with certainty (Golders, 2021; R. Fensham, W. Ponder, 2010a).

Edge of the basin (E); Outcropping basement (O); Basement high (B); Surface fault (S); Deep fault (D); Thinned aquitard (T). The dashed line above the deep fault represents an inferred fault (not visible).

GAB springs

Low conductivity confining layer

Basement

Artesian aquifer

Figure removed due to copyright restriction.

Figure 5. Conceptual diagrams of the hydrogeological settings for artesian springs in this study (Fensham et al., 2021)**.**

Fensham *et al.* (2020) and Golders (2022) have used the term outcrop spring to describe gravity fed springs, which are not under artesian pressure and can fluctuate in size with recent rainfall events. Outcrop springs also occur in units that are not part of the GAB sediments such as those that occur in Paleogene to Neogene sandstone overlying the GAB. The permeable nature of the Tertiary sediments produces spring systems fed by local recharge from rainfall.

2.4 Bores

As the number of artesian water bores drilled into the GAB has increased extraction since 1890, the artesian pressure has decreased and caused discharge springs to cease to flow. Many springs in the Bourke and Bogan supergroup have been heavily impacted by aquifer drawdown, as a result of the uncontrolled discharge of artesian water from pastoral bores (Fensham et al., 2021). A well-known example of this is Yantabulla springs, which once ceased to flow causing the township of Yantabulla to become an abandoned ghost town (Powell et al., 2015). Over 520 water bores have ceased to flow, another 840 have continued free flowing, and a total of 1360 artesian bores are drilled into the artesian units within the study area (NSW, Australia). The NSW government is working towards capping free-flowing bores, which have the potential to increase artesian pressures and cause springs and bores that have ceased to flow to start to flow again.

2.5 Simplified Hydrogeological Conceptual Model

The regional approach to intra-basinal connectivity (Figure 4) that was first proposed in the GAB Water Resource Assessment (Ransley & Smerdon, 2012) and subsequently in the Hydrogeological Atlas of the Great Artesian Basin (Ransley et al., 2015) was largely conceptual because of the very limited knowledge of the hydrogeology of many underlying basins. The basic hydrogeological model for the study area produced as part of the Hydrogeological Atlas (Ransley et al., 2015) is only accessible by querying the stratagraphic layers in a geographical information system program. The major hydrogeological units are the Cenozoic sequence (stratigraphic layer 2), Rolling Downs Group aquitard (stratigraphic layer 4), Cadna-Owie and Hooray Sandstone and equivalents aquifer (stratigraphic layer 5), Hutton Sandstone aquifer (stratigraphic layer 7) and the granite/metamorphic basement (stratigraphic layer 10).

The major aquifer forming unit in NSW GAB is collectively referred to as the Cadna-Owie and Hooray Sandstone. This includes interconnected hydrogeological units including the Pilliga Sandstone equivalents, the Mooga Sandstone, Pilliga Sandstone and Hooray Sandstone (Radke & Ransley, 2019; New South Wales Government, 2020).

These early assessments were based on indirect or variable criteria to ascribe a broad hydraulic characterisation to individual formations (Radke & Ransley, 2019), especially for the south-eastern extent of the GAB and the Cadna-Owie and Hooray Sandstone aquifer.

Before this study, southeastern GAB regional connectivity mapping (i.e., the regional GAB groundwater flow map generated by (Ransley et al., 2015)) remained qualitative due to difficulties parameterising the basins under standard criteria used across the other parts of the GAB. Therefore conceptual uncertainty remained one of the major sources of uncertainty in groundwater flow modelling, which is often the case in other groundwater studies (Sreekanth et al., 2019b).

3. METHODOLOGY

Characterising the hydrogeology of springs is particularly difficult in the remote study area of the southeast GAB due to the large spatial and temporal variability of recharge and overall low water fluxes. Assessing the hydrogeological characteristics of the springs is made more complex by the paucity of data concerning bores, the limited availability of existing data (aquifer parameters and spring geochemistry), and the remote location of the study sites.

The research approach was to initially focus on enhancing the overall understanding of the hydrogeochemistry of the GAB springs. The GAB spring environmental tracer component of the investigation was complemented by a program of targeted bore sampling to build on the fundamental hydrogeological understanding of the Candna-Owie and Hooray sandstone and Equivalents (Pilliga) in the study area which was data-poor. A field sampling program was conducted between March 2018 and July 2019 to collect water samples and other hydrogeological information from springs and proximate bores within the study area. The sample preservation and laboratory analysis methods used in this study are described in detail in *Hydrogeology and ecology survey of the Great Artesian Basin springs in NSW Survey methodology* (Thompson et al., 2021).

Table 1. Existing datasets

Dataset document	Existing data relevant to this study
Hydrogeology and ecology survey of the Great Artesian Basin springs in New South Wales – survey methodology and site description (J. Thompson *et al.,* 2021)	Field observation and understanding of the landscape setting at the springs from my observations during the 2018 and 2019 field investigations informed the spring profiles in this report. Personal communications with local landholders and Indigenous groups also helped me to inform the description of springs in this report. Individual spring profiles and results limited to raw data from surveys are provided in this report. The report does not incorporate results collected by other studies and does not analyse results.
Water Sharing Plan for the NSW Great Artesian Basin Groundwater Sources 2008	DPIE is the custodian of the WSP. The springs are documented as a single coordinate in a table of the published WSP, Schedule 4. Schedule 4 was developed by NSW Government based on historical datasets. Historical information used includes outcomes reported by (Pickard,

Dataset document	**Existing data relevant to this study**
	1992) of Macquarie University, who surveyed artesian springs in the western division of NSW.
Spring Database (Government Queensland, 2018)	The Queensland dataset is information that has emerged since the WSP was implemented in 2008. The documentation has GAB spring data from 1995 to 2015. The data has been checked, tested, and compiled by the Queensland Herbarium.
Final Report Volume 2 – Hydrogeological profiles of Great Artesian Basin springs; Springsure, Eulo, Bourke, and Bogan River supergroups (The University of Queensland, 2014)	A technical resource used to inform the advice in the two reports commissioned by the Department of the Environment, 'Ecological and hydrogeological survey of the Great Artesian Basin springs - Springsure, Eulo, Bourke and Bogan River supergroups' Volume 1 and Volume 2.
NSW GAB Bore Integrity Assessment ((Klorn Crippen Berger, 2018b)	*Measured and Predicted Head Variance Conditions – 2018 Verification Data Set* (table 2 in the report) used in compiling GAB bore potentiometric levels for analysing and evaluating hydrodynamics. The 'calculated head (m)' was adopted for converting bore potentiometric levels to relative level (mAHD) and is assumed to be corrected for temperature and density.
NSW Cap and Pipe the bores bore integrity survey results ((Geospatial Australia Pty Ltd, 2021)	GAB bore data for general and laboratory chemistry and bore integrity, located within a 50-kilometre radius of GAB springs investigated in this study (Figure 1). A subset of this data includes some isotope results (I selected these sites for Geospatial Australia to sample in 2018 and 2019). The dataset was provided as an excel spreadsheet (unpublished) from NSW Government.

Dataset document	**Existing data relevant to this study**
Groundwater Dependant Ecosystems spatial database (Referred to as Commonwealth GDE dataset).	The Groundwater Dependant Ecosystems spatial dataset has lineage to data in the WSP spring schedules, Commonwealth listed EBPC Act 1999 listed GDEs and other datasets to map springs for the extent of NSW. It is a spatial layer stored in DPIE’s geospatial databases. It was extracted as a table using ESRI ArcMap into an MS Excel file for the NSW GAB groundwater sources extant. The dataset includes a single spring complex name, coordinate, and brief description of the data source and justification for site selection. Justifications include descriptors referring to work done by (Pickard, 1992).
Great Artesian Basin geological and hydrogeological surfaces update: report and data package (Geoscience Australia, 2022)	Updated surface extent layers and thicknesses for key hydrogeological units, reconciling geology across borders and providing the basis for a consistent hydrogeological framework at a basin-wide scale. These layers were interrogated in conjunction with (Scheibner & Basden, 1998)) for constructing the conceptual model for this study.
*Atlas of the Great Artesian Basin (*Ransley et al., 2015)	Map 10 shows the Potentiometric surface map of the C-H sandstone aquifer, which is largely conceptualised for the southeastern GAB.
Geology of NSW - Synthesis Volume 1 Structural Framework (Scheibner & Basden, 1998)	Hardcopy book with a schematic structural map of the Eromanga and Surat Basin (refer to figure 7.2 on page 71).
Artesian Springs in the Western Division of NSW (Pickard, 1992)	Synopsis of spring profiles described during site visits to selected sites in 1994 in the study area. This was used more so in the preparation for the field surveys in October 2018, March 2019, and July 2019.

Dataset document	Existing data relevant to this study
Springs of the Great Artesian Basin (Arthington et al., 2020)	Papers in this Special Issue, 19 in total, are an assembly of scholarly papers relating to springs of the GAB contribute to these broad objectives Commonwealth *Environment Protection and Biodiversity Conservation Act 1999* and *The 2010 Recovery Plan* (R. Fensham, W. Ponder, 2010b) from a wide range of sectors, individuals and perspectives.

3.1 Revised Dataset

This new spring and bore data collected during the 2018-19 field investigations was integrated with existing datasets provided by the Queensland Herbarium (Queensland Herbarium, 2015) for springs, and from Geospatial Australia (GA, 2018; 2019) for artesian bores. A total of 51 unique 'spring complex' names and 379 spring vent locations were identified before fieldwork activities. Of the 51 identified 'complexes', 45 were visited during the 2018 and 2019 fieldwork.

Following the 2018-19 field investigations, refinements to the dataset were applied to clean up spring descriptions where there were inconsistencies with spring nomenclature and address data gaps, such as assigning vent identification (vent ID) numbers to new spring expressions and existing spring locations without vent ID's. The consolidated data set presents 38 spring complexes representing 400 spring vents. The updated count of spring complexes closely fits the expected number of complexes for the Bourke and Bogan supergroups (35 complexes), which was similar to what was reported (Commonwealth of Australia, 2014b). The updated list of springs with consolidated complex naming applied is presented in Figure 1. Further details on the datasets and methodology for the refinements are described in the report *Site selection methodology for the Great Artesian Basin springs survey* (Thompson, 2019).

Six spring complexes were not visited in the 2018-19 field investigations: Sweetwater, Deadman, Toulby, Log, Yantabangee, Towry and Tego due to logistical issues. A further seven spring expressions did not present clear surface expression formation and were unable to be located: Sandy, Jacomb, Old Morton Plains, Tanawanta Mud, Tooloomi, Waroo and Tyngnynias.

Thoroo mud spring was an emerging spring vent (Jessica Thompson pers. Comms with landholder Adam Robertson, Mascot Station), and only a single sample was collected. The vent location was new to GAB spring records.

The surveyed spring sites were predominantly on private landholder properties, and some were situated on public nature reserves and stock routes. Extensive consultation was necessary to negotiate access to sites, as most bores and springs were located on private property. This also provided the opportunity for the collection of anecdotal information from local landholders and the traditional custodians, Aboriginal Elders while on country. Anecdotal information and field observations provided an additional line of evidence for the permanence of groundwater discharge at the spring.

Of note, this was the first scientific survey of Bingewilpa ever, a site which was once a spring: 'a beautiful spot' according to Tietkens, who saw it in 1865, but it was soon dug out and made into a well and a bore was sunk nearby on what is now Tero Station. Bingewilpa ("*birndi walpi*") also holds significant cultural value to the Two Ngatyi (rainbow serpents) who join up at this site where they make the rain (Beckett & Hercus, 2016).

3.2 Water Sampling and Laboratory Analysis

Of the 38 spring sites, 27 samples were collected from 19 springs. Two-hundred bore samples were also obtained during 2018-19 (Geospatial Australia Pty Ltd, 2022). Samples collected during field investigations that were analysed for major ions were analysed by Enviro Lab Pty Ltd, whilst stable isotopes of water, oxygen (^{18}O) and deuterium (^{2}H), radiocarbon (^{14}C and $^{13}C/^{12}C$ (or $\delta^{13}C_{DIC}$) of Dissolved Inorganic Carbon (DIC), elsewhere referred to as δ13CDICchlorine-36 (^{36}Cl), tritium and strontium ($^{87}Sr/^{86}Sr$) were analysed at Australian Nuclear Science and Technology Organisation (ANSTO) (Appendix A).

Both laboratories were National Association of Testing Authorities accredited. Anions were determined by Ion Chromatography. Total Dissolved Solids was determined gravimetrically. Alkalinity was determined titrimetrically both in the field and in the laboratory. Conductivity and salinity were measured using a conductivity cell at 25°C. Metals were determined by metals by Inductively Coupled Plasma Atomic Emission Spectroscopy (ICP-AES) and Inductively Coupled Plasma Mass Spectrometry (ICP-MS). Ionic balance was calculated and did exceed the recommended +/- 10% error range for some samples.

$\delta^{2}H$ and $\delta^{18/16}O$ was analysed by Picarro Cavity Ring-Down Spectroscopy (CRDS). $\delta^{13}C_{DIC}$ samples were run using an established equilibration method on Gas Bench II coupled to continuous-flow Delta V Advantage Isotope Ratio Mass Spectrometer (IRMS). ^{14}C and ^{36}Cl was analysed by accelerator mass spectrometry (AMS).

Tritium was analysed using liquid scintillation spectrometry, conducted using Perkin Elmer Quantulus™ instruments. Tritium data was assessed by ANSTO to ensure it fits a Poisson distribution with a confidence interval of 95%.

The sampling program involved:

- a review of accessible groundwater bores in the eastern GAB to establish reliable sampling points for the Hooray sandstone (e.g. bores with known construction and geology logs)
- the collection and analysis of spring, rainfall, runoff, and GAB bore groundwater samples for the following parameters:
    - physical characteristics (pH, redox potential (mV), electrical conductivity (µS/cm), temperature (°C), dissolved oxygen (% and mg/L), total alkalinity (mg/L),
    - major ion and trace element chemistry,
    - environmental tracers including ^{36}Cl, ^{14}C DIC, $^{13}C/^{12}C$, $\delta^{18}O$ and $\delta^{2}H$, $^{87}Sr/^{86}Sr$ and ^{3}H.

The grab-sampling methodology was generally adopted from the Australian Guideline for Water Quality Monitoring and Reporting (NWQMS 2000) for surface water (springs) and the Groundwater Sampling Analysis – A Field Guide (Sundaram et al., 2010) for bores. Field filtering equipment used was WATERRA 0.45 µm filter, 0.45 µm stericup or 0.45 µm sandwich, hand pump and silicone tubing and lure lock syringe to connect to sandwich filter.

Bottles were supplied and prepared by the laboratories. For general chemistry, unpreserved 500 ml bottles were triple rinsed with water from the sample point before filling. For each site, 2 100 ml nitric acid preserved bottles were not rinsed before filling and one 100 ml acid preserved bottle was field filtered using a 0.45 µm filter. For isotope chemistry, Tritium was collected in a 2 litre bottle, thoroughly rinsed with 0.45 µm filtered sample and discard rinsate, with 3 rinses in total. After rinsing was completed, the bottle was gently filled up to the top, leaving no bubbles and no head space. The cap and sealed with electrical tape, placed into an individual sealed plastic bag and the bottle was not refrigerated. The similar sample process was followed for ^{36}Cl and ^{14}C DIC in a 1 litre bottles each, and refrigerated to 4 °C. $\delta^{18}O$ and $\delta^{2}H$ followed the same process in two 30 ml containers, without refrigeration. $^{87}Sr/^{86}Sr$ was collected in a 60 ml plastic bottle pre-treated by ANSTO with nitric acid preservative, filled to near-top with 0.45µm filtered sample and refrigerated to 4 degrees

Celsius. Samples were dispatched to the laboratories in eskies with ice bricks. $^{13}C_{DIC}$ was collected in two 12 ml glass exetainers, with a triple rinsed syringe body with 0.45 µm filtered sample (via luer lock fitting attachment), then attach 0.20µm blue inline filter to syringe).

The 27 water samples were collected from the following sites:

- four samples collected at Tego in March of 2012 (Queensland Herbarium, 2017),
- three samples were collected repeatedly at the same Peery and Boongunyarra spring vents in October 2018, March 2019, and July 2019,
- two samples at each of the Cumborah spring vents in July 2019,
- one sample at each of Lila, Old Gerara, Wapweelah, Thully, Tharnowanni, Coonbilly, Youngerina, Native Dog, Thooro Mud, Bingewilpa, Nulty, Scrubber, Colless, Muleyo, Youltoo, and Coolabah,
- one rainfall sample collected from a 34 mm rainfall event in October 2018, and
- one rainfall-runoff sample was collected in October 2018.

Peery spring was also the site for quality assurance and quality control of duplicate laboratory samples, which provided an additional data point in the geochemical analysis during the field investigations.

Most springs represented low-flow, diffuse zones of discharge. These were a challenge to sample for water chemistry because the low and diffuse spring discharge is by surficial process and evapotranspiration, and at some sites surface water runoff from recent rainfall. For this reason, samples were collected as close as possible to known discharge points or vents, consistent with other artesian springs studies of similar environments (Flook et al., 2020).

A rainfall and runoff sample were also collected for the full suite of analytes including isotopes in the middle (145°E, 29°S) of the study area in October 2018. A reference seawater sample has been included in the major ion results. A reference strontium isotope result measured in the Surat Basin, an equivalent unit to represent the C-H sandstone aquifer has been included in the strontium isotope analysis.

Other sites that were dry including Kallyna, Eliza Lake, Yantabulla, Nupunyah are also not present in the following sections as hydrochemical data does not exist for these sites. Refer to the spring profiles in Hydrogeology and ecology survey of the Great Artesian Basin springs in New South Wales – survey methodology and site description (J. Thompson *et al.,* 2021) for results from the 2018 and 2019 surveys for more information on the observation results and status of these GAB spring sites.

A comprehensive groundwater sampling program was undertaken across the southeastern GAB (Figure 1). A focus of the groundwater sampling and analysis program aimed to investigate the spatial distribution of mean groundwater residence times of the springs and the Hooray and Equivalents aquifer. This study also characterised the ionic and isotopic composition of springs and groundwater to delineate flow paths and investigate source waters and potential mixing (e.g. groundwater, runoff, or through flow from Paleogene to Neogene units) between the GAB groundwater and the assumed discharge springs.

Bores were required for comparing the hydrochemistry of aquifers from known depths with springs. The ability to identify source aquifers for GAB springs surveyed is dependent on groundwater data from nearby GAB bores. Flowing artesian bores within a 50-kilometre radius of springs sampled were targeted for general chemistry using data collected by (Geospatial Australia Pty Ltd, 2021). A subset of artesian bores within a 5-kilometre radius was sampled for an advanced suite of chemistry collected during field investigations for this study and supplemented by (Geospatial Australia Pty Ltd, 2021).

The method for site selection of bores selection was using a GIS spatial analysis of priority GAB bores located within a 5-kilometre radius of the centroid of spring complexes. This was done using ArcMap (ESRI, 2011) software package and bore data from the WaterNSW Hydstra bore database.

Bores shortlisted for sampling were further refined by geographical distribution across the south-eastern GAB groundwater sources, to ensure even coverage across the study area and within the vicinity of the targeted GAB springs.

Further refining of the shortlisted GAB bores was applied for bore construction details (depth, groundwater source, casing, and slotted section). Checks on these criteria were done using WaterNSW Hydstra, the NSW Department of Primary Industries Groundwater Database System (GDS), and the Groundwater Explorer (BoM 2018).

The GAB bores were also required to be flowing artesian. A further selection criterium for GAB bores was the ability to physically access bores for sampling during fieldwork.

3.3 Groundwater Level and Pressure Data sets

GAB bore level and pressure datasets were compiled from publicly available literature (Klorn Crippen Berger, 2018a). Most existing bores in the region have been drilled for stock and domestic use and do not have good control over geology or construction detail. Bore selection was based on bores with depth ranges from 100 to 1000 metres within the Cadna-

Owie and Hooray Sandstone aquifer across the investigation area. The bores selected were also required to have available construction details including surveyed elevation at the top of the casing, screen depth, and pressure or level data to create the potentiometric surface.

Bore levels were converted to a reduced standing water level according to the surveyed top of casing height in metres above the height datum. The potentiometric head level points were plotted on a map with the GAB hydraulic boundaries and GAB major structural elements (Geoscience Australia, 2013) in QGIS. The map was then printed out, and potentiometric surface contours were hand-drawn on the paper map and scanned to generate a digital image. The flow lines in the digital image were then digitised within ArcGIS.

3.4 Potentiometric Surface and Groundwater Flow

The potentiometric head level points were plotted on a map with the GAB hydraulic boundaries and GAB major structural (Geoscience Australia, 2013) in QGIS. The map was then printed out, and potentiometric surface contours were hand-drawn on the paper map and scanned to generate a digital image. The hand-drawn image was then rectified within ArcGIS and faults lines were digitised on screen.

Regional groundwater flow directions within the Cadna-owie – Hooray Aquifer and Equivalents were inferred from a potentiometric surface and five-meter contours using measurements of groundwater head. The potentiometric surface is inferred from 414 water bore head measurements obtained in 2018, and 2019 (Geospatial Australia Pty Ltd, 2022; Klorn Crippen Berger, 2018b)(Klorn Crippen Berger, 2018b)(Klorn Crippen Berger, 2018b)(Klorn Crippen Berger, 2018b)(Klorn Crippen Berger, 2018b) and 1985-1994 (NSW Government, 2018) (Table 10).

Published geological information, including interpreted elevation top of aquifers and aquitards and fault locations (Geoscience Australia, 2013; Ransley & Smerdon, 2012) was used to identify zones that may potentially be associated with enhanced vertical permeability. Where the thickness of the aquitard is lower, resistance to vertical flow is also reduced.

A property of the artesian groundwater systems is there is a large difference in the rate of spread of the cone of depression around a discharging well (National Ground Water Association, 2023a). This is a feature of the potentiometric surface that can occur in the study area given there is a lot of agricultural groundwater withdrawal from the GAB aquifers.

3.4.1 Comparative plots

Major ion analysis was undertaken using graphical approaches including piper plots and ion concentration graphs (Flook et al., 2020). Hydrogeochemical ratios have been used extensively in groundwater investigations to trace the evolution of meteoric water in groundwater. Rain waters have an ionic signature that reflects their oceanic origin (Commission National Water, 2013). Processes such as rock–water interaction, precipitation, and dissolution of minerals and ion exchange reactions alter the ionic ratio of rainwater after infiltration (Jankowski & Ian Acworth, 1997). Assessment of ionic ratios makes it possible to identify the dominant processes affecting the chemical composition of groundwater (Commission National Water, 2013).

Major ions were also analysed using a multivariate statistical approach (principal component analysis) to identify hydrochemical patterns and assess the processes that control hydrochemical evolution (Moya, Raiber, Taulis, & Cox, 2015) within the major GAB aquifers (from bore samples) and discharge springs.

3.4.2 PHREEQC

PHREEQC aqueous geochemical analysis of major ions was used to identify the hydrogeochemical processes that drive or control hydrochemical variability (Parkhurst & Appelo, 2013). The input parameters used in PHREEQC modelling were analytes pH, Ca, K, Na, Mg, Alkalinity, S, Cl, Al, As, Cd, Cr, Cu, Fe, Li, Pb, Mn, Hg, Ni, Au, Sr and Zn in mg/L at 20°C, pe = 4, for springs and bores using the 'Phreeqc.dat' input database as standard.

Baublys et al. (2019) have previously described the role of mineral phases in hydrogeochemical processes that drive or control hydrochemical variability in the northern Surat Basin, where the increase in bicarbonates leads to the precipitation of calcite ($CaCO_3$) and strontianite (SrCO3). These constituents have therefore been selected for further investigation from the PHREEQC modelling (Parkhurst & Appelo, 2013).

Saturation indices can be particularly useful for identifying hydrogeochemical processes. Saturation indices are a measure of the propensity for a solution to precipitate (+) or dissolve (-) a given mineral. Positive SI suggest the minerals in question are over saturated and therefore like to precipitate. If a mineral has a negative SI in water, it is more likely to dissolve if said water encounters said mineral.

Strontinate and calcite phase saturation indices can be selected for generating a plot, as this was considered useful to understand hydrogeochemical processes and separating groundwater versus meteoric-dominated spring water.

3.4.3 Principal Component Analysis (PCA)

PCA is a dimensionality-reduction method that is used to reduce the dimensionality of large data sets, by distilling a large set of variables (i.e. hydrochemical data) into a smaller dataset that still contains most of the information in the large set (Appendix D – Table 11 and Table 12).

The PCA method allows a large dataset of variables (measured physical and chemical parameters in water samples) to be compressed into a smaller number of uncorrelated orthogonal factors by interpreting the correlation matrix. The PCA transforms the raw dataset to produce eigenvectors of a variance or correlation matrix (observations and variables).

In this study, PCA was applied using MATLAB (The MathWorks Inc, 2021) to measure the physical and chemical parameters (variables) of 314 samples that have a complete data set of 42 variables. This includes eleven major ions, ionic balance, pH, EC, and 28 total and dissolved metal analytes.

Of the 314 samples, there are 24 spring samples, one rainfall sample, and 289 samples from artesian bores (156 of these bores are within a 50 km radius of the springs and range from 100 to 580m depth).

Eighteen variables of the initial 42 were selected for PCA, based on laboratory results being above the limit of detection. This allowed the reduction of 18 variables to four significant Principal Components (PC) that then can be used to analyse driving hydrogeochemical processes for the dataset.

3.5 Isotope Data Analysis

Several publications have focused on flow systems in other parts of the GAB using various isotope techniques such as ^{36}Cl (Zhang et al., 2007), $\delta^{13}C$ of DIC (Herczeg et al., 1991), strontium ($^{87}Sr/^{86}Sr$) and stable water isotopes ($\delta^{2}H$ and $\delta^{18}O$). This study applied a similar methodology.

3.5.1 Strontium isotopes ($^{87}Sr/^{86}Sr$)

Strontium isotope ratio ($^{87}Sr/^{86}Sr$) analysis of groundwater systems is a well-established method of identifying water sources, degree of water-rock interactions, and in many cases mixing relationships between the sources of dissolved constituents in water (Taylor et al., 2015). The most common mixing is between dissolved constituents from aquifer mineral weathering, and those arising in rainfall (usually dominated by sea spray or atmospheric dust).

Twenty samples were collected from fifteen spring sites, as well as five GAB bores plus a rainfall sample for $^{87}Sr/^{86}Sr$ analysis. Reference data identified in the literature have been included in the results for Hooray Sandstone and individual minerals assumed to be within the composition of the aquifer matrix (e.g., muscovite and plagioclase). Strontium isotope results from these sites along with strontium concentration, 1/[Sr], and the calculated end-member strontium source mixing ratios are presented in Appendix A – Table 5.

As a relatively high-mass element, strontium isotope fractionation in nature is very small (Baublys et al., 2019). Thus if the strontium isotope ratios of the sources of strontium to an ecosystem are known, the ratio found in each component of the hydrological system will reflect the proportions of strontium that are derived from each of the strontium sources (Green, Bestland, & Walker, 2004). This study explored strontium sources from end-members and compared results with samples collected from springs and bores. End-members are rainfall, seawater, and minerals within the GAB aquifer matrix. The strontium values used from existing sources include

End-member Sr values were a data gap and have been sourced from existing literature, including rainfall and mineralogy (muscovite and K-feldspar) from Bailey et al. (1996), Hooray aquifer material values were adopted from (Baublys et al., 2019), and values for seawater from (Taylor et al., 2015). These values and the data measured from the field sampling campaign were utilised in a mixing equation (below).

The mixing equation assumes mixing between two end-members, and results show the proportion of each end member contributing to the observed strontium ratio of the spring or bore groundwater sample. The mixing equation is shown below, and was identified by Capo *et al*. (1998) and presented in Green *et al*. (2004):

$$\frac{M_1^{Sr}}{M_1^{Sr}+M_2^{Sr}} = \frac{(^{87}\mathrm{Sr}/^{86}\mathrm{Sr})_{mix} - (^{87}\mathrm{Sr}/^{86}\mathrm{Sr})_2}{(^{87}\mathrm{Sr}/^{86}\mathrm{Sr})_1 - (^{87}\mathrm{Sr}/^{86}\mathrm{Sr})_2} \qquad \text{Equation 1}$$

Numerous studies have used strontium isotope ratios to trace and quantify the sources and fluxes of base cations in spring and groundwaters (Green et al., 2004; Shand, Darbyshire, Love, & Edmunds, 2009,Keppel et al., 2013). The chemical similarity of strontium to calcium, having a similar ionic radius and the same valence, means that strontium tends to behave similarly to calcium in most systems (Bailey et al., 1996). Sr concentrations compared with TDS to investigate sources and fluxes of base cations in spring and groundwaters is another existing method (Baublys et al., 2019) that has been used in this study.

3.5.2 Stable water isotopes deuterium (^{2}H) and oxygen (^{18}O)

Stable isotopes of hydrogen and oxygen are useful for determining the source of the water sampled. Groundwater sample results were compared to meteoric (rainfall) and marine (seawater) origin end-member samples. Processes that dictate the stable water isotope changes of water sampled include mixing of water sources, condensation, and evaporation (Kendall & Doctor, 2003).

Stable water isotope samples were collected from 22 spring sites, one rainfall sample, one rainfall-runoff site and 13 artesian bores (Figure 20 and Appendix A – Table 6).

The water sample laboratory analysis by ANSTO is expressed as isotope ratios, δ, of $^{2}H/^{1}H$ and $^{18}O/^{16}O$. Values are reported as parts per thousand (‰) compared to an internationally agreed standard (called the Vienna Standard Mean Ocean Water (VSMOW)). Water signatures that have more 'heavier' isotopes are referred to as 'enriched', such as seawater. Alternatively, the water signatures have less of the 'heavy' water isotopes referred to as 'depleted', such as water vapour.

$\delta^{2}H$ and $\delta^{18}O$ concentrations from springs, bores, meteoric water, and runoff collected in the study area have been plotted against the Cobar Local Meteoric Water Line (LMWL) and the Global Meteoric Water Line (GMWL) in Figure 20.

The Cobar LMWL has been derived from monthly weighted $\delta^{2}H$ and $\delta^{18}O$ taken from the Global Network of Isotopes in Precipitation program conducted by the International Atomic Energy Agency (International Atomic Energy Agency, 2018).

Cobar (NSW) GNIP station (number 9471100) is the closest to the south-eastern GAB and shares similar climatic conditions. The climate condition classification for Cobar and GAB groundwater source extent is warm temperate, dry winter, and hot summer (Kottek, Grieser, Beck, Rudolf, & Rubel, 2006).

3.5.3 Radiocarbon carbon (^{14}C of DIC)

Estimating groundwater residence times (or age dating) in such a large system as the GAB is not straightforward as there is often a myriad of assumptions required, no matter what approach is used. One of the most common techniques to estimate groundwater age is the application of groundwater dating techniques using natural environmental tracers (Herczeg & Love, 2007).

Evaluating groundwater residence times can be done using an isotopic tracer such as ^{14}C (Risha et al., 2009). Despite the complex chemistry of carbonates in groundwater, ^{14}C is widely used in dating groundwaters recharged between 500 and 30,000 years before the present. Results are expressed in percent modern carbon (pMC), and models have been applied by the laboratory, ANSTO, to determine groundwater residence time. Radiocarbon is useful for waters whose age ranges between 3,000 and 45,000 years.

This study uses the modelled “age” of the water sampled to indicate the relative residence time of the springs and GAB aquifer. The Cadna-Owie Hooray sandstone and Equivalents contain “dead” carbon, therefore ^{14}C content is expected to be towards a 0 pMC ^{14}C result. The relative indication of modern water spring water could be interpreted as mixing with meteoric or shallow (“young”) groundwater. The modern atmospheric ^{14}C content is around 100 pMC (pre-nuclear test) (S. Priestley, 2018), therefore samples close to this level may be considered to contain modern water. Measurable ^{14}C could indicate mixing with GAB water or a completely different source, such as the Paleogene to Neogene alluvium or outcrops that occur in a part of the study area.

Twenty-six radioactive carbon (^{14}C of DIC) isotope samples were collected at 16 spring sites over the three sampling campaigns, as well as 19 bore sites, plus one rainfall runoff sample.

There are, however, uncertainties present in calculating the percentage of ^{14}C of DIC species that originated from living plants in the aquifer outcrop and the atmosphere as opposed to that added by ancient carbonaceous deposits in the aquifer matrix. For this reason, radiocarbon dating of groundwater is most useful when repeated sampling occurs. In this case, obtaining absolute ages with their attendant uncertainties are not the primary numbers used in site interpretations. The uncorrected apparent ages are the primary numbers; they are used to compare with other apparent ages in the study. This will largely obviate the correction uncertainty. In all cases, the most useful data will come from these comparisons and not from absolute ages. Also, the uncorrected apparent ages can be interpreted as maximum ages, i.e. the real age of the groundwater is equal to or less than the apparent age (Beta Analytic, 2023; Stuiver & Polach, 1977).

3.5.4 Chlorine-36 (^{36}Cl)

Fourteen samples for chlorine-36, expressed as 36Cl/Cl-, were collected from eleven spring sites, as well as thirteen GAB bore samples. Results are presented in Appendix B – Hydrochemistry datasets, Table 8.

Chlorine (Cl^-) concentration can be useful to determine if mixing is the mechanism responsible for a change in a groundwater system.

It is noted that during the field campaign tritium (^{3}H) and Chlorine-36 (^{36}Cl) were sampled from springs and a subset of bores, which can be useful for dating groundwater with ages younger than 60 years and between 46,000 and 1 million years, respectively. Due to time constraints, the age-corrected results were not assessed in this report.

3.6 Hydrogeological Conceptual model

The conceptual model was designed to present the association of GAB discharge springs with the hydrogeological setting that has already been recognised. There was a limitation in that there was no hydrogeological model with detailed structural features in the transect where the springs in the southeastern GAB exist. A hydrogeological model across a transect of the springs in the Bourke Supergroup Eromanga and Surat Basin was developed by reviewing the literature (Geoscience Australia, 2022; Ransley et al., 2015; Scheibner & Basden, 1998).

The method is strongly dependent on the quality of data that informs the hydrogeological setting, and it is recognised that the absence of a geological structural feature (i.e. a fault) may represent a deficiency in the model—for example, there may be unmapped faults that are critical for the formation of a spring or the resolution of the hydrogeological layers used may not be sufficiently fine to find an association. The depth and extent of structural features through the geological setting were also not clear in the literature reviewed. Based on the available information, the structural features were interpreted and annotated in the conceptual model cross-section (refer to Section 7 for the Conceptual model). As future data becomes available, the conceptual model presented in this study will provide a more comprehensive understanding of hydrogeological associations.

4. RESULTS

4.1 Hydrogeology

4.1.1 Potentiometric surface

Based on inferred regional groundwater flow, two major flow systems can be delineated from Figure 6 – a westward and a northward flow system. The westward flow system begins in the highlands associated with the extensive recharge zone in the Surat Basin (150°E, 29°S) at 248 metres above height datum (mAHD) and flows in a south-westerly direction through the Eromanga Basin (144°E, 30°S) with levels down to 80 mAHD. Similarly, the start (148°E, 31°S) of the northward flow system is associated with the southern recharge zone and elevated strata have a potentiometric level measurement of 227 mAHD, which then flows into the Coonamble Embayment at 130 mAHD before connecting to the westward regional flow system (148°E, 30°S). There also appear to be localised groundwater flow direction changes in the central region of the study area in proximity to faults. This flow pattern is consistent with the interpreted GAB-wide scale contours by (Ransley et al., 2015).

A feature of the potentiometric surface map is two cones of depressions in the vicinity of 146°E, 30°S from 110 mAHD to 89 mAHD, and again from 150 mAHD to 140 mAHD at 147.5°E, 30.5°S. There are GAB bores located within these two areas, and there are no springs or known faults identified at these locations.

The hydraulic gradient in the west of the system lessens significantly, down to 80m AHD near Peery Springs. The Canda-Owie and Hooray aquifer and Equivalents rising near the surface are due to a basement high (Figure 6).

Figure removed due to copyright restriction.

Figure 6. Interpreted groundwater contours for the C-H sandstone, groundwater levels and inferred flow directions in the study area of the south-eastern Great Artesian Basin. Potentiometric surfaces are represented by contours of equal hydraulic head, shown by the 5 metres contour line gradient colour from 80m in blue to 230 m in yellow. The potentiometric surface implies groundwater flow direction (black arrows) and provides information on the current hydraulics of the system. Inset map: Study area within the GAB.

4.2 Spring Field Observations

Observations from the field investigations found that artesian mound springs were a rare landform in the southeast GAB, with only one active mound spring complex identified at Peery Springs, located at the Paroo overflow. There were estimated to be 300 active vents at this complex. Most other springs were found to be mud soaks or bubbling at ground level, or inactive springs with remnant white carbonate mounds left weathering into the landscape.

Most water discharging from the springs was less than 30°C. Away from the vents the water temperature in smaller springs quickly approaches that of the air temperature. GAB bore waters were generally alkaline (7.1 to 9 pH units) with high levels of dissolved solids. Generally, pH is expected to gradually increase along the flow path through the GAB. Spring samples pH varied from 6.6 at Lila to 9.2 at Thooro Mud, and rainfall was neutral.

Springs were very restricted in their patch sizes, ranging from a few centimetres to approximately 100 metres in diameter. Generally, individual springs were isolated by tens of kilometres from the next nearest spring.

The discharge spring wetlands vary in size from minuscule (< $1m^2$) to over 100 hectares, with the largest at the Peery Spring complex. In some locations (i.e. Bingewilpa, Boongunyarra, Cumborah and Lake Eliza) the spring wetlands include pools. In all cases, the spring wetlands can be distinguished from most other wetlands of the region because they are not subject to seasonal drying out and are sustained by a relatively constant water supply. This latter characteristic of spring wetlands supports a suite of organisms including perennial wetland plants that are distinct from those in seasonal wetlands. GAB spring species were also identified at some vents, including *Utricularia fenshamii* and *Eriocaulon carsonii*. Inland freshwater crab were also identified at Coolabah spring, which was a new ecological finding during the spring surveys. Inland crab habitat is typically within clayey ephemeral wetlands.

4.3 Hydrochemistry

4.3.1 Major ions

The GAB water bores for the C-H sandstone aquifer were sodium bicarbonate (with minor potassium) was the dominant major ion chemistry constituent for most water bores (Figure 7). This ion water type is a well-known characteristic of GAB groundwater (Golders, 2021), and a group of these samples trend towards higher chloride. Spring sites that also shared the same water type were Peery, Bingewilpa, Muleyo, Wapweelah, Coolabah and Tego.

Total dissolved solids (TDS) and pH are elevated for the GAB bores and discharges springs. Outcrop springs generally had lower pH levels, similar to rainfall (Figure 8).

Chloride concentrations are generally below 200 mg/L for most springs and bores (Figure 9). The exception to this is Bingewilpa spring and bores in the vicinity of this spring, which is situated on the west side of the Eromanga Basin Bulloo Embayment-Tibooburra Ridge junction (i.e., GW004634, GW030963), and present elevated chloride concentrations generally between 500 to 1400 mg/L.

Sites that plot above the rainfall dilution line in Figure 9, Figure 14 and Figure 12 indicate the addition of bicarbonates and sodium relative to meteoric water (Commission National Water, 2013). Conversely, sites that plot below the rainfall dilution line in Figure 11 indicate the removal of calcium in spring and bore samples compared to meteoric water. A mixed signal of addition and removal of potassium compared to meteoric water across the springs sampled, whereas most bores plot below the rainfall dilution line is shown in Figure 13.

Bingewilpa consistently is substantially more saline than all other spring sites. Consistent with the elevated TDS and EC, sodium chloride dominates the ion chemistry. The levels of sodium (1200 mg/L) and chloride (1400 mg/L) are the highest compared to all other sites.

Sites sampled that had low chloride (Cl) ion and total dissolved solids (TDS), concentrations were Lila (3 mg/L Cl, 26 mg/L TDS) and Native Dog (3 mg/L Cl, 160 mg/L TDS) (Figure 10 and Appendix A – Table 4).

The Lila sample plots questionably below the rainfall sample in the laboratory analysed ion results. It is not clear how this result would be achieved in the field. Repeat sampling at Lila is recommended to constrain the discrepancy, whether it be from contamination (i.e. dilution of the water sample from deionised water) or confirm that the ion results presented here are representative of the site.

Bicarbonate alkalinity was dominant across all samples. Bicarbonate alkalinity was highest at Bingewilpa and Peery, ranging from 720 to 730 mg/L for these. Thooro mud spring had 72 mg/L carbonate alkalinity (as $CaCO_3$), and one sample from Culla Wilallee spring (Mother Nosey complex) spring with 28 mg/L. All other spring samples are below the detection level for carbonate alkalinity.

Tego's total alkalinity value was patched using the HCO3, and CO3 was assumed to be 5 mg/L, which was the limit of reporting from the laboratory. The assumptions made to patch these alkalinity results are consistent with the actual results of other spring sites (Figure 10 and Appendix A – Table 4). Patching the alkalinity data enables Tego to be plotted on the Piper Plot in Figure 7.

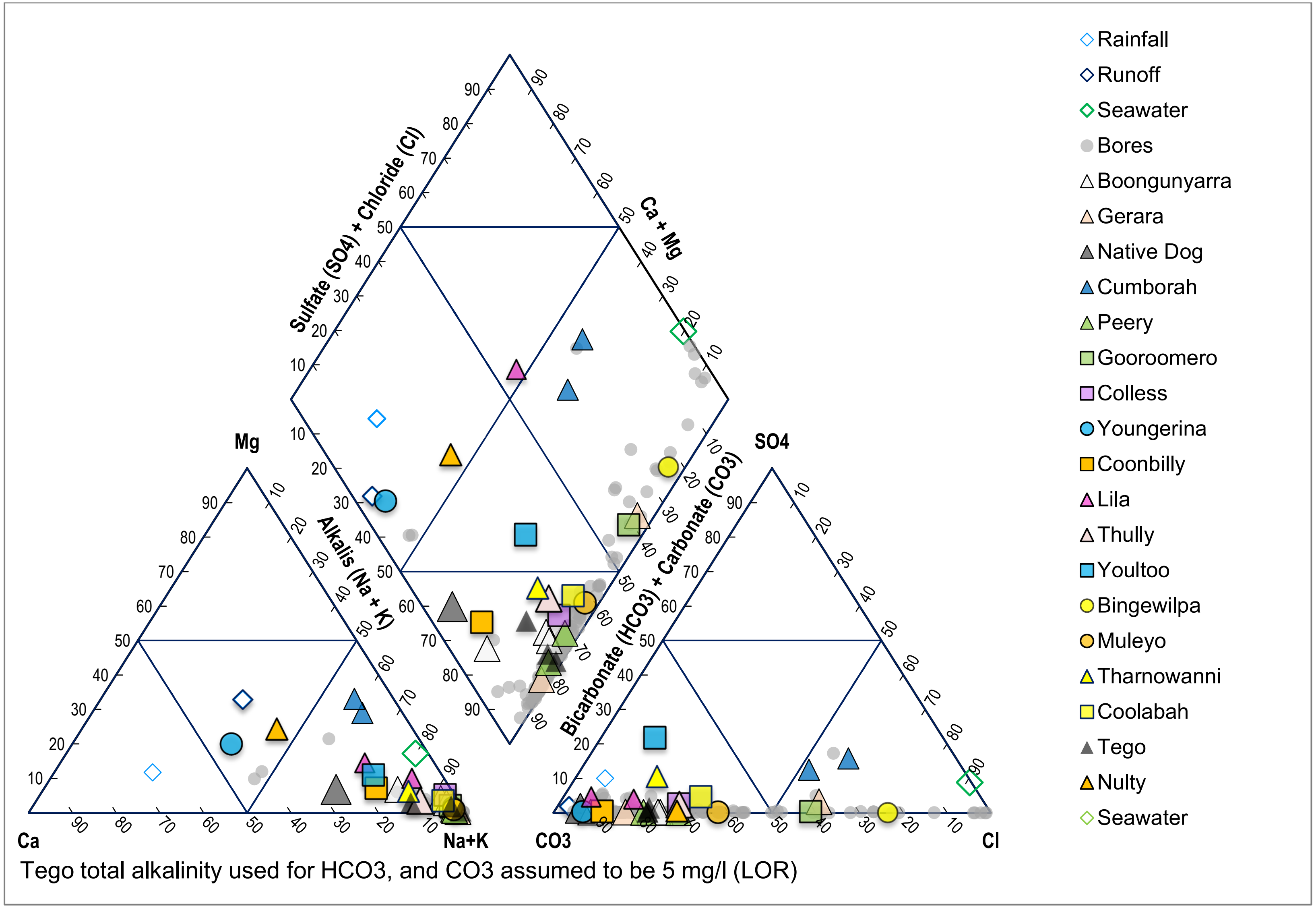

Figure 7. The piper plot shows relative proportions of cations (Ca, Mg, N + K) and anions (Cl, CO_3 +HCO_3, and SO_4).

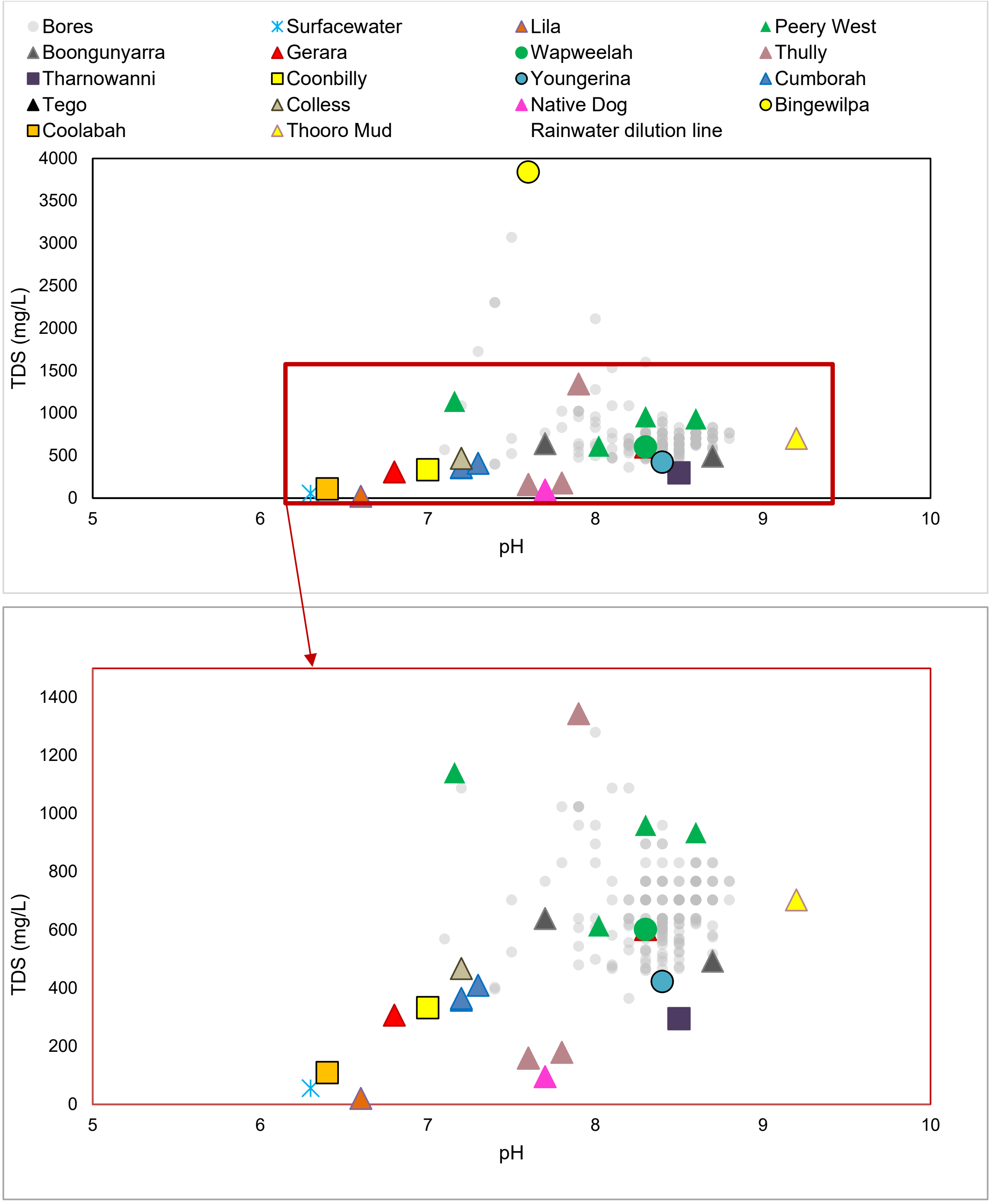

Figure 8. TDS versus pH for springs and artesian bores in the C-H sandstone aquifer.

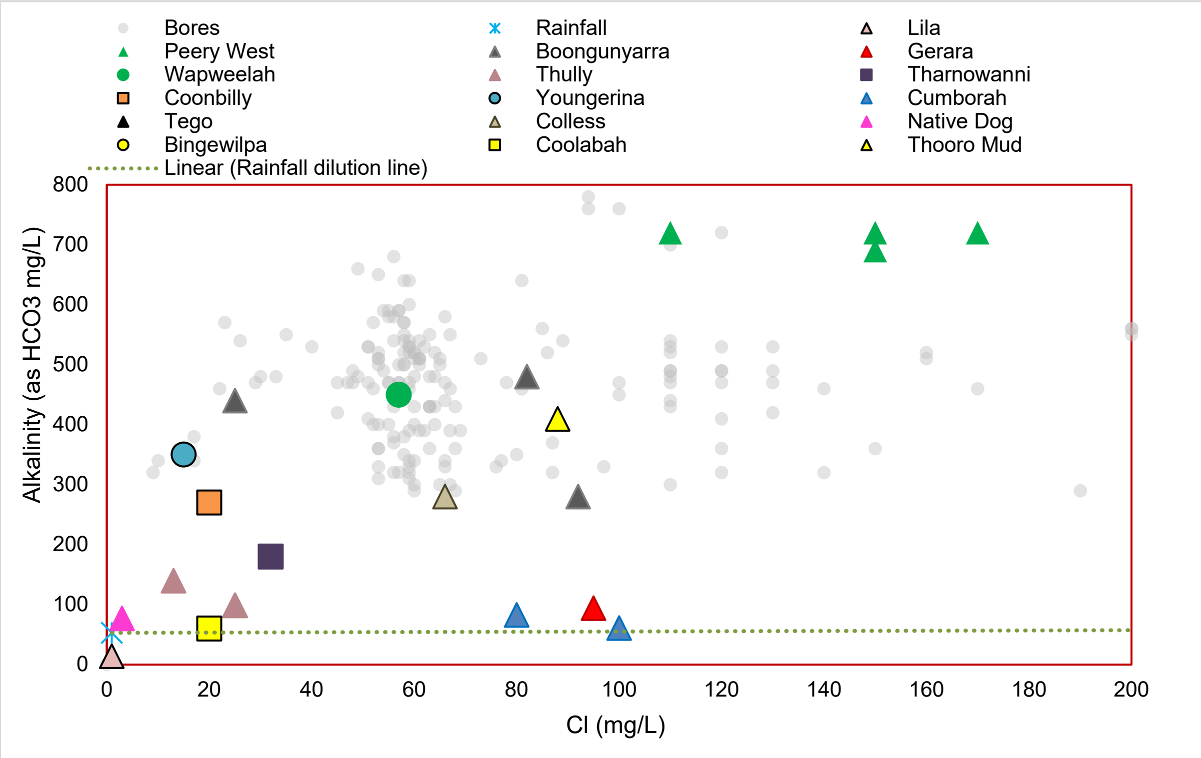

Figure 9. Alkalinity versus chloride for springs and artesian bores in the C-H sandstone aquifer. The dotted line represents the rainfall dilution line, which the majority of samples plotted above.

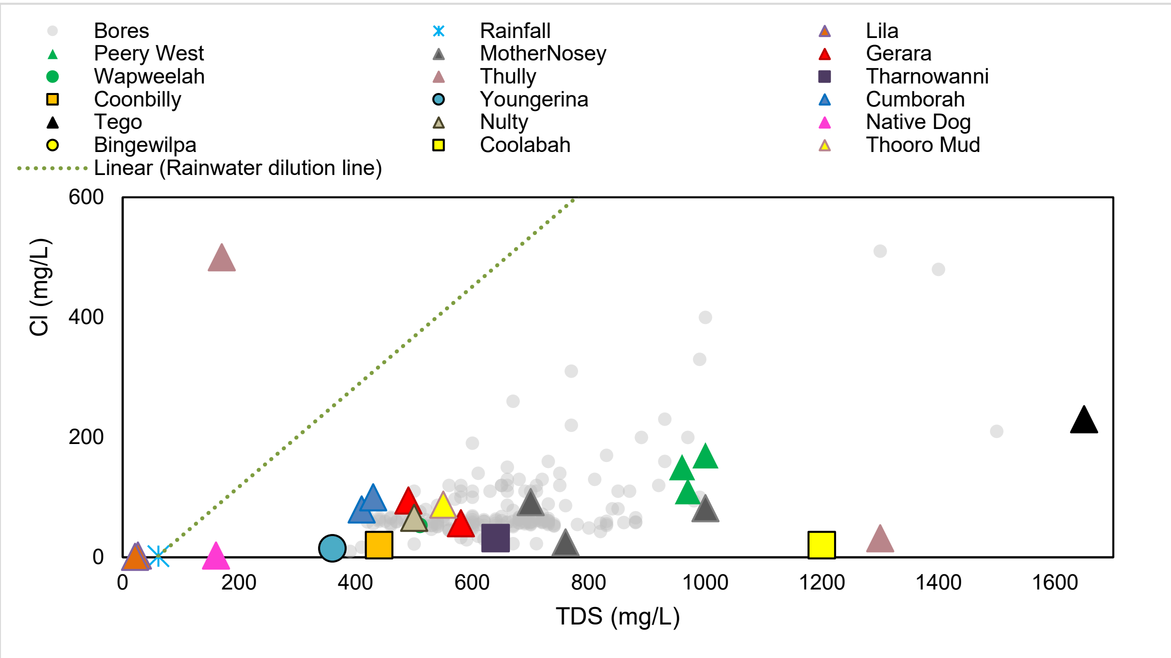

Figure 10. Chloride versus TDS cross plot for springs and artesian bores in the C-H sandstone aquifer. The dotted line represents the rainfall-seawater mixing line, which the majority of samples plot below.

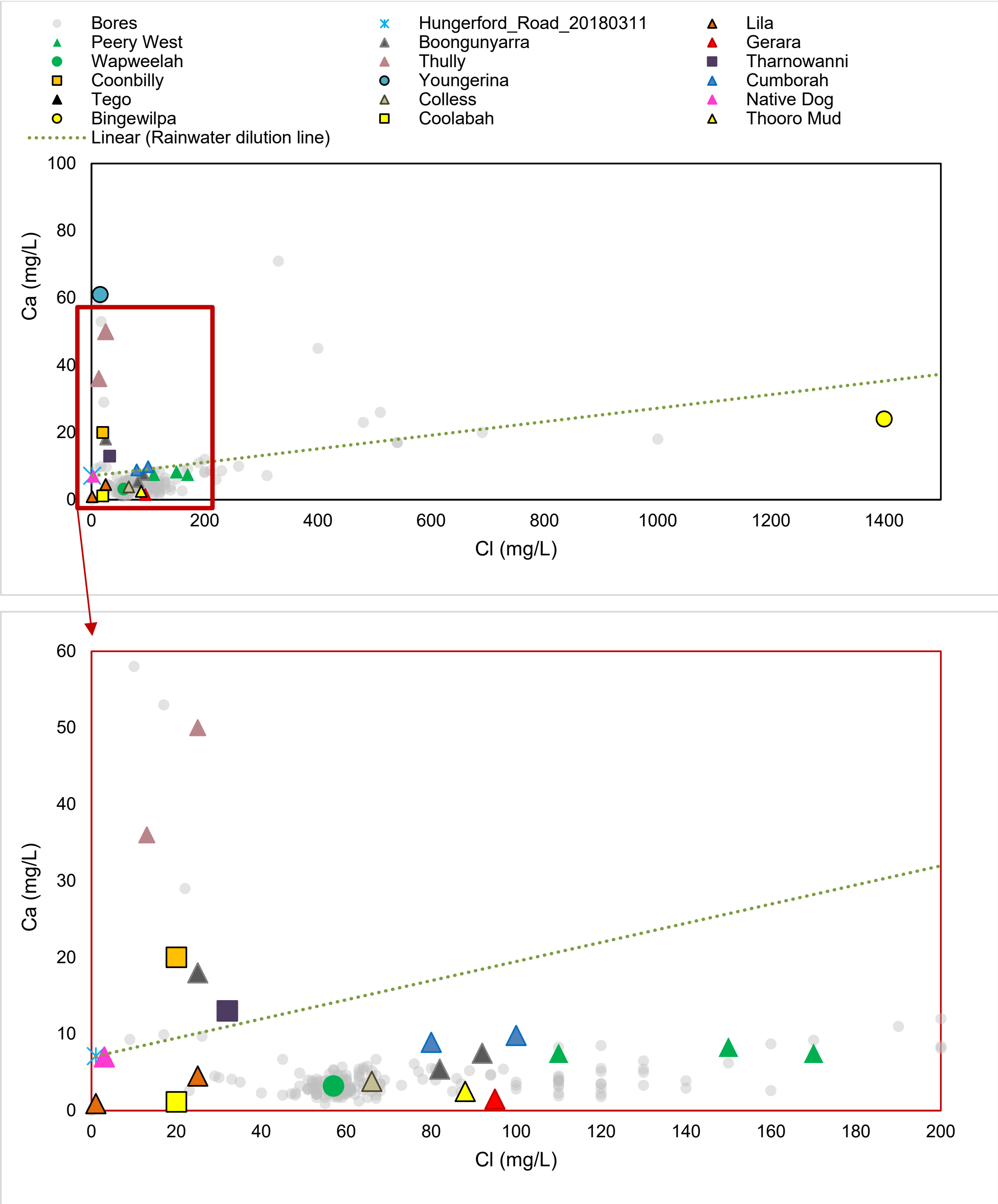

Figure 11. Calcium versus chloride for all sites with outliers at Thully, Youngerina and Bingewilpa. Most GAB spring and bore sites are below the rainfall dilution line.

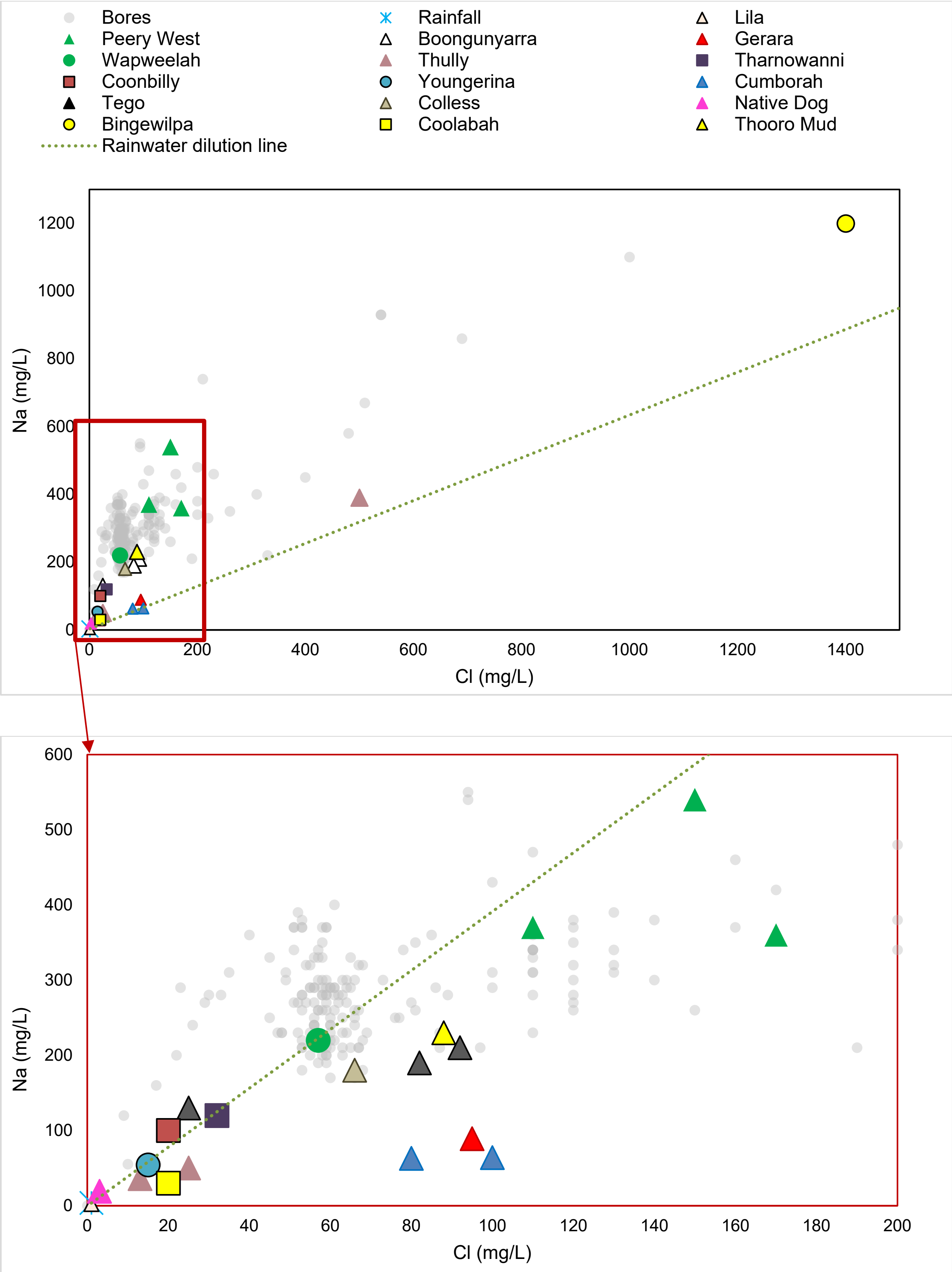

Figure 12. Sodium versus chloride for all sites with an outlier at Thully and Bingewilpa (top). Most sites are above the rainfall dilution line and are below 540 mg/L for Na and 200 mg/L for Cl (bottom inset).

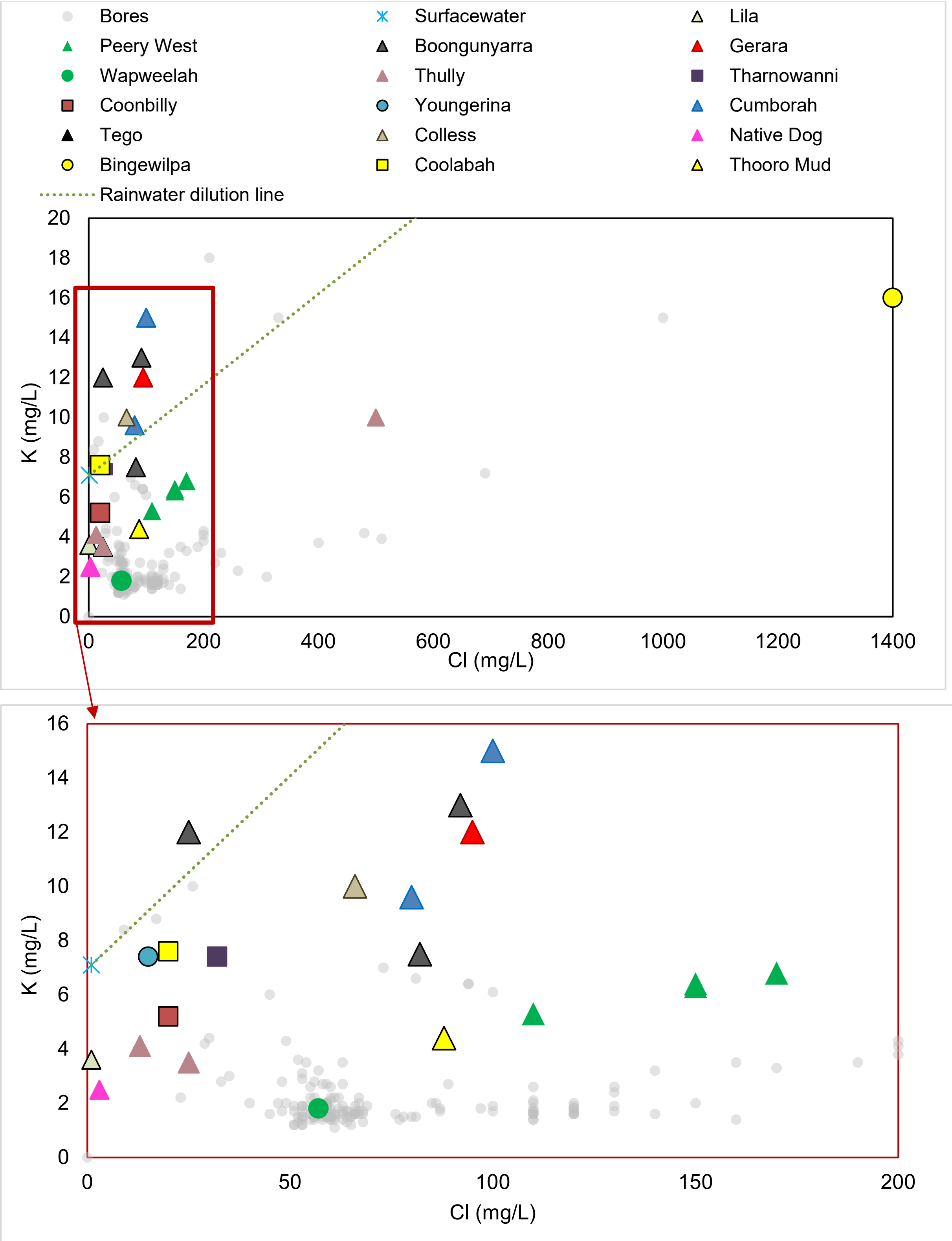

Figure 13. Potassium (K) versus chloride for all sites with an outlier at Thully and Bingewilpa (top) and most sites below 16 mg/L for K and 200 mg/L for Cl (bottom inset).

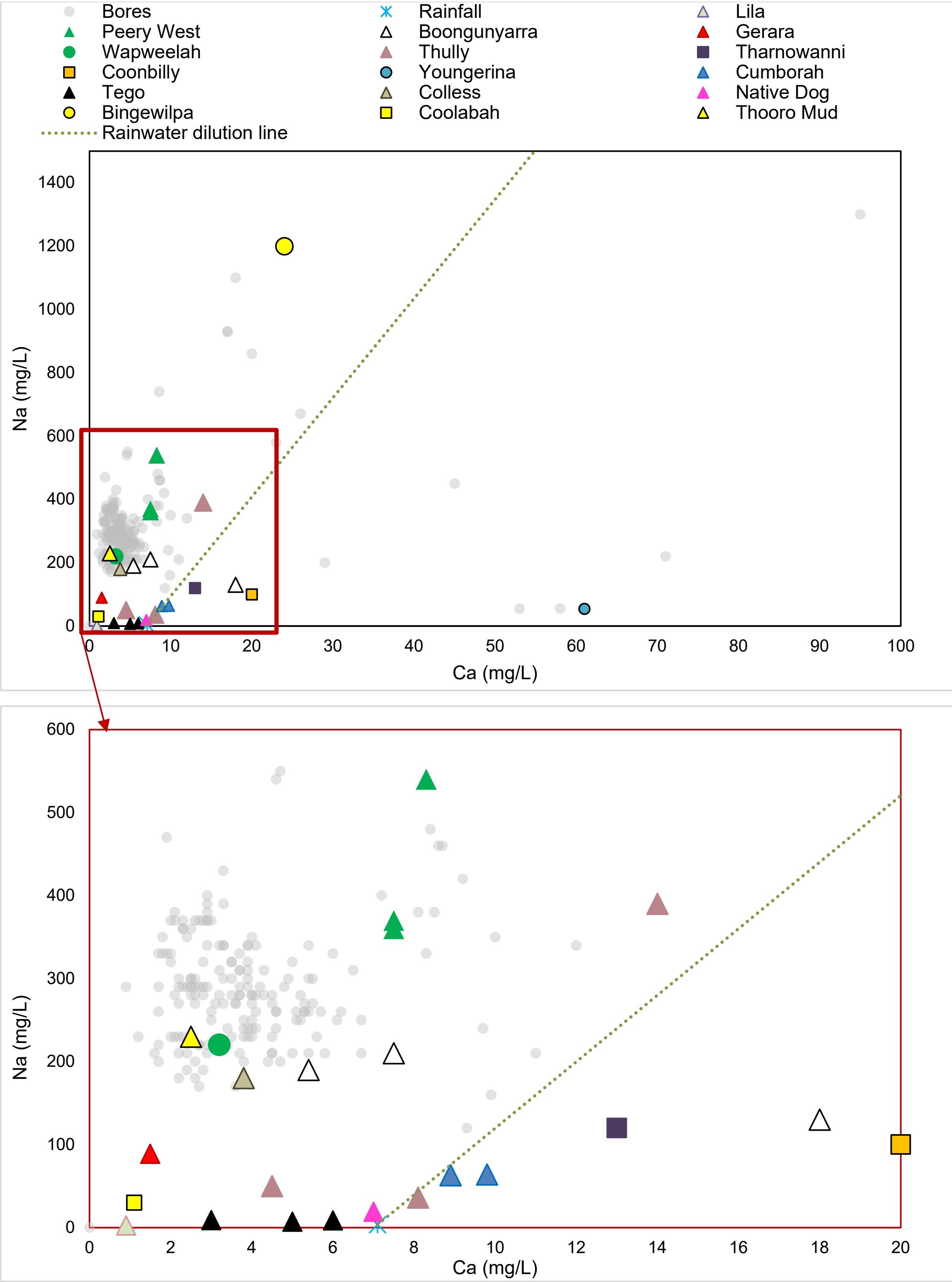

Figure 14. Sodium versus calcium for all sites with an outlier at Youngerina, Bingewilpa and some bores (top) and a cluster of sites below 540 mg/L for Na and 20 mg/L for Ca (bottom inset).

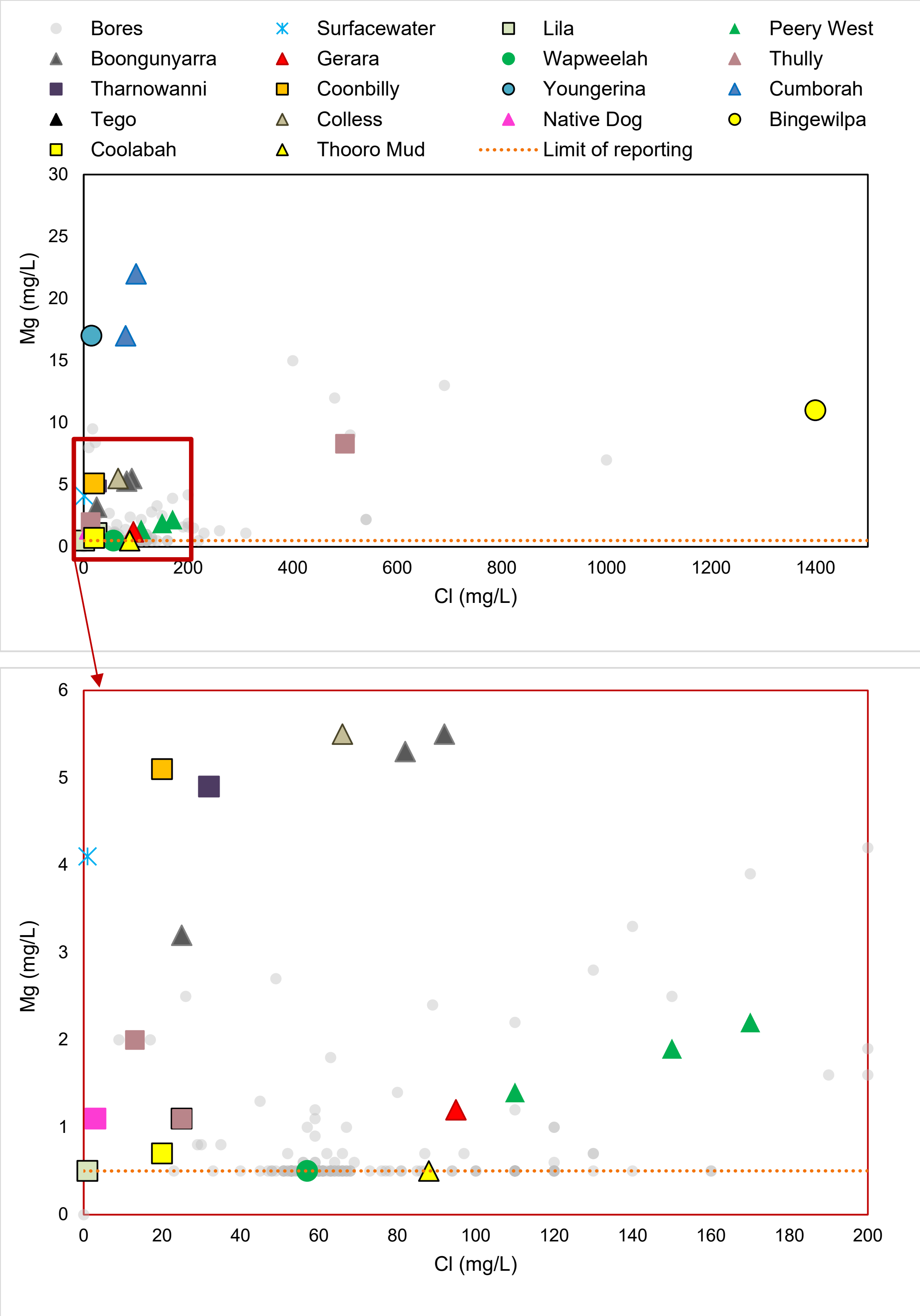

Figure 15. Magnesium versus chloride for all sites.

4.3.2 Trace Metals

Springs and bores were analysed for dissolved and total metals (aluminium, arsenic, cadmium, chromium, copper, iron, lithium, lead, manganese, mercury, nickel, silver, strontium and zinc). Dissolved cadmium and silver were not found in any locations. Concentrations of the remaining metals varied widely across the springs with aluminium, iron, and strontium in particular reporting concentration ranges (above the limit of detection) across all bores (Appendix A – Table 4).

Dissolved aluminium (Figure 16) for most bores and several spring samples (Coolabah, Tharnowanni, Wapweelah, two Peery samples, and one Boongunyarra sample) analysed plot below the limit of detection (10 µg/L). Gerara (100 ug/L), Thooro mud (88 ug/L) two Boongunyarra samples (20 and 50 ug/L) and one Peery (100 ug/L) plot above the rainfall dilution line. A cluster of samples has substantially elevated dissolved aluminium compared to the Canda-Owie Hooray sandstone and Equivalents aquifer including Youngerina, Native Dog, Lila, Thully and Coonbilly.

A similar pattern of separation is observed for dissolved iron (Figure 17), where bores fed by the Canda-Owie Hooray sandstone and Equivalents aquifer and discharge spring vents plot generally below the rainfall dilution line (< 250 µg/L). The same cluster of springs plot with substantially elevated iron 370 to 3400 µg/L.

Dissolved strontium concentrations were varied across the bore and spring samples, with a wide range of 39 to 2300 µg/L for bores, with the median value calculated at 95 µg/L. Samples with repeat sample ranged from 290 to 320 µg/L for Peery, Cumbora ranged from 210 to 250µ/L, Boongunyarra ranged from 110 to 250 µg/L and Thully ranged from 44 to 71 µg/L.

During the analysis, redox potential measured in the field was compared with these dissolved metals, however, the correlation was weak, at $R^2 = 0.15$ or less for each metal compared with redox. These results are insignificant and therefore have been excluded from this report.

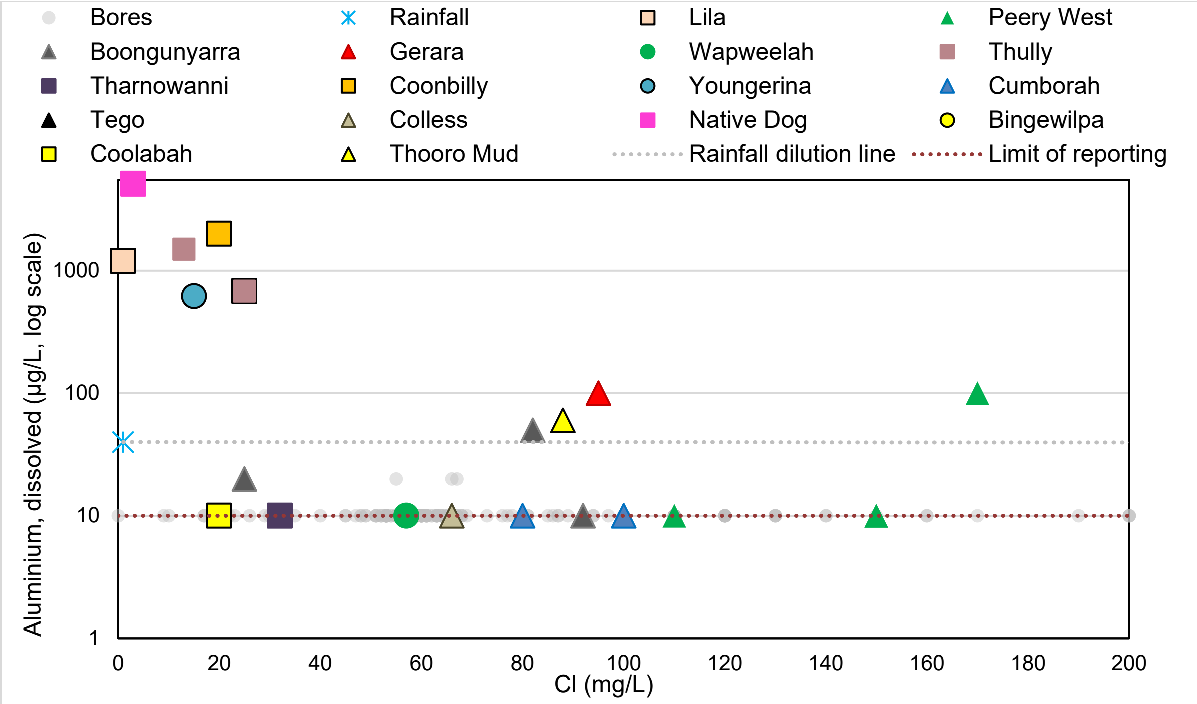

Figure 16. Aluminium (dissolved) versus chloride, with showing bores fed by the Canda-Owie Hooray sandstone and Equivalents aquifer and discharge spring vents plot generally below the limit of detection (10µg/L), while a cluster of springs with substantially elevated aluminium concentrations plot in the 650 to 5100 µg/L range.

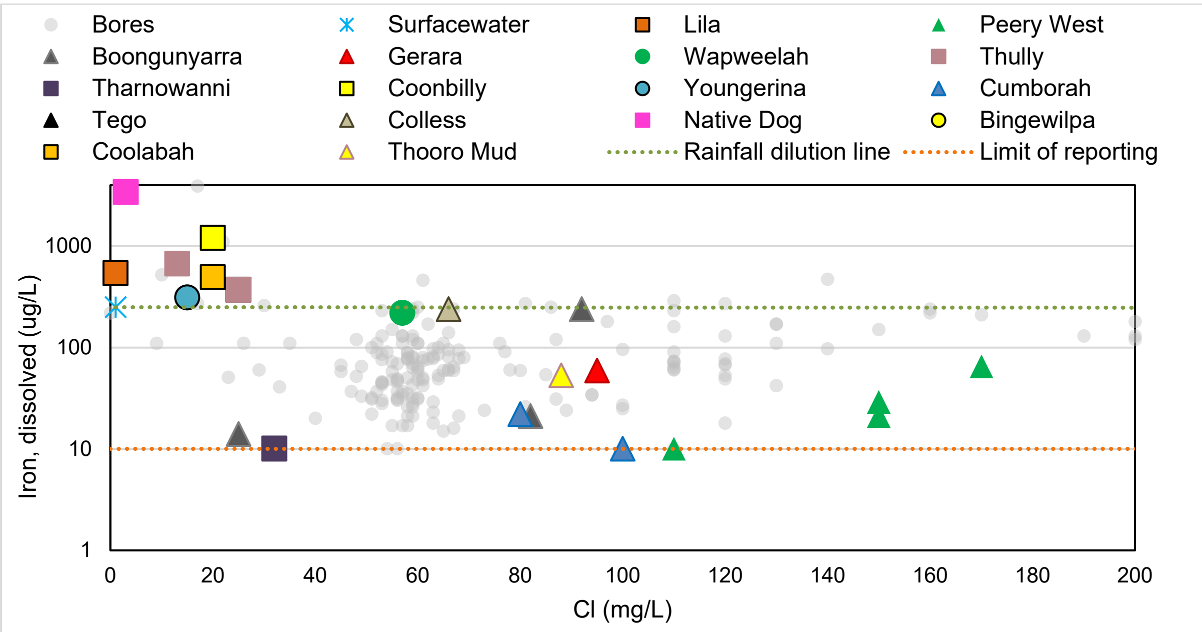

Figure 17. Iron (dissolved) versus chloride, with showing bores fed by the Canda-Owie Hooray sandstone and Equivalents aquifer and discharge spring vents plot generally below the rainfall dilution line (< 250 µg/L), while a cluster of springs with substantially elevated iron 370 to 3400 µg/L.

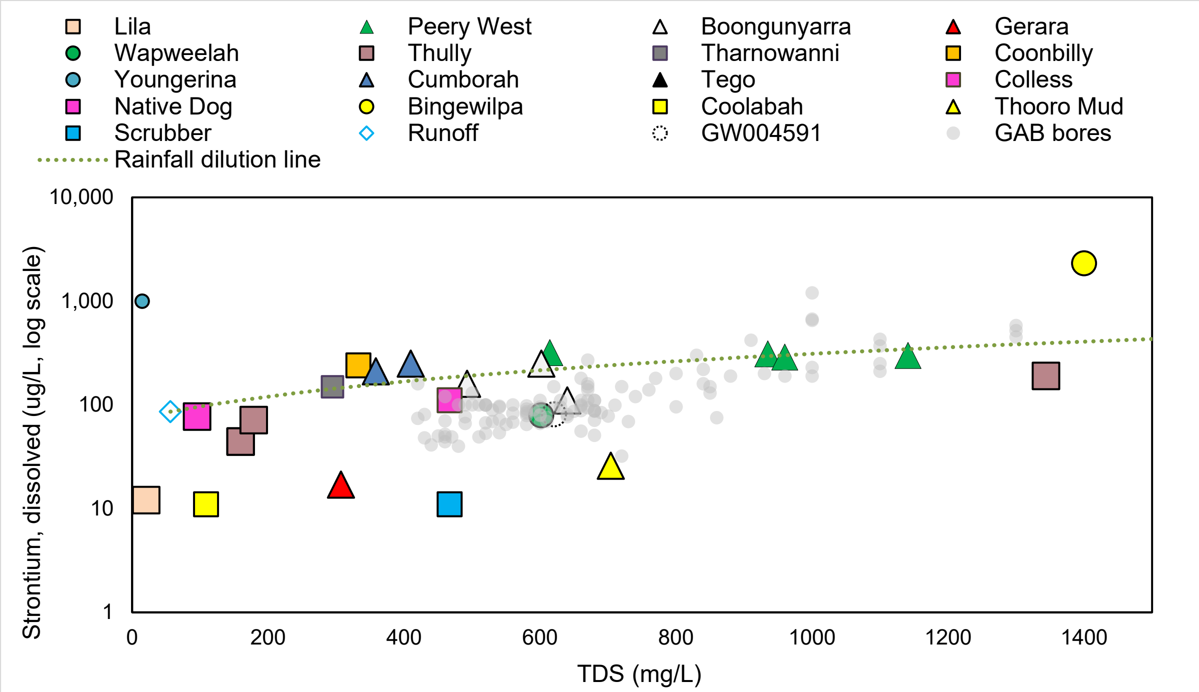

Figure 18. Strontium versus TDS shows common bores and several spring sites (Peery, Thooro Mud, Boongunyarra, Wapweelah) overlapping, while other spring sites are separated from the grouping.

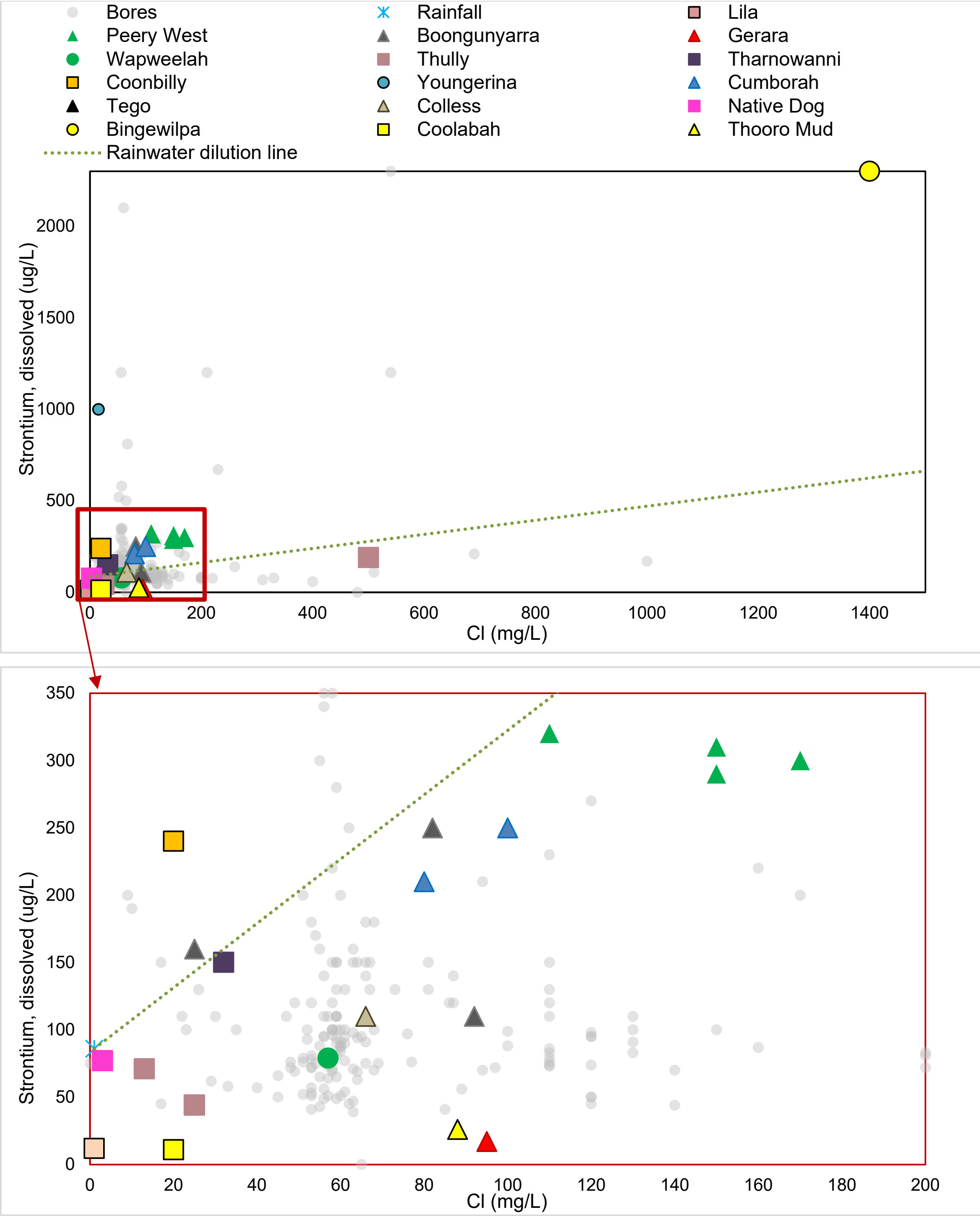

Figure 19. (a) Strontium versus chloride concentration for all sites. The dotted line is the rainfall dilution line. There are some notable outliers with higher concentrations, including Thully, Youngerina, Bingewilpa and some bores. (b) Zoomed view of strontium versus chloride concentration data below 200 mg/L Cl and 350 mg/L strontium.

4.3.3 Stable water isotopes

The GAB bore results and a cluster of the spring sample points are showing generally higher rainfall events (60-130mm/month or greater) recharged the Cadna-Owie Hooray sandstone and Equivalents aquifer. All the samples plot below the LMWL and above the GMWL, which indicate evaporation signatures at the time of recharge.

The GAB bores present as a cluster in Figure 20, ranging from δ^2H= -41.4 and $\delta^{18}O$= -6.67 to δ^2H= -36 and $\delta^{18}O$= -5.05. Springs that plot within this range are Peery, Bingewilpa, Thooro, Scrubber, Colless, Toulby and one Tego sample and two of the three Boongunyarra samples (sampled in March and October 2018). The weather conditions preceding these sampling events were dry and any localised rainfall (Figure 2) did not affect the water at these spring sites.

Cumbora stable water isotope signatures (δ^2H= -22.6, $\delta^{18}O$= -3.91 and δ^2H= 22, $\delta^{18}O$= -4.06) are akin to the monthly weighted average rainfall for Cobar (δ^2H= -23.64 and $\delta^{18}O$= -4.66 (pink circle in Figure 20)).

Coonbilly stable water isotope signatures (δ^2H= -22.2, $\delta^{18}O$= -1.14) are akin to the standing water rainfall-runoff sample (δ^2H= -22.5, $\delta^{18}O$= -1.15). These points are also akin to the monthly weighted average rainfall with strong evaporation signatures. Of note, the rainwater sample collected during the 27 mm rainfall event during the field campaign (16 October 2018) also plots (δ^2H= -18.5, $\delta^{18}O$= -0.61) more similar to the standing water rainfall-runoff sample compared to the calculated monthly weighted average rainfall.

All remaining sample points are below the monthly weighted average rainfall with isotopic enrichment indicating strong evaporation signatures ($\delta 18O$ >-1‰). Strong evaporation is likely to have occurred after the spring water has emerged. The water at the spring points is likely to have been recharged by historically 10-30mm rainfall events. Evaporation processes are likely to have occurred while the sample has been exposed to the atmospheric conditions leading up to the sampling time.

The equation of the LMWL for the Cobar GNIP station and rainfall data collected during the fieldwork is provided in Figure 20.

$$\delta^2H = 6.8 \cdot \delta^{18}O + 6.7 \qquad \text{Equation 2}$$

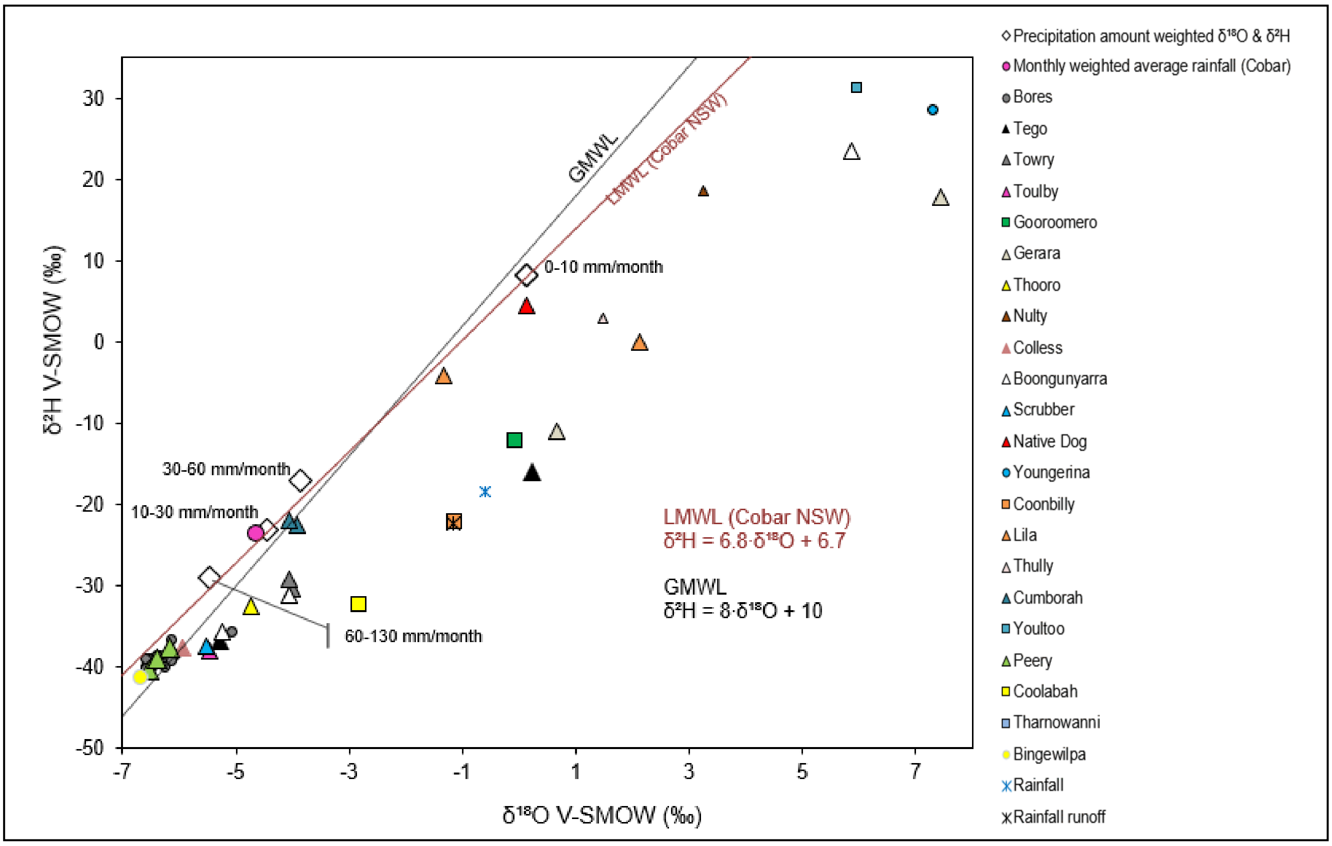

Figure 20 Stable water isotopes of springs (triangles = GAB natural flows, circles = bore free flowing at spring site, and square associated with outcrop spring), with hollow diamonds, represent the amount-weighted mean δ^2H and $\delta^{18}O$ composition of different size rainfall events (0-10, 10-30, 30-60 and 60-130 mm/month) for Cobar rainfall.

4.3.4 Strontium

Strontium isotope ratios for spring samples range from 0.708 to 0.710, and bore values range from 0.705 to 0.708. End-member values of strontium are 0.710 for rainfall, 0.709 for seawater and 0.704 for Hooray sandstone mineralogy.

Strontium isotope ratios (using Equation 1) suggest that the greater proportion (79-81%) of the strontium content in groundwater (bores) sampled (GW004591 and GW004282 respectively) are likely to have originated from weathering from the Hooray sandstone.

The spring values have a higher strontium isotope ratio range (using Equation 1), indicating other geochemical processes such as cation exchange at the surface, are occurring in addition to the aquifer material weathering.

Variation of strontium isotope ratios with strontium concentration in spring samples indicates the mixing of end-members with distinct strontium isotope ratios (Figure 21). Silicate weathering of plagioclase (K-feldspar) and muscovite across the Surat Basin has been described by (Baublys et al., 2019) to present, however, this is at low levels across the basin.

Peery springs have a complex hydrogeochemistry but in general, are relatively high in TDS with a lack of evaporation trends in $\delta^{18}O$ and $\delta^{2}H$ suggesting mostly mineral dissolution along the groundwater flow path from aquifer material and at the spring expression is the main source of dissolved ions.

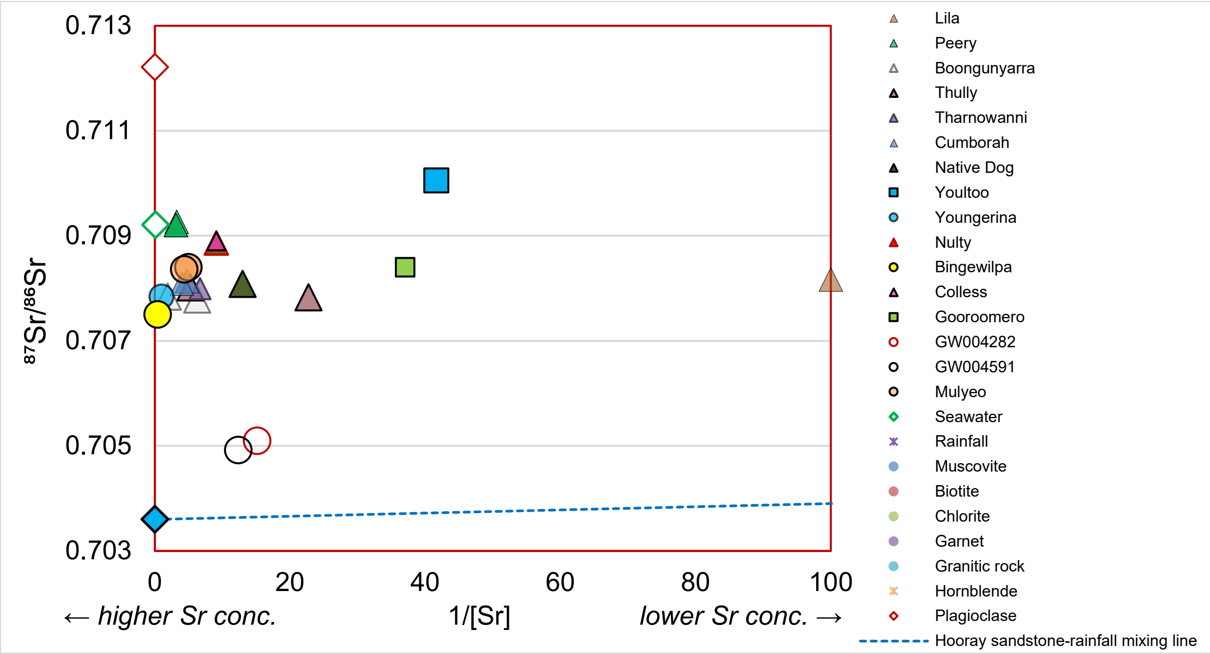

Figure 21. $^{87}Sr/^{86}Sr$ versus 1/Sr concentration.

Figure 21 note: Only the $^{87}Sr/^{86}Sr$ result has been plotted for Hooray sandstone and used to generate the mixing line, as strontium concentration was not available and has been plotted at 0 on the x-axis in the absence of this data point. While this is a limitation, the Hooray sandstone 1/[Sr] value is assumed to be plotted in this vicinity on the graph.

Figure 22 shows that with increasing TDS there is increased Sr concentration in the samples. The GAB groundwater samples generally plot above the Hooray sandstone-rainfall mixing line (Figure 19), indicating that Sr is gained due to mineral weathering in the aquifer, especially considering their Sr isotope ratios. Thooro mud spring has low strontium concentration and high TDS (Figure 22) which plots near results for GAB bore GW010785 (406 m deep). This indicates that other ions are contributing to the TDS at this site. Thooro mud spring also presents slightly lower stable water isotope ratios compared to the C-H sandstone aquifer and plots below the LMWL (Figure 20). This indicates source water is potentially evaporated water (Figure 22) compared to the Hooray sandstone aquifer.

Tharnowanni and Coonbilly water matrix are also likely to be sourced from long-standing surface runoff from rainfall events which evaporated leading up to the sampling period.

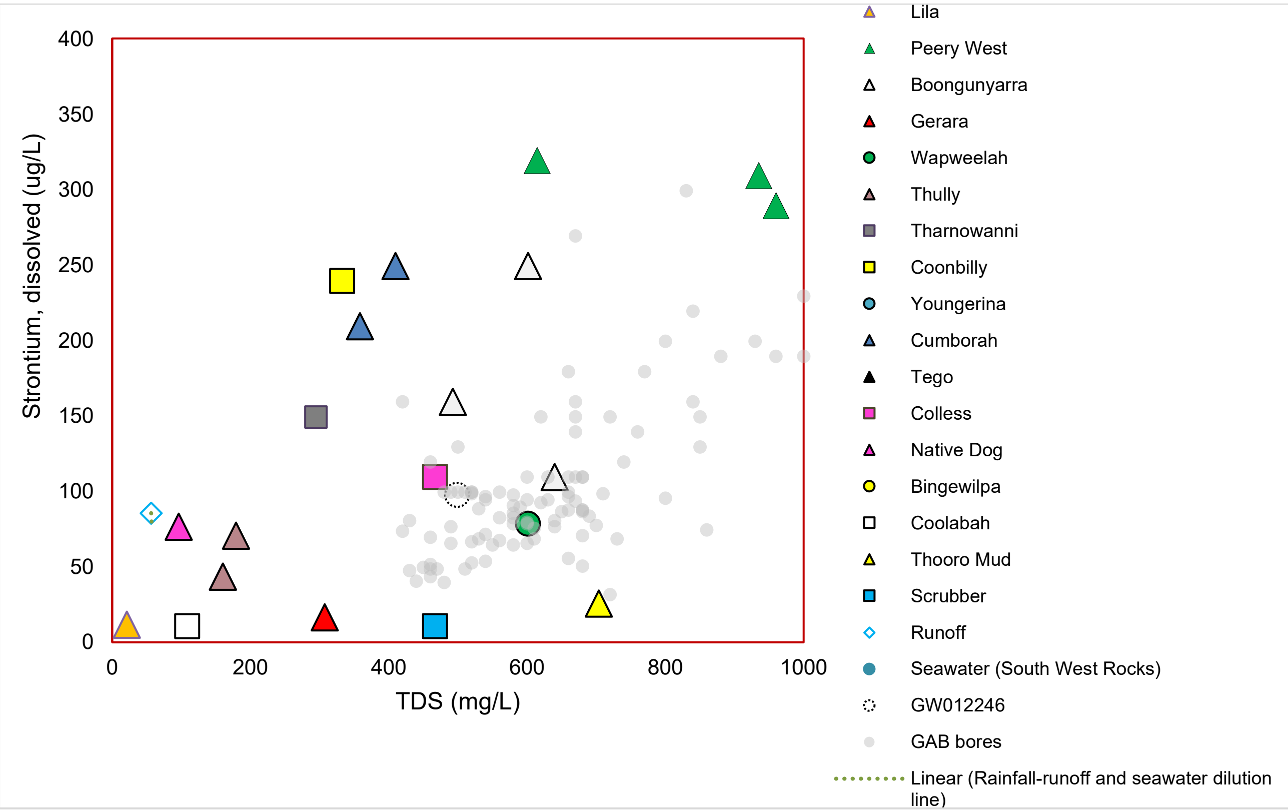

Figure 22. Strontium concentrations versus total dissolved solids (TDS, mg/L) for the springs fed by natural seeps (triangles), springs with leaking bores (circles) and surface water dominated spring sites (squares), with Hooray sandstone groundwater (grey dots).

4.3.5 PHREEQC

Hydrogeochemical complexities observed from PHREEQC (Parkhurst & Appelo, 2013) include re-equilibrium of solute as groundwater flows through the aquifer and discharges at the springs, particularly for Strontinate and calcite saturation indices. Figure 23 shows a strong positive correlation (R^2 = 0.98) between strontianite and calcite for springs and GAB bores. There also is an apparent separation of water types, with groundwater-dominated water matrix having an increased saturation index for strontianite at 2.9, and 1.1 for calcite (i.e., Peery, Boongunyarra, Bingewilpa, Cumborah). Meteoric-dominated water types have lower values of -3.9 for strontianite and -2.3 for calcite (i.e., Lila and Coolabah).

For all springs and bores, the majority of mineral phase results are reported as negative values, except for gibbsite, goethite, Fe(OH)3(a) and jarosite-K (Table 13 - Appendix D).

Saturation indices for the full range of analytes reported from PHREEQC (Parkhurst & Appelo, 2013) modelling for results presented in Figure 23 are presented in Table 13 -

Appendix D. These results are only a subset of the output file, which has been excluded from this report due to the large output file size which is 96060 rows in excel.

The full output file includes results for each of the Phreeqc.dat modules (i.e., SOLUTION_MASTER_SPECIES, SOLUTION_SPECIES, PHASES, EXCHANGE_MASTER_SPECIES, EXCHANGE_SPECIES, SURFACE_MASTER_SPECIES, SURFACE_SPECIES and RATES).

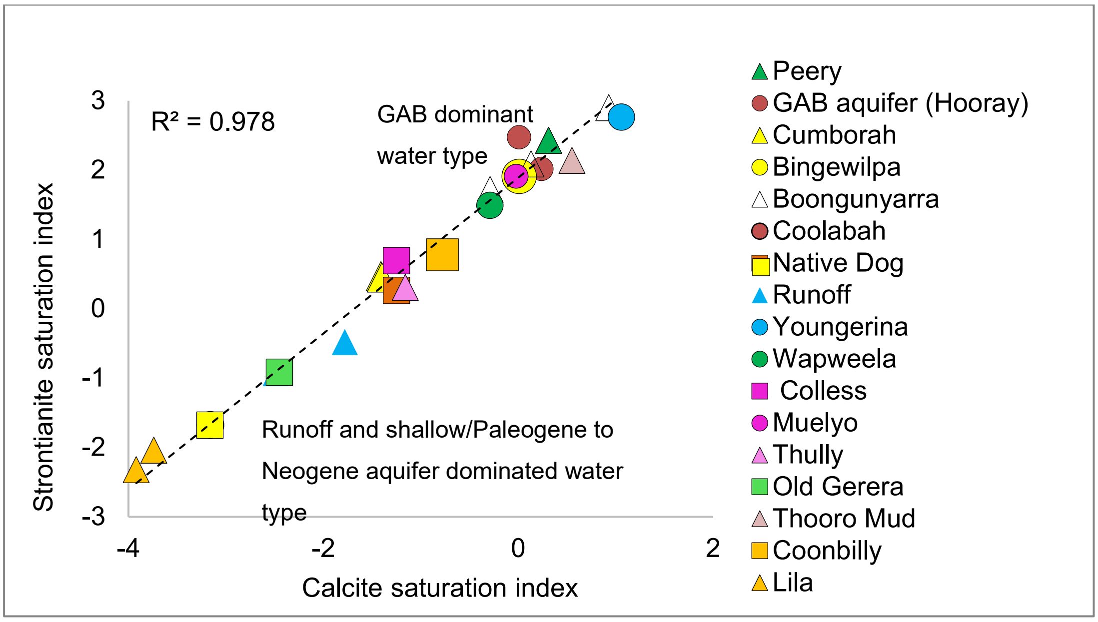

Figure 23. Calcite and strontianite saturation indices relationship, modelled using PHREEQC (Parkhurst & Appelo, 2013) for springs, GAB bores, rainfall and surface water.

4.3.6 Principal component analysis (PCA)

PC1 explains the groundwater mineralisation and salinity processes, whereas PC2 shows redox and carbonate-driven processes. These are the focal principal components for explaining overall processes. It is not clear what processes are driving the combination of results for PC3 and PC4, as there are only three seemingly unrelated significant variables for PC3 and one for PC4.

Factor analysis was carried out on the dataset which shows that significant (>0.5 or <-0.5 coefficient score) PC1 variables were dominated by major ions. This includes Ca (0.94), Na (0.93), K (0.86), HCO3 (0.95), ionic balance (0.95), Mn (0.85), Sr (0.95) and electrical conductivity (0.95). This explains the groundwater mineralisation and salinity processes.

Significant PC2 variables are $CaCO_3$ (0.63), Fe (-0.62) and pH (0.54). Calcium carbonate precipitation and dissolution processes from pressure, temperature or turbulence change inherent with rapid spring water ejection are expected to be driving these results. PC1 and

PC2 seem to be independent processes, as there is not a clear relationship between the respective variables (Figure 24).

The eigenvalues totalled 18 which matches the total input variables, and the variance totalled 100%, indicating the PCA model script applied in MATLAB (The MathWorks Inc, 2021) was executed correctly for the dataset (Table 2, Table 12).

Table 2. PCA factor loadings for four principal components, with significant values (>0.5 or <-0.5 coefficient score) in bold blue text.

Variable	PC1	PC2	PC3	PC4
Ca^{2+}	**0.935**	0.017	-0.110	-0.211
Mg^{2+}	0.726	-0.077	0.270	0.354
Na^{+}	**0.931**	0.260	0.001	-0.006
K^{+}	**0.864**	-0.073	-0.389	0.132
HCO_3	**0.952**	-0.020	-0.228	-0.079
$CaCO_3$	-0.231	**0.631**	0.066	**0.540**
SO_4	-0.332	0.360	-0.335	-0.423
Cl^{-}	0.357	-0.180	**-0.527**	0.455
Ionic balance	**0.948**	0.100	0.053	-0.081
Al^{3+}	0.164	0.347	-0.243	0.104
Fe^{2+}	-0.005	**-0.626**	0.143	-0.162
Li^{+}	0.537	-0.461	-0.205	0.180
Pb^{2+}	0.597	0.339	**0.532**	0.231
Mn^{4+}	**0.845**	-0.056	-0.158	-0.258
Sr^{2+}	**0.947**	0.143	0.111	-0.199
Zn^{2+}	0.381	0.087	**0.512**	-0.350
pH	-0.360	**0.539**	-0.384	-0.271
EC	**0.946**	0.183	0.028	-0.005

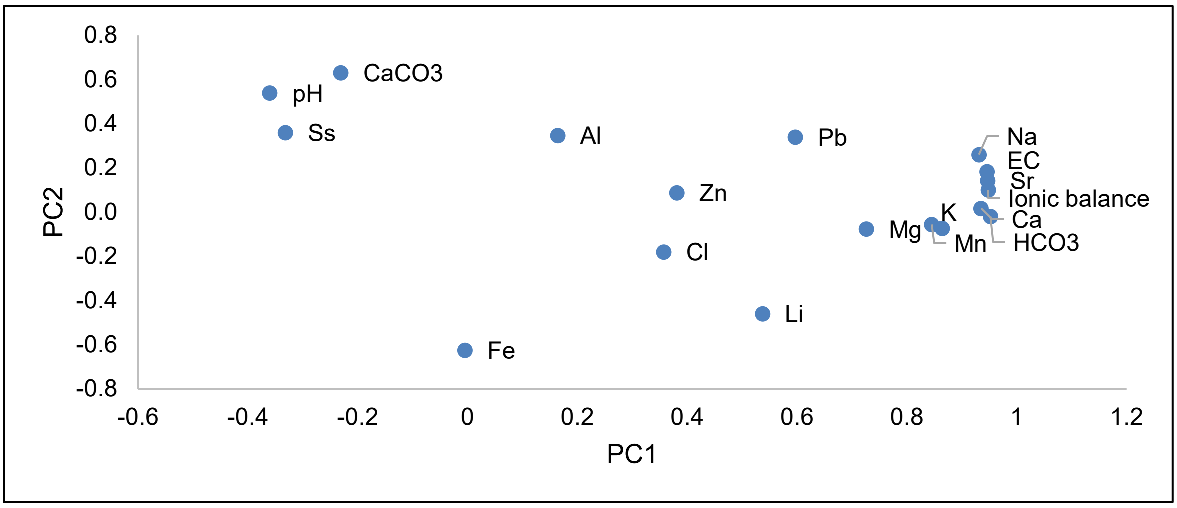

Figure 24. PC1 versus PC2 plot for eighteen variables.

4.3.7 Radiocarbon

There are generally two groupings split for the ^{14}C versus chloride (Figure 25) and for ^{14}C versus $\delta^{18}O$ (Figure 26). Group 1 shows GAB dominant water type and Group 2 shows runoff and shallow/Paleogene to Neogene aquifer-dominated water type.

The modern atmospheric ^{14}C content is 100 pMC (pre-nuclear test). Surface runoff and shallow/Paleogene to Neogene aquifer-dominated water types have a 14C value between 92 and 103 pMC.

GAB bores consistently plot in the low range ^{14}C, generally <1.5 pMC. Peery also plotted consistent pMC values in radiocarbon grouped with GAB dominant water type 2.5 to 4.2 pMC for the three sampling events. By contrast, Boongunyarra plots variably within the GAB 15.9, 35.1 and 93.5 pMC. Residence time ranges from modern to 49,700 years old.

Radiocarbon dating analysis of groundwater is highly uncertain, as there are many variables related to carbon sources that may skew the result.

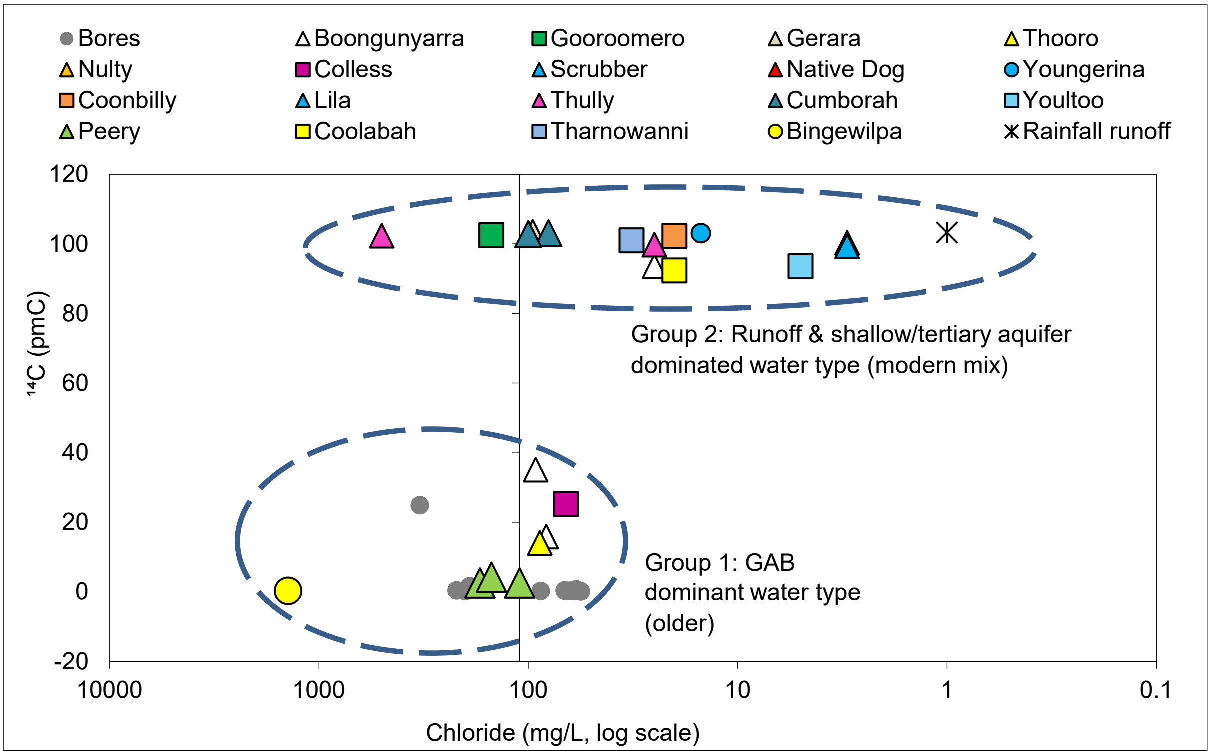

Figure 25. ^{14}C (pMC) versus chloride for springs, GAB bores and surface runoff sample

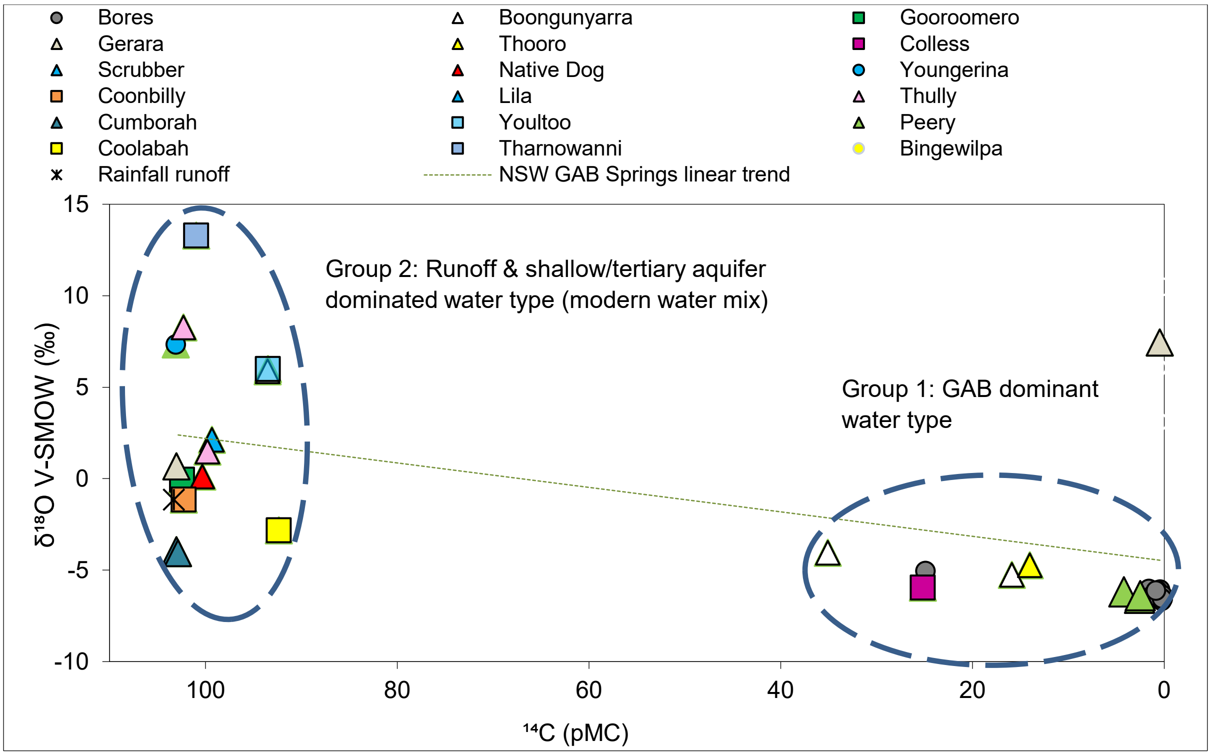

Figure 26. 14C (pMC) versus δ¹⁸O for springs, GAB bores and surface runoff samples.

Figure removed due to copyright restriction.

Figure 27. Radiocarbon activity (^{14}C DIC pMC) and modelled conventional 'age' distribution of radiocarbon samples. Site-specific results can be found in Appendix B –Table 8.

4.3.8 Chlorine isotopes (^{36}Cl/Cl)

^{36}Cl concentrations in groundwater vary from 1.3×10^{-14} to 5.5×10^{-13} (Appendix A – Table 8). This is presented in Figure 28, along with the inferred groundwater flow directions (arrows), C-H sandstone aquifer potentiometric surface levels, and the modelled regional ^{36}Cl/Cl distribution by (Ransley et al., 2015) for the C-H sandstone aquifer.

Figure removed due to copyright restriction.

Figure 28. Map of ^{36}Cl distribution of springs (open circle), and bores (circle with crosshair) sampled as part of this study. This has been overlaid onto the ^{36}Cl/Cl modelled regional distribution across the C-H sandstone aquifer by (Ransley et al., 2015) and potentiometric surface contours.

5. DISCUSSION

5.1 Hydrochemistry and environmental tracers

Hydrochemical analysis was done using environmental tracers to compare spring types with the C-H sandstone aquifer water origins for discharge springs, and rainfall origins for outcrop springs. There were two other spring-type settings identified in this study, bore-fed springs and inactive springs, which totals four spring-type settings identified in this study. The following discussion section focuses primarily on using hydrochemistry and environmental tracers to decipher the water sources flowing to discharge springs compared to outcrop spring expressions. Overall, there are clear lines of hydrochemical evidence characterising discharge springs compared to outcrop springs.

The discharge springs, such as the Bourke and Bogan Supergroup, can be characterised typically by long residence times, have Na-Cl and Na-HCO_3 type water, and have higher strontianite and calcite saturation indices compared to outcrop springs. This is akin to the C-H sandstone aquifer environmental tracer and hydrochemistry fingerprint. This is also consistent with numerous other GAB aquifer and discharge spring studies in South Australia by (S. C. Priestley et al., 2019) and in Queensland by Moya et al. (2015 and 2016) and Herczeg *et al*. (1991). Outcrop springs are typically characterised by strontianite and calcite saturation indices that are more similar to rainfall results. The discharge springs have a more depleted stable water isotope composition and are recharged by rainfall events of at least 60-130 mm. Outcrop springs have a more enriched stable water isotope composition reflects smaller rainfall events (<60 mm rainfall events) and appear to be more influenced by evaporation, especially those with $\delta^{18}O$ >1‰. The larger discharge spring pools appear to undergo more evaporation compared to the smaller spring expressions. The discharge springs also have higher TDS compared to outcrop springs. Dissolved trace metals results were generally inconclusive about separating discharge springs from outcrop springs. Comparison of spring with bores is however limited, since bores targeted during the sampling campaign was only concentrated on the C-H aquifer, and the Paleogene to Neogene units remain a knowledge data gap.

The Peery spring complex represents one of the main natural discharge points in the southeastern GAB. The physical, chemical and stable water isotopic signatures are quite similar to the GAB groundwater samples. The ^{14}C activity for Peery springs (2.51 to 4.2 ^{14}C DIC pMC) is slightly higher than background levels in the Cadna-Owie and Hooray Sandstone aquifer (0.17 to 1.62 ^{14}C DIC pMC). This suggests a tiny amount of mixing with the Peery Lake water table (Paleogene to Neogene units of the overlying Murray-Darling Basin) as the GAB artesian water bubbles up to the surface. All samples from Peery have a similar isotopic signature, indicating that the δ^2H and $\delta^{18}O$ ratios do not vary seasonally, consistent with the C-H sandstone groundwater source.

For discharge springs and bores within the C-H sandstone aquifer, the elevated alkalinity and the presence of dissolved minerals in the water reflect the long residence time of the groundwater. The basic pH, increasing EC levels along the flow path, and HCO_3-Na water type of GAB springs and bores reflect processes of mineralisation coming from the groundwater flowing through aquifer matrix material. This process was also found by (Dupuy et al., 2021) while investigating thermal spring hydrosystems on Corsica Island (Western Mediterranean, France).

The PCA analysis showed that mineralisation is an overall primary driving process for the salinity signatures for all spring and bore water samples, with secondary reduction-oxidation processes. The salinity signature was the first principal component of the PCA analysis, demonstrating that hydrochemistry for all springs and bores is generally dominated by electrical conductivity, ionic balance, Na^+, Ca^{2+}, Mn^{2+}, Sr^{2+} and K^+, which is a result of water-rock mineralisation processes. Solute concentrations in percolating discharge springs and any infiltrating water are additionally modified by the dissolution of surficial minerals such as carbonates and gypsum, as water moves through the unsaturated zone. This has also been described and explained with cation exchange causing dissolution of these ions by other studies in the western GAB by (Priestley et al., 2019).

Calcium dissolution and precipitation processes are the second principal component of the hydrochemistry PCA analysis, demonstrated by the significant variables being $CaCO_3$, Fe and pH for all springs and bore water samples. Calcium dissolution and precipitation has also been recognised in numerous studies as a major process controlling the hydrochemical evolution in the GAB (Moya, 2015). Calcium dissolution and precipitation processes likely a result of reactions in response to a pressure, temperature, turbulence change inherent with groundwater flow at the surface for all spring expressions are taking place. For discharge springs, this occurs as the C-H sandstone artesian groundwater approaches the shallow subsurface of the springs. This is where pH reduces towards neutral levels and there is an oxidation process happening with irons, and bicarbonates increase. The increase in bicarbonates leads to the precipitation of calcite ($CaCO_3$) and strontianite ($SrCO_3$). A similar geochemical process has also been described by Baublys et al. (2019), who investigated the fate of hydrochemical constituents between GAB groundwaters and surface waters in the northern GAB artesian aquifer. Similarly, for outcrop springs, reduction-oxidation processes occur in the relatively shorter, through-flow paths, where shallow groundwater flows through the localised Paleogene to Neogene unit to the outcrop spring. Further investigation into dissolution of minerals, such as gypsum, or precipitation, such as iron oxides, with accompanying figures is recommended to further benefit the data analysis and interpretations.

The stable water isotope data for both discharge and outcrop springs showed that the composition of all water is completely local with meteoric origins. Outctop springs have undergone evaporation at the spring vent site due to a more enriched stable water isotope composition, compared to discharge springs which show a more depleted stable water isotope composition. The enrichment of stable water isotopes at outcrop springs also indicates that evaporation plays a control in concentrating salts mobilised during runoff at these spring sites.

Based on the stable water isotope data, the discharge springs and C-H sandstone groundwater in the southeastern GAB have values corresponding to diffuse recharge. Previous studies by Priestley (2018) have reported groundwater recharge at the western GAB and compared the isotopic signatures of groundwater in the recharge zone. They recognised that groundwater infiltrated by diffuse recharge is characterised by $\delta^{18}O$ values above -6.8‰, whereas groundwater from localised recharge sources at the eastern GAB, $\delta^{18}O$ values of approximately 90% of depleted $\delta^{18}O$ values, typically below -9.3‰.

The discharge spring Boongunyarra, however, had three samples collected from the same vent and conversely has a greater variety in the distribution of δ^2H and $\delta^{18}O$ ratios. This is likely to be a result of the water matrix across the three sampling periods having varied amounts of diffuse recharge from runoff compared to GAB groundwater. The nature of the spring site, being at the lowest point in the landscape on a clay pan set, would enhance the diffuse recharge to the springs as runoff and throughflow would migrate to the lowest point in the landscape where this spring lies.

These stable water isotope results also indicate that the discharge springs have a degree of sensitivity to evaporation and the influence of localised groundwater recharge processes, which confirms that the springs can be vulnerable to potential climate change impacts. The vulnerability of discharge springs due to evaporation which has been enhanced by climate change is a contemporary issue discussed by many researchers, such as de Graaf *et al.* (2019) who discussed where and when the environmentally critical flow will be reached because of climate change and groundwater pumping. The ^{14}C activity measurements in this study also show there are signals of “younger” water in some spring water which reflects (#1) the influence of rainwater in the spring sample water matrix from rainfall events leading up to the field sampling campaigns, and (#2) some contributions of localised recharge at springs, particularly in the centre of the study area where there are also faults and lineament zones. Geoscience Australia (2013) has described areas of localised GAB aquifer recharge in the southwestern GAB, which supports the interpretation in statement #2.

The ^{14}C of dissolved inorganic carbon cross plots show there are two distinct groupings between GAB dominant water type springs and runoff and shallow/Paleogene to Neogene aquifer-dominated water-type springs. The runoff and shallow/Paleogene to Neogene aquifer-dominated water types fall within the range of 92 to 103 pMC, which is similar to the modern atmospheric ^{14}C content of 100 pMC. GAB bores consistently plot in the low range ^{14}C, generally <1.5 pMC. Peery also plotted consistent pMC values in radiocarbon grouped with GAB dominant water type 2.5 to 4.2 pMC for the three sampling events. By contrast, Boongunyarra plots variably within the GAB 15.9, 35.1 and 93.5 pMC, indicating that the effect of rainfall leading up to the sampling period can affect tracer results. These results are comparable with the western GAB groundwater ^{14}C activities reported by (S. C. Priestley et al., 2019), where low-range (<3pMC) across most of the western regions, whereas several samples between the south-west and southern margin have a wide range of 14C activities (2–90 pMC) which were close to rivers.

The geological basin appears to be a control in the salinity and major ion chemistry of waters associated with the C-H sandstone flow through. The major ion graphs for most springs and bores that exist in the Surat Basin have chloride concentrations generally below 200 mg/L for most springs and bores. Whereas Bingewilpa spring and the bores (i.e., GW004634, GW030963) in the vicinity of this spring have elevated chloride concentrations (generally 500 to 1400 mg/L) and some elevated major ions (Na^+, K^+) and dissolved metals (Sr^{2+}) which are situated on the west side of the Eromanga Basin Bulloo Embayment-Tibooburra Ridge junction (Figure 9 to Figure 19). The long flow paths and time the groundwater is in contact with the rock within the geological basins can contribute to salinity processes with mineral dissolution. The PHREEQC SI modelling shows that some minerals in saturation can contribute dissolved ions to the groundwater, particularly Jarosite-K which has the highest SI across all spring sites.

Flows at the discharge springs are primarily controlled by the artesian pressure from the hydraulic head gradient in the C-H Sandstone aquifer (elevated at around 230 mAHD at the eastern recharge area to 80 mAHD to the west). Consistent with several spring investigations on Australia’s GAB (Commonwealth of Australia, 2014a; Keegan-Treloar et al., 2022) and the world (i.e., United States (NRC, 2010; Egger, Glen, and McPhee, 2014)), the major controls on water expressing at discharge springs is the local and regional hydraulic gradients.

Of the springs that were sampled over three field campaigns, there was some variation in the chemistry which reflects the influence of rainfall mixing with GAB groundwater for discharge springs that exist in lower-lying areas of the landscape. For example, Boongunyarra spring is a discharge spring that has physical, chemical and stable water isotopic signatures quite similar to GAB groundwater samples, however, ^{14}C activity was elevated in two samples compared to the C-H Sandstone groundwater, which reflects the mixing of the GAB groundwater with modern water table of the Paleogene to Neogene units. The variations of rainfall before each sampling event reflect the occurrence of seasonal recharge to these springs, which are in a low-lying claypan that receives local catchment drainage. The low flow rate at the spring also enables mixing, probably in the hyperopic zone where local catchment runoff drains.

The ^{14}C crossplots show that Colless plots towards GAB-type water, however, the ^{14}C residence time is up to around 6,500 years and indicates the water source at this spring may be associated with the local GAB recharge zone. Fensham *et al.* (2020) and Golders (2022) have previously associated Colless with outcrop springs typology.

Boongunyarra also ^{14}C residence times up to 14,700 years. This suggests that the localised recharge zone in the central southeastern GAB where there are basement highs potentially influences the southwestern Eromanga discharge spring water. Given that the residence times for other springs, such as Peery, is 47,000 years, and the distance to the nearest local recharge zone is ~250 km in the direction of flow, the flow rate could be interpreted to be approximately 5 m/day. Similarly, given the 70 km distance of Boongunyarra from the local recharge zone, residence times up to 14,700 years, the flow rate could be approximated to be 4.6 m/day. There is, however, the potential for the addition of ^{14}C in the spring, such as from the exchange of CO_2, which can be a limitation.

For potential secondary sources of water to springs, the ^{36}Cl data indicates that some springs located along the Walgett Lineament zone and the Yanda Creek Lineament zone have a modern groundwater contribution. Notably, springs within this general vicinity contained a percent modern carbon range from 92 to 103% (Cumborah, Lila, Coonbilly, Youltoo, Cowgrial, Tooloomi, Gooroomeroo, Coolabah, Native Dog, Youngerina and Nulty).

The lack of Paleogene to Neogene aquifer end-member, however, limits the interpretation of subsurface processes utilising groundwater from this aquifer because water samples cannot be directly compared. Whilst there may be limited ways to address this, the limitation will always be present without that data. Process argument is therefore strongest where endmember samples are present and processes can therefore be directly inferred. Sampling of Paleogene to Neogene aquifer end members are therefore recommended for future investigation of outcrop springs. Further end-member sampling from other aquifers and rainfall is recommended to address this knowledge gap.

5.2 Conceptual hydrogeological model development

The development of a hydrogeological conceptual model aims to provide the science that will ultimately underpin effective groundwater management. Using the results of the various geochemical tracers, a conceptual hydrogeological model of the regional spring setting and groundwater flow was developed (Figure 29). This study identifies two broad types of natural active springs that emanate from the GAB spring sediments; discharge (artesian) springs and outcrop springs. There are also bore-fed springs, where landholders have drilled bores into spring sites that have free-flowing artesian bores, and inactive (dry) spring sites. The following section identifies where these spring sites fit into the four spring-type groups described and discusses conceptual hydrogeological understandings used in the development of the model.

Overall, the springs can be categorised into four spring-type groups. These are:

- Discharge springs: Peery, Boongunyarra, Sweetwater, Tego, Towry, Log, Lake Eliza, Colless and Thooro.
- Outcrop springs: Cumborah, Lila, Coonbilly, Youltoo, Cowgrial, Tooloomi, Gooroomeroo, Coolabah, Native Dog, Youngerina and Nulty.
- Bore fed springs: Bingewilpa, Wapweela, Muleyo, Hawkes,
- Inactive springs: Kulluna, Yantabulla, Goonery, Wee Wattah, Sandy, Jacomb.

The potentiometric surface from the recharge area at the eastern margins of the Cadna-Owie and Hooray Sandstone aquifer is sufficient to provide flow to the discharge springs to the west (Figure 6). Flow rates from the recharge area to the spring natural discharge point are the superposition of long flow paths and long timescales, between 30,000 to 50,000 years for most discharge springs (Figure 27). On the other hand, outcrop springs consist of modern water (Figure 27) and are likely to be associated with short-term pulse-type events due to aquifer head changes following local rainfall (Criss, 2010).

The model shows the relationship between hydraulic pathways from the C-H sandstone aquifer leakage through the Rolling Downs aquitard via faults predominantly in the Walgett, Cunnamulla and Paroo Lineament zones to discharge springs. Polygonal faulting previously identified by (Ransley et al., 2015) is expected to have played a significant role in the leakage from the C-H sandstone to the surface as discharge springs. Discharge springs that overlie the immediate vicinity of the lineament zones were active spring expressions (i.e., Peery, Boongunyarra, Lake Eliza, Thooro and Gerera) during the GAB spring field surveys in 2018 and 2019. This relationship is consistent with the review of key artesian spring characteristics by (Keegan-Treloar et al., 2022), and investigations of discharge springs in the western GAB by the National Water Commission (2013).

Some GAB spring sites in the vicinity of Cunnamulla and Paroo Lineament zones are inactive (i.e., Kulluna, Yantabulla) or are low-flow mud soaks (i.e. Lake Eliza). Some GAB springs are now the site for artesian bores (i.e., Muleyo, Hawkes, Wapweela and Bingewila). Peery spring was estimated to have over 300 spring vents from the 2018 and 2019 field investigations, which had highly varied flow rates from each spring expression. National Water Commission (2013) found that for western GAB springs, there are no predictable relationships between the hydraulic head differences and the rate of spring discharge suggesting the fault conductance was highly variable between springs. As the fault conductance is unknown in the southeastern GAB, which was also the case for the study by the National Water Commission (2013), it can be challenging to predict how spring discharge might vary in response to future changes in the aquifer hydraulic head. Furthermore, the lineament zones in the hydrogeological model (Figure 29) are inferred from the cross-section developed from a transect from the 3D hydrogeological (Geoscience Australia, 2016). This is a limitation of the hydrogeological model, further investigation into the depth and extent of the lineament zones is recommended.

There is no clear evidence of a deep aquifer source for the springs between the Yanda Creek Lineament and Walgett Lineament zones. A better understanding of the fault zones is an important component of understanding and developing models of the GAB springs. The stratigraphic model of the GAB in this area indicates that the springs in this area are underlain by up to around 250 m of Rolling Downs Group aquitard. Given there is no direct evidence for such a fault or fracture the possibility that the springs are outcrop springs gravity-fed by a meteoric source cannot be discounted. If this is the case, they may be emerging from unconformable contact with the surface of the Rolling Downs Group aquitard mudstone. This interpretation is consistent with a description of outcrop spring flow by Fensham et al. (2021), who describe this type of setting around the nearby Culgoa Lineament as a potential source for outcrop spring flow. The degree of connectivity of springs with underlying aquifers is partly influenced by fault networks, and mapping faults or the fracture network can be challenging at all scales, as their locations are not easy to predict. The conceptual model would benefit from improving the detail in mapping subsurface fracture systems, particularly with depth ranges of faults, and assessing their roles in facilitating or preventing the circulation of geothermal fluids.

There is an area of shallower granite that follows the line of the Sweetwater, Kullyna and Native Dog spring complexes. This may indicate an unmapped lineament or other structural feature related to the shallow basement. The University of Queensland (2014) noted in a spring profile report that these three springs are likely to be outcrop springs. Unfortunately, radiocarbon or other advanced tracer data was unable to be collected at Sweetwater and Kullyna for this current study, which makes it challenging to decipher the spring water type. Radiocarbon tracer data collected at Native Dog indicates this site is fed by modern rainfall and is outcrop spring typology.

Nulty and Scrubber springs are also associated with the Cenozoic sequence outcrop east of Enngonia and are assumed to emanate from the base of Cenozoic sequence sandstone where it contacts the top of the Rolling Downs Group confining. This translates the spring typology to be an outcrop characteristic spring. In an ecological assessment and hydrogeological assessment (with hydrochemistry limited to ions, pH, EC and TDS) of these springs Fensham *et al.* (2020) and Golders (2022) also characterised this spring as outcrop-type springs.

Extraction from bores was not measured in this study but can cause anomalies in the potentiometric surface. The significance of extraction from bores is the apparent cone shapes in the potentiometric surface and the impact of the direction of groundwater flow. This pattern in the potentiometric surface and flow direction is apparent in Figure 6.

The lack of recent head measurements, temperature and salinity data remains a limitation for the potentiometric surface. The lack of datum (survey height) data for water bores with recent head measurements meant that some recent data points were excluded from the potentiometric surface dataset (Table 9). Nonetheless, a comparison of Figure 6 with the previous, largely conceptual whole of the GAB groundwater flow map generated by Ransley et al. (2015) (refer to Map 10 in the *Hydrogeological Atlas of the GAB*) indicates the lack of data for correction does not compromise the interpretation of groundwater flow direction across the C-H sandstone aquifer.

It may be useful to examine the head differences between aquifers and seal characteristics of aquitards to get a sense of the direction of leakage (if pathways exist) and also to assess the seal characteristics of the intervening Rolling Downs Group clay aquitard. Potentiometric surfaces of two aquifers are overlain, and one is subtracted from the other. In areas where the head difference residual is less than ±10 m, the heads are assumed to be approximately equal. Conversely, where the head difference residual is larger than 10 m (i.e. a value less than –10 m or a value greater than +10 m), this indicates areas where significant pressure differences exist between the two aquifers. Such a condition is interpreted as indicating areas where the intervening aquitard may be acting as a tight seal or where inter-aquifer leakage is negligible (Love *et al.*, 2013).

The inferred flow lines in the potentiometric surface map for this study confirm that regional groundwater within the C-H sandstone is driven by pressure heads. There are two major flow systems interpreted from the flow lines: a westward and a northward flow system. This is consistent with the generalised flow paths presented in the GAB Atlas (Ransley et al., 2015).

This work highlights that individual GAB spring systems, while broadly similar in setting, are strongly influenced by local hydrological and geological controls (fault zones and localised runoff catchment areas), and each GAB spring requires detailed characterisation to achieve a comprehensive conceptual model. The additional sites for which there was no hydrogeological survey before this study (including Bingewilpa, Thooro Mud and numerous discharge spring vents) further highlight the novelty of the hydrogeological investigations disseminated from this project.

5.3 Conceptual model

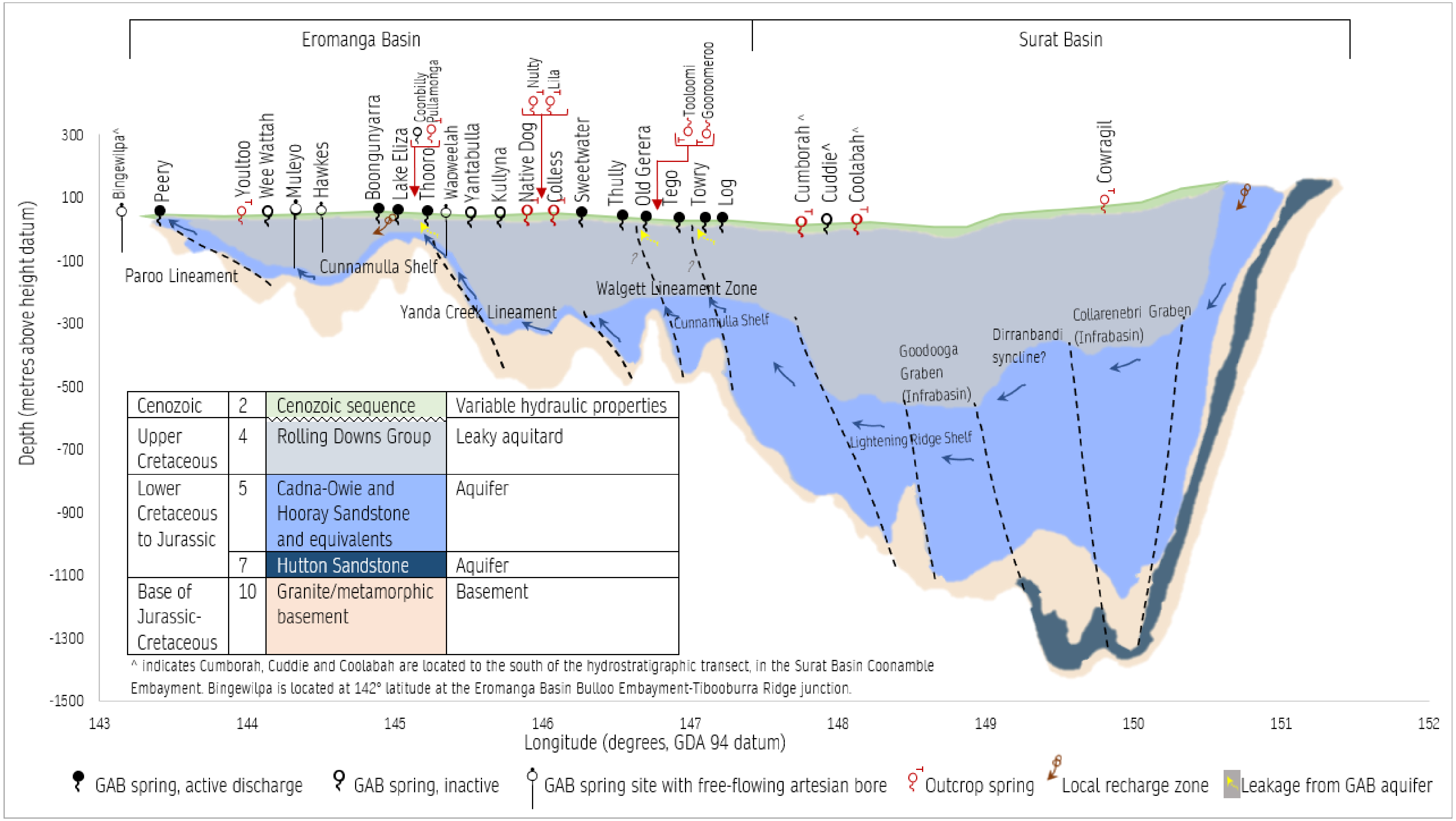

Figure 29. Hydrogeological diagram of the southeastern portion of the GAB with springs and symbolised flow status. Dashed lines and symbols represent an inferred fault (Geoscience Australia, 2022; Scheibner & Basden, 1998). Inset table: Corresponding regional hydrogeological stratigraphy showing age and hydraulic properties of units relevant to the Bourke and Eulo supergroups. The layer numbers in the stratigraphic model (Geoscience Australia, 2022) are indicated on the left.

6. CONCLUSION

Australia is not immune to the challenge posed by declining groundwater resources. As the artesian pressure in the GAB has declined due to anthropogenic impacts and climate change, many of the artesian springs have shown declining flow rates and, in some instances, ceased to flow altogether. Whilst several works have been undertaken in the western and northern GAB, this study has addressed a knowledge gap in the hydrogeological understanding of the southeastern GAB.

Of the 38 springs in the 600 km^2 study area, there were four main spring groups. This includes GAB springs, outcrop springs, springs with bores sunk into them and inactive spring sites. Only 9 were active with natural GAB flows. The study findings also showed that water emanating from the GAB springs is up to 30,000 years old, are generally fresh (EC up to 1,500 µS/cm) and overall has a similar hydrogeochemical fingerprint to the C-H sandstone aquifer. Added complexities have been teased out, with the mixing of water from different aquifers, localised GAB recharge systems and that the discharge springs are proximate to either faults or the GAB boundary. Also, compared to these GAB springs, there were outcrop springs that looked like they belonged with the GAB, however, these are gravity fed through Paleogene to Neogene unit outcrops and have water chemistry akin to rainfall and runoff. The environmental tracers show that the water is young, flows reflect this as they are dependent on recent rain, or rains in the preceding few years.

The outcomes from this study provide key baseline data and information for future monitoring campaigns. Follow-up surveys are recommended to check the discharge status and collect additional samples to improve the baseline dataset. Comparative datasets in time can help identify the change in GAB springs' condition and assist in groundwater resource assessments. Recommended analytes for follow-up monitoring campaigns include sampling for major ions, dissolved metals, radiocarbon isotopes and stable water isotopes. Monitoring the potentiometric surface is also important to evaluate the rise or decline in the artesian pressure of the C-H sandstone aquifer that feeds the GAB spring. An improvement of the endmember library for future works is also recommended, which should to include more potential aquifers as mentioned in this report, as well as better understanding of the relationship to faulting.

Future hydrogeochemical assessment of GAB springs is recommended as it can help deduce the degree of benefits of initiatives to reduce GAB water wastage, such as the federally funded Cap and Pipe program, where the management of free-flowing water is aimed at restoring GAB artesian pressures. This may result in increased spring discharge or recommencement of flow from current dry springs. The degree of impacts to springs from existing and future GAB bore extraction of groundwater should also be considered, as interference with artesian flows can impact spring expressions. The conceptual hydrogeological model coupled with the key baseline data that has emerged from this study should be considered for incorporation into future hydrogeochemical assessments of the GAB springs.

7. BIBLIOGRAPHY

Arthington, A. H., Rossini, R. A., Flook, S. C., Jackson, S. E., Tomlinson, M., & Walton, C. S. (2020). Springs of the Great Artesian Basin. *Proceedings of the Royal Society of Queensland*, *126*, 334. http://www.royalsocietyqld.org/2020-springs-special-issue-vol-126/

Bailey, James W. Hornbeck,: Charles T. Driscoll, and H. E. G. (1996). Calcium inputs and transport in a base-poor forest ecosystem as interpreted by Sr isotopes. *WATER RESOURCES RESEARCH, VOL.*, *32*(3), 707–719.

Baublys, K. A., Hamilton, S. K., Hofmann, H., & Golding, S. D. (2019). A strontium (87Sr/86Sr) isotopic study on the chemical evolution and migration of groundwaters in a low-rank coal seam gas reservoir (Surat Basin, Australia). *Applied Geochemistry*, *101*(2019), 1–18. https://doi.org/10.1016/j.apgeochem.2018.12.020

Beckett, J., & Hercus, L. (2016). The Two Rainbow Serpents Travelling - Geographical names in the Two Ngatyi stories. *ANU Press*.

Beta Analytic. (2023). Groundwater Radiocarbon Dating – Concept and Practical Application. *Website Cited 17 September 2023*, *Miami, Flo*. https://www.radiocarbon.com/groundwater-carbon-dating.htm

Brake, L., Harris, C., Jensen, A., Keppel, M., & Lewis, S. (2020). *Great Artesian Basin Springs: a Plan for the Future*. *January*.

Cantonati, M., Fensham, R. J., Stevens, L. E., Gerecke, R., Glazier, D. S., Goldscheider, N., Knight, R. L., Richardson, J. S., Springer, A. E., & Tockner, K. (2021). Urgent plea for global protection of springs. *Conservation Biology*, *35*(1), 378–382. https://doi.org/10.1111/cobi.13576

Commission National Water. (2013). *Groundwater Recharge, Hydrodynamics and Hydrochemistry in the Western GAB: Vol. VI*.

Commonwealth of Australia. (2014a). *Aquifer connectivity within the Great Artesian Basin , and the Surat , Bowen and Galilee Basins*. *June*.

Commonwealth of Australia. (2014b). *Ecological and hydrogeological survey of the Great Artesian Basin springs - Springsure, Eulo, Bourke and Bogan River supergroups Volume 1*.

Criss, R. E. (2010). A darcian model for the flow of big spring and the hydraulic head in the ozark aquifer, Missouri, USA. *Acta Carsologica*, *39*(2), 379–387. https://doi.org/10.3986/ac.v39i2.106

CSIRO. (2018). *The Great Artesian Basin and Coal Seam Gas*. *5 July 2018*.

Currell, M. J., & Katz, B. G. (2022). Threats to Springs in a Changing World : Science and Policies for Protection. *Book, Library of Congress*.

de Graaf, I. E. M., Gleeson, T., (Rens) van Beek, L. P. H., Sutanudjaja, E. H., & Bierkens, M. F. P. (2019). Environmental flow limits to global groundwater pumping. *Nature*, *574*(7776), 90–94. https://doi.org/10.1038/s41586-019-1594-4

Dupuy, M., Garel, E., Huneau, F., Santoni, S., Di Rosa, M., & Mattei, A. (2021). Geochemical and isotope characterisation of thermo-mineral springs of corsica island: From geological complexity to groundwater singularity. *Water (Switzerland)*, *13*(17). https://doi.org/10.3390/w13172413

Fensham, R. J., Doyle, T., Habermehl, M. A., Laffineur, B., & Silcock, J. L. (2021). Hydrogeological assessment of springs in the south-central Great Artesian Basin of Australia. *Hydrogeology Journal*, *29*(4), 1501–1515. https://doi.org/10.1007/s10040-021-02335-x

Flook, S., Fawcett, J., Cox, R., Pandey, S., Schöning, G., Khor, J., Singh, D., Suckow, A., & Raiber, M. (2020). A multidisciplinary approach to the hydrological conceptualisation of springs in the Surat Basin of the Great Artesian Basin (Australia). *Hydrogeology Journal*, 219–236. https://doi.org/10.1007/s10040-019-02099-5

Fu, G., Zou, Y., Crosbie, R. S., & Barron, O. (2019). Climate changes and variability in the Great Artesian Basin (Australia), future projections, and implications for groundwater management. *Hydrogeology Journal*, 375–391. https://doi.org/10.1007/s10040-019-02059-z

Geoscience Australia. (2013). *Great Artesian Basin major geological structural elements*. 50.

Geoscience Australia. (2016). Three-dimensional visualisation of the Great Artesian Basin. *Geoscience Australia 3D Data Viewer*, *catalogue*(produced by the Great Artesian Basin Water Resource Assessment (GABWRA)), software tool.

Geoscience Australia. (2022). *Great Artesian Basin geological and hydrogeological surfaces update: report and data package*. *eCat ID 14*.

Geoscience Australia. (2023a). Great Artesian Basin. *Website Cited 29 January 2023*.

Geoscience Australia. (2023b). Stratigraphic Unit Details: Cadna-owie Formation. *Australian Stratigraphy Database, Website Cited 15 February 2023*. https://doi.org/10.1007/978-981-13-2538-0_2349

Geospatial Australia Pty Ltd. (2021a). *GAB bores within 50km radium of springs (GABS_MS50km_LABRESULTS_2018_2019)*. on behalf of New South Wales Department of Planning, Industry and Environment. Unpublished MS Excel spreadsheet.

Geospatial Australia Pty Ltd. (2021b). *GAB bores within 50km radium of springs (GABS_MS50km_LABRESULTS_2018_2019)*. on behalf of New South Wales Department of Planning, Industry and Environment. Unpublished MS Excel spreadsheet.

Geospatial Australia Pty Ltd. (2022). *List of GAB bores surveyed Round 1 2018 and Round 2 2019* (p. Microsoft Excel Spreadsheet dataset). unpublished.

Golders. (2021). *Great Artesian Basin Springs Conceptualisation in NSW*. *August*.

Government Queensland. (2018). *Springs database*. Open Data Portal.

Gray, C. M. (1978). Geochronology of granulite-facies gneisses in the western musgrave block, central Australia. *Journal of the Geological Society of Australia*, *25*(7–8), 403–414. https://doi.org/10.1080/00167617808729050

Green, G. P., Bestland, E. A., & Walker, G. S. (2004). Distinguishing sources of base cations in irrigated and natural soils: Evidence from strontium isotopes. *Biogeochemistry*, *68*(2), 199–225. https://doi.org/10.1023/B:BIOG.0000025743.34079.d3

Habermehl, M. (1982). *Springs in the Great Artesian Basin, Australia - Their origin and nature*. *Report 235*(Bureau of Mineral Resources Geology and Geophysics).

Habermehl, M. A. (1980). The Great Artesian Basin, Australia. *BMR Journal of Australian Geology & Geophysics*.

Habermehl, M. A. (2019). Review: The evolving understanding of the Great Artesian Basin (Australia), from discovery to current hydrogeological interpretations. *Hydrogeology Journal*, 13–36. https://doi.org/10.1007/s10040-019-02036-6

Hasegawa, T., Nakata, K., Mahara, Y., Habermehl, M. A., Oyama, T., & Higashihara, T. (2016). Characterization of a diffusion-dominant system using chloride and chlorine isotopes (36Cl, 37Cl) for the confining layer of the Great Artesian Basin, Australia. *Geochimica et Cosmochimica Acta*, *192*, 279–294. https://doi.org/10.1016/j.gca.2016.08.002

Hayes, P., Nicol, C., La Croix, A. D., Pearce, J., Gonzalez, S., Wang, J., Harfoush, A., He, J., Moser, A., Helm, L., Morris, R., & Gornall, D. (2019). Enhancing geological and hydrogeological understanding of the Precipice Sandstone aquifer of the Surat Basin, Great Artesian Basin, Australia, through model inversion of managed aquifer recharge datasets. *Hydrogeology Journal*, 175–192. https://doi.org/10.1007/s10040-019-02079-9

Herczeg, A. L., & Love, A. J. (2007). Review of Recharge Mechanisms for the Great Artesian Basin. *Water*, *November*.

Herczeg, A. L., Torgersen, T., Chivas, A. R., & Habermehl, M. A. (1991). Geochemistry of ground waters from the Great Artesian Basin, Australia. *Journal of Hydrology*, *126*(3–4), 225–245. https://doi.org/10.1016/0022-1694(91)90158-E

Independent Expert Scientific Committee. (2018). *Bioregional Assessment Program*.

International Association of Hydrogeologists Australia. (2020). Advances in hydrogeologic understanding of Australia ' s Great Artesian Basin. *Hydrogeology Journal*, *28:01*.

International Atomic Energy Agency. (2018). *Australian Global Network of Isotope in Precipitation (GNIP) database 1960-2014* (p. MS Excel dataset).

Jankowski, J., & Ian Acworth, R. (1997). Impact of debris-flow deposits on hydrogeochemical processes and the development of dryland salinity in the Yass River Catchment, New South Wales, Australia. In *Hydrogeology Journal* (Vol. 5, Issue 4, pp. 71–88). https://doi.org/10.1007/s100400050119

Jones, C., Stanton, D., Hamer, N., Denner, S., Singh, K., Flook, S., & Dyring, M. (2019). Field investigation of potential terrestrial groundwater-dependent ecosystems within Australia's Great Artesian Basin. *Hydrogeology Journal*, 237–261. https://doi.org/10.1007/s10040-019-02081-1

Katz, B. G., & Currell, M. J. (2022). *Towards a Collective Effort to Preserve and Protect Springs*. 209–212. https://doi.org/10.1002/9781119818625.ch15

Keegan-Treloar, R., Irvine, D. J., Solórzano-Rivas, S. C., Werner, A. D., Banks, E. W., & Currell, M. J. (2022). Fault-controlled springs: A review. *Earth-Science Reviews*, *230*(April). https://doi.org/10.1016/j.earscirev.2022.104058

Kendall, C., & Doctor, D. H. (2003). Stable Isotope Applications in Hydrologic Studies. *Treatise on Geochemistry*, *5.11*, 319–364. https://doi.org/10.1016/j.jamda.2016.01.002

Kent, C. R., Pandey, S., Turner, N., Dickinson, C. G., & Jamieson, M. (2019). Estimating current and historical groundwater abstraction from the Great Artesian Basin and other regional-scale aquifers in Queensland, Australia. *Hydrogeology Journal*, 393–412. https://doi.org/10.1007/s10040-019-02074-0

Keppel, M., Karlstrom, K., Crossey, L., Love, A., & Priestley, S. (2019). Evidence for intra-plate seismicity from spring-carbonate mound springs in the Kati Thanda–Lake Eyre region, South Australia: implications for groundwater discharge from the Great Artesian Basin. *Hydrogeology Journal*, 297–311. https://doi.org/10.1007/s10040-019-02049-1

Keppel, M., Karlstrom, K., Love, A., Priestley, S., Wohling, D., & De Ritter, S. (2013). *Allocating Water and Maintaining Springs in the Great Artesian Basin: Hydrogeological Framework of the Western Great Artesian Basin: Vol. I*.

Klorn Crippen Berger. (2018a). NSW GAB Bore Integrity Assessment (Draft). *Technical Assessment*.

Klorn Crippen Berger. (2018b). *NSW GAB Bore Integrity Assessment (Final)*. *Table 2*.

Kottek, M., Grieser, J., Beck, C., Rudolf, B., & Rubel, F. (2006). World map of the Köppen-Geiger climate classification updated. *Meteorologische Zeitschrift*, *15*(3), 259–263. https://doi.org/10.1127/0941-2948/2006/0130

Mahara, Y., Habermehl, M. A., Hasegawa, T., Nakata, K., Ransley, T. R., Hatano, T., Mizuochi, Y., Kobayashi, H., Ninomiya, A., Senior, B. R., Yasuda, H., & Ohta, T. (2009). Groundwater dating by estimation of groundwater flow velocity and dissolved 4He accumulation rate calibrated by 36Cl in the Great Artesian Basin, Australia. *Earth and Planetary Science Letters*, *287*(1–2), 43–56. https://doi.org/10.1016/j.epsl.2009.07.034

Matic, V., Costelloe, J. F., & Western, A. W. (2020). An integrated remote-sensing mapping method for groundwater dependent ecosystems associated with diffuse discharge in the Great Artesian Basin, Australia. *Hydrogeology Journal*, 325–342. https://doi.org/10.1007/s10040-019-02062-4

Miles, C., White, M., & Scholz, G. (2012). *Assessment of the impacts of future climate and groundwater development on Great Artesian Basin springs A technical report to the Australian Government from the CSIRO Great Artesian Basin Water Resource Assessment*. *December*, 68.

Moggridge, B. J. (2020). Aboriginal people and groundwater. *Proceedings of the Royal Society of Queensland*, *126*, 11–27. https://doi.org/10.5962/p.357835

Moya, C. E. (2015). H Ydrostratigraphic and Hydrochemical Characterisation of Aquifers , Aquitards and Coal Seams in the G Alilee and E Romanga Basins , Central Q Ueensland , a Ustralia. *Thesis for Degree of Doctor of Philosophy*, *Queensland University of Technology*.

Moya, C. E., Raiber, M., Taulis, M., & Cox, M. E. (2015). Hydrochemical evolution and groundwater flow processes in the galilee and eromanga basins, great artesian Basin, Australia: A multivariate statistical approach. *Science of the Total Environment*, *508*, 411–426. https://doi.org/10.1016/j.scitotenv.2014.11.099

Moya, C. E., Raiber, M., Taulis, M., & Cox, M. E. (2016). Using environmental isotopes and dissolved methane concentrations to constrain hydrochemical processes and inter-aquifer mixing in the Galilee and Eromanga Basins, Great Artesian Basin, Australia. *Journal of Hydrology*, *539*, 304–318. https://doi.org/10.1016/j.jhydrol.2016.05.016

Mudd, G. M. (2000). Mound springs of the Great Artesian Basin in South Australia: A case study from Olympic Dam. *Environmental Geology*, *39*(5), 463–476. https://doi.org/10.1007/s002540050452

National Ground Water Association. (2023a). Confined or Artesian Groundwater. *Website*.

National Ground Water Association. (2023b). Springs. *Website Cited 15 September 2023*, *Groundwate*. https://www.ngwa.org/what-is-groundwater/About-groundwater/springs

National Research Council. (2010). Management and Effects of Coalbed Methane Produced Water in the Western United States. In *Management and Effects of Coalbed Methane Produced Water in the Western United States*. The National Academies Press. https://doi.org/10.17226/12915

National Water Commission. (2013). *Groundwater Recharge , Hydrodynamics and Hydrochemistry: Vol. II* (A. Love, D. Wohling, S. Fulton, P. Rousseau-Gueutin, & S. De Ritter, Eds.). Commonwealth of Australia, National Water Commission.

Negus, P. M. (2020). *Girt by dirt: The ecology of spring ecosystems in north-eastern Australia*.

New South Wales Government. (2020). Groundwater Resource Description - NSW Great Artesian Basin Groundwater Sources. *WATER SHARING PLAN FOR THE NSW GREAT ARTESIAN BASIN GROUNDWATER SOURCES*, 1–39.

NSW Department of Planning Industry and Environment. (2019). *Cap & Pipe the Bores Program*. *June*.

Ordens, C. M., McIntyre, N., Underschultz, J. R., Ransley, T., Moore, C., & Mallants, D. (2020). Preface: Advances in hydrogeologic understanding of Australia's Great Artesian Basin. *Hydrogeology Journal*, *28*(1), 1–11. https://doi.org/10.1007/s10040-019-02107-8

Pandey, S., Singh, D., Denner, S., Cox, R., Herbert, S. J., Dickinson, C., Gallagher, M., Foster, L., Cairns, B., & Gossmann, S. (2019). Inter-aquifer connectivity between Australia's Great Artesian Basin and the overlying Condamine Alluvium: an assessment and its implications for the basin's groundwater management. *Hydrogeology Journal*, 125–146. https://doi.org/10.1007/s10040-019-02089-7

Parkhurst, D. L., & Appelo, C. A. J. (2013). PHREEQC (Version 3)-A Computer Program for Speciation, Batch-Reaction, One-Dimensional Transport, and Inverse Geochemical Calculations. *Modeling Techniques, Book 6*, 497.

Perez, K. E., Ponder, W. F., Colgan, D. J., Clark, S. A., & Lydeard, C. (2005). Molecular phylogeny and biogeography of spring-associated hydrobiid snails of the Great Artesian Basin, Australia. *Molecular Phylogenetics and Evolution*, *34*(3), 545–556. https://doi.org/10.1016/j.ympev.2004.11.020

Pickard, J. (1992). *Artesian Springs in the Western Division of New South Wales* (p. 128). Maquaried University.

Powell, O., Silcock, J., & Fensham, R. (2015). Oases to Oblivion: The Rapid Demise of Springs in the South-Eastern Great Artesian Basin, Australia. *Groundwater*, *53*(1), 171–178. https://doi.org/10.1111/gwat.12147

Priestley, S. (2018). *Inter-aquifer connectivity : investigating groundwater movement through a regional- scale aquitard using a multi- scale and multi-tracer approach by*. *May*.

Priestley, S. C., Shand, P., Love, A. J., Crossey, L. J., Karlstrom, K. E., Keppel, M. N., Wohling, D. L., & Rousseau-Gueutin, P. (2019). Hydrochemical variations of groundwater and spring discharge of the western Great Artesian Basin, Australia: implications for regional groundwater flow. *Hydrogeology Journal*, 263–278. https://doi.org/10.1007/s10040-019-02071-3

Queensland Herbarium. (2015). *Queensland Spring Database*. Department of Science Information Technology and Innovation.

Queensland Herbarium. (2017). *196_TEGO*.

Fensham R, W. Ponder, R. F. (2010b). Recovery plan for the community of native species dependent on natural discharge of groundwater from the Great Artesian Basin. *Report to Department of the Environment, Water, Heritage and the Arts, Canberra. Queensland Department of Environment and Resource Management, Brisbane*, 1–41. http://espace.library.uq.edu.au/view/UQ:177715%5Cnpapers2://publication/uuid/E0408F0C-C4AE-4CC3-855D-D23CFF2CDFDA

Radke, B., & Ransley, T. (2019). Connectivity between Australia's Great Artesian Basin, underlying basins, and the Cenozoic cover. *Hydrogeology Journal*, 43–56. https://doi.org/10.1007/s10040-019-02075-z

Ransley, T. R., Radke, B. M., Feitz, A. J., Kellett, J. R., Owens, R., Bell, J., Stewart, G., & Carey, H. (2015). Hydrogeological Atlas of the Great Artesian Basin. In *Hydrogeological Atlas of the Great Artesian Basin*. Commonwealth of Australia, Geoscience Australia. https://doi.org/10.11636/9781925124668

Ransley, T. R., & Smerdon, B. D. (2012). *Hydrostratigraphy, hydrogeology and system conceptualisation of the Great Artesian Basin. A technical report to the Australian Government from the CSIRO Great Artesian Basin Water Resource Assessment. December*.

Richey, A. S., Thomas, B. F., Lo, M. H., Reager, J. T., Famiglietti, J. S., Voss, K., Swenson, S., & Rodell, M. (2015). Quantifying renewable groundwater stress with GRACE. *Water Resources Research*, *51*(7), 5217–5237. https://doi.org/10.1002/2015WR017349

Risha, U. A. A., Clark, I., Beecham, S., Author, C., Boulevard, M. L., & Lakes, M. (2009). *Evaluation of Groundwater Flow and Travel Times 1 . Introduction and General Background*. 1349–1362.

Sandiford, M., Lawrie, K., & Brodie, R. S. (2019). Hydrogeological implications of active tectonics in the Great Artesian Basin, Australia. *Hydrogeology Journal*, 57–73. https://doi.org/10.1007/s10040-019-02046-4

Scheibner, E., & Basden, H. (ed). (1998). Geology of New South Wales - Synthesis Volume 1 Structural Framework. *Memoirs - Geology*, *1*(13), 295.

Shand, P., Darbyshire, D. P. F., Love, A. J., & Edmunds, W. M. (2009). Sr isotopes in natural waters: Applications to source characterisation and water-rock interaction in contrasting landscapes. *Applied Geochemistry*, *24*(4), 574–586. https://doi.org/10.1016/j.apgeochem.2008.12.011

Smerdon, B. D., Ransley, T. R., Radke, B. M., & Kellett, J. R. (2012). *Water resource assessment for the Great Artesian Basin*. *December*.

Sreekanth, J., Crosbie, R., Pickett, T., Cui, T., Peeters, L., Slatter, E., Northey, J., Merrin, L. E., Davies, P., Miotlinski, K., Schmid, W., & Herr, A. (2019a). Regional-scale modelling and predictive uncertainty analysis of cumulative groundwater impacts from coal seam gas and coal mining developments. *Hydrogeology Journal*, 193–218. https://doi.org/10.1007/s10040-019-02087-9

Sreekanth, J., Crosbie, R., Pickett, T., Cui, T., Peeters, L., Slatter, E., Northey, J., Merrin, L. E., Davies, P., Miotlinski, K., Schmid, W., & Herr, A. (2019b). Regional-scale modelling and predictive uncertainty analysis of cumulative groundwater impacts from coal seam gas and coal mining developments. *Hydrogeology Journal*, 193–218. https://doi.org/10.1007/s10040-019-02087-9

Stuiver, M., & Polach, H. A. (1977). Groundwater Radiocarbon Dating – Concept and Practical Application. *Website Cited 17 September 2023*, *19*(3), 355–363. https://doi.org/10.1016/j.forsciint.2010.11.013

Suckow, A., Deslandes, A., Raiber, M., Taylor, A. R., Davies, P., Gerber, C., & Leaney, F. (2019). Reconciling contradictory environmental tracer ages in multi-tracer studies to characterize the aquifer and quantify deep groundwater flow: an example from the Hutton Sandstone, Great Artesian Basin, Australia. *Hydrogeology Journal*, *36*, 75–87. https://doi.org/10.1007/s10040-019-02042-8

Sundaram, B., Feitz, J. A., Caritat, D. P., APlazinska, A., Brodie, S. R., Coram, J., Ransley, T., & Geosicence Australia. (2010). *Groundwater Sampling and Analysis - A Field Guide*.

Taylor, A. R., Pichler, M. M., Olifent, V., Thompson, J., Bestland, E., Davies, P. J., Lamontagne, S., Suckow, A., Robinson, N., Love, A., & Munday, T. (2015). *Groundwater Flow Systems of North-eastern Eyre Peninsula (G-FLOWS Stage-2): Hydrogeology, geophysics and environmental tracers*. *15*.

The MathWorks Inc. (2021). MATLAB® R2021b - academic use. *MATLAB® Computer Program*, *MathWorks*.

The University of Queensland. (2014). *Final Report Volume 2 – Hydrogeological profiles of Great Artesian Basin springs ; Springsure , Eulo , Bourke and Bogan River supergroups*. *2*(April), 267.

Thompson, J. E. (2019). *DOC19 51177 Great Artesian Basin Springs Survey Site Selection Methodology*.

Thompson, J., Rumpf, C., Coleman, D., Bowen, S., & Haeusler, T. (2021). *Hydrogeology and ecology survey of the Great Artesian Basin springs in New South Wales - Results and site descriptions* (Issue August). NSW Department of Planning, Industry and Environment dpie.nsw.gov.au.

https://water.dpie.nsw.gov.au/__data/assets/pdf_file/0011/482897/hydrogeology-and-ecology-survey.pdf

Viljoen, R., Pinder, B., Mukherjee, S., & Herbert, S. J. (2020). Hydrogeological implications of fault behaviour from in situ pressure measurements of the Horrane Fault in the Surat Basin (Great Artesian Basin, Australia). *Hydrogeology Journal*, 161–174. https://doi.org/10.1007/s10040-019-02093-x

Wallace, L., & Ransley, T. (2022). *Assessing the Status of Groundwater in the Great Artesian Basin Summary Report* (Record 202). Geoscience Australia.

Wang, W., Fan, Y., Li, K., Wang, X., & Kang, J. (2022). Challenges of Spring Protection and Groundwater Development in Urban Subway Construction: A Case Study in the Jinan Karst Area, China. *Water (Switzerland)*, *14*(9). https://doi.org/10.3390/w14091521

Wolaver, B. D., Priestley, S. C., Crossey, L. J., Karlstrom, K. E., & Love, A. J. (2019). Elucidating sources to aridland Dalhousie Springs in the Great Artesian Basin (Australia) to inform conservation. *Hydrogeology Journal*, 279–296. https://doi.org/10.1007/s10040-019-02072-2

Yang, J., Liu, H., Tang, Z., Peeters, L., & Ye, M. (2022). Visualization of Aqueous Geochemical Data Using Python and WQChartPy. *Groundwater*, *March*. https://doi.org/10.1111/gwat.13185

Zhang, M., Frape, S. K., Love, A. J., Herczeg, A. L., Lehmann, B. E., Beyerle, U., & Purtschert, R. (2007). Chlorine stable isotope studies of old groundwater, southwestern Great Artesian Basin, Australia. *Applied Geochemistry*, *22*(3), 557–574. https://doi.org/10.1016/j.apgeochem.2006.12.004

Appendix A – Hydrostratigraphy

Table 3. Hydrostratigraphic sequence of the Eromanga, Carpentaira Surat and Clarence-Moreton basins (Ransley and Smerdon, 2012)

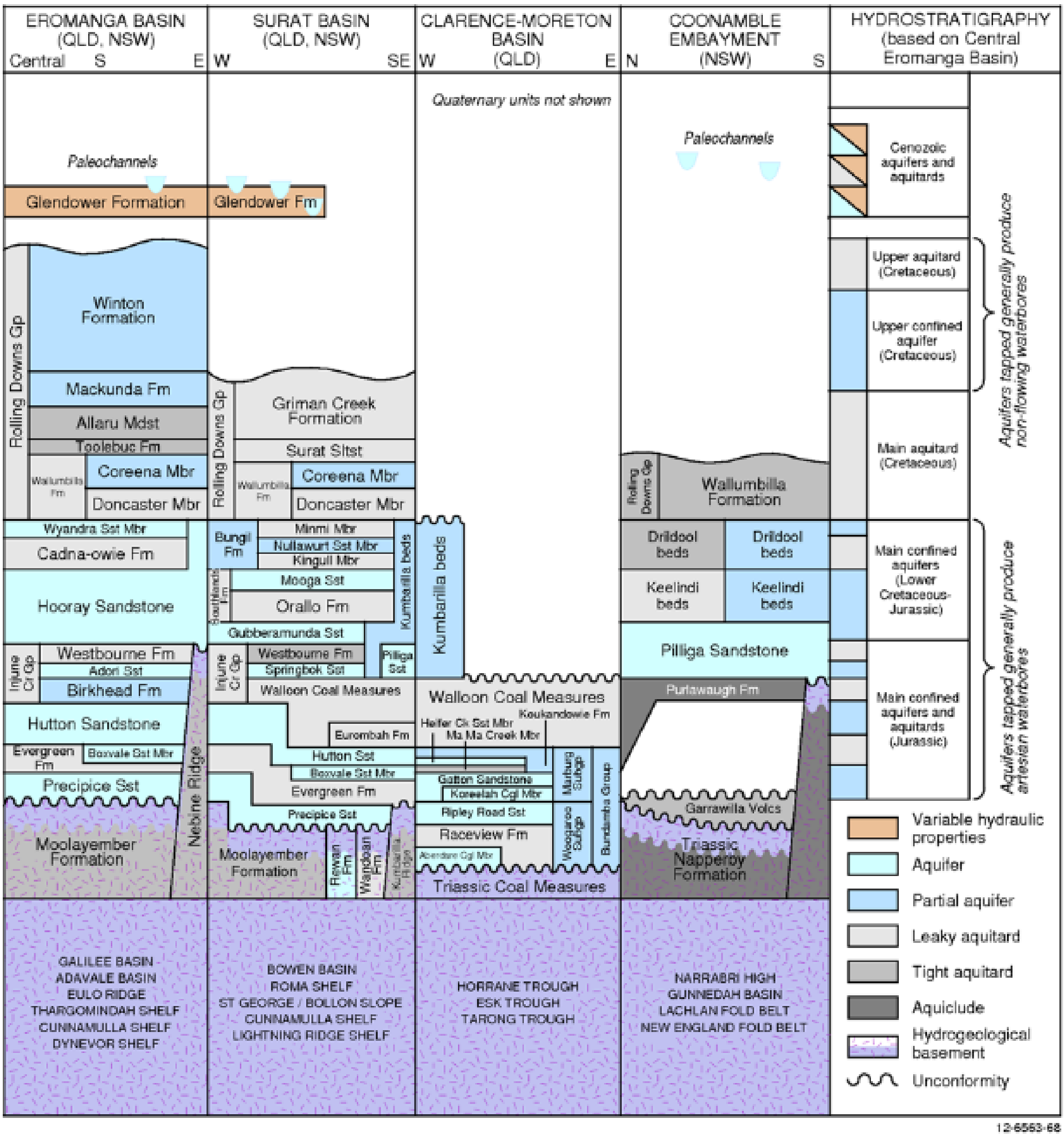

Figure 4.4 Hydrostratigraphic sequence of the Eromanga,Carpentaira Surat and Clarence-Moreton basins
[Note: this figure is reproduced at a larger scale in the compendium of A3 figures as A3 Figure 9]

Appendix B – Hydrochemistry datasets

Dataset notes for this section (Table 3 to Table 8):

- Name[a] indicates data obtained from (Queensland Herbarium, 2017),
- Name[b] indicates bore data from Geospatial Australia (2019), and
- dash (-) indicates no spring vent identification number (ID) assigned to site.

Table 4. Electrical conductivity, pH and total dissolved solids data for springs, bores, and rainfall in the south-eastern GAB study area.

Name	pH as pH units	Conductivity as SPC µS/cm	TDS mg/L
Tego[a]	-	-	1650
Gooroomero	7.5	890	570
Gerara	8.3	940	602
Old Gerara	6.8	480	307
Thooro Mud	9.2	1100	704
Colless	7.2	730	467
Boongunyarrah	7.7	1000	640
Boongunyarrah	8.3	940	602
Boongunyarrah	8.7	770	493
Native Dog	7.7	150	96
Youngerina	8.4	660	422
Coonbilly	7.0	520	333
Lila	6.6	43	28
Lila	6.6	33	21
Thully	7.6	250	160
Thully	7.8	280	179
Thully	7.9	2100	1344
Cumborah	7.2	560	358
Cumborah	7.2	570	365
Cumborah	7.3	640	410
Youltoo	6.8	120	77
Peery	7.2	1783	1141
Peery	8.0	960	614
Peery	8.6	1461	935
Peery West[a]	8.3	1500	960
Peery West[a]	7.6	6000	3840
Peery West[a]	7.5	2550	1632
Peery West[a]	7.4	2890	1850
Peery West[a]	7.5	750	480
Peery West[a]	7.0	2250	1440
Peery West[a]	7.8	2620	1677
Peery West[a]	8.6	2780	1779
Peery West[a]	8.0	2750	1760
Peery West[a]	9.5	2787	1784
Peery West[a]	9.2	2690	1722

Name	pH as pH units	Conductivity as SPC µS/cm	TDS mg/L
Peery West[a]	7.8	2740	1754
Peery West[a]	7.9	2585	1654
Peery West[a]	8.8	4840	3098
Peery West[a]	7.9	3130	2003
Peery West[a]	7.7	2110	1350
Peery East 7[a]	8.9	7310	4678
Scrubber	7.2	730	467
Coolabah	6.4	170	109
Wapweelah	8.3	940	602
Bingewilpa	7.6	6000	3840
Muleyo	7.9	1600	1024
Tharnowanni	8.5	460	294
Runoff (Hungerford_Road)	6.3	88	56
Rainfall	7.0	89	57
Seawater (South West Rocks)	8.1	48000	30720
Seawater (South West Rocks)	8.1	48000	30720
16783A	8.4	880	563
GW004339	7.5	1100	704
GW003823	7.9	750	480
GW004666	8.3	1000	640
GW010786	8.3	970	621
GW011260	8.4	980	627
GW040866	7.2	1700	1088
GW010756	8.3	730	467
GW004047	8.5	890	570
GW012285	7.5	820	525
GW004705	8.4	910	582
GW008253	8.0	1300	832
GW004659	8.3	730	467
GW012246	8.0	780	499
GW004591	8.5	970	621
GW004267	7.9	1600	1024
GW004262	8.6	1200	768
GW004262	8.6	1200	768
GW004602	8.8	1200	768
GW004619	8.6	1000	640
GW004677	8.7	1200	768
GW008339	8.5	1000	640
GW012483	8.6	1000	640
GW025018	8.7	1200	768
GW039438	8.7	1300	832
GW001648	8.6	1100	704
GW004469	8.1	730	467

Name	pH as pH units	Conductivity as SPC µS/cm	TDS mg/L
GW008045	8.2	570	365
GW012135	8.7	1100	704
GW021037	8.6	1100	704
GW064371	8.6	1100	704
GW004117	8.5	1000	640
GW004118	8.5	1200	768
GW004173	8.6	980	627
GW004205	8.7	1100	704
GW004205_control	8.7	1100	704
GW010433	8.6	1000	640
GW004300	8.7	960	614
GW004733	8.8	1100	704
GW004753	8.6	1200	768
GW008035	8.7	1300	832
GW021322	8.6	1300	832
GW021322_control	8.6	1300	832
GW014672	8.4	960	614
GW039377	8.7	900	576
GW039445	8.7	810	518
GW003761	8.6	1100	704
GW027500	8.4	1000	640
GW027500	8.4	1000	640
GW010441	8.3	2500	1600
GW012310	8.6	1100	704
GW021414	8.7	1200	768
GW038300	8.6	1100	704
GW014627	8.6	1100	704
GW004367	8.7	1100	704
GW001346	8.5	1100	704
GW001551	8.4	1100	704
GW004125	8.5	970	621
GW004165	7.4	620	397
GW004311	8.5	1100	704
GW004374	8.3	1300	832
GW008351	8.5	1100	704
GW010608	8.0	1000	640
GW012177	8.6	1200	768
GW012259	8.5	1100	704
GW039435	8.4	1400	896
GW039504	7.4	630	403
GW039584	8.8	1200	768
GW273148	8.6	1300	832
GW003333	7.6	12000	7680

Name	pH as pH units	Conductivity as SPC µS/cm	TDS mg/L
GW003627	7.8	1600	1024
GW004035	8.5	1100	704
GW004311	8.5	1100	704
GW004505	7.7	1200	768
GW004506	7.8	1300	832
GW004634	7.5	4800	3072
GW030963	7.4	3600	2304
GW030963_control	7.4	3600	2304
GW039505	7.3	2700	1728
GW273269	8.5	1100	704
GW004536	8.0	950	608
GW007251	7.0	7000	4480
GW014564	8.2	1000	640
GW014992	7.9	1500	960
GW020109	8.4	1100	704
GW965066	8.4	1500	960
GW004215	8.4	950	608
GW004303	8.3	960	614
GW004432	8.1	1100	704
GW004558	8.5	870	557
GW041048	8.4	880	563
GW273060	8.4	970	621
GW273061	8.4	950	608
GW273270	8.3	1100	704
GW004119	8.5	930	595
GW004295	8.3	970	621
GW004719	8.3	1100	704
GW010491	8.4	980	627
GW010491_duplicate	8.4	980	627
GW011136	8.4	980	627
GW012121	8.6	1200	768
GW021603	8.6	1200	768
GW030868	8.6	970	621
GW004659	8.5	730	467
GW007210	8.5	780	499
GW008053	8.4	770	493
GW008449	8.5	820	525
GW011266	8.5	890	570
GW004252	8.4	1200	768
GW025066	8.5	1100	704
GW004048	8.3	830	531
GW004048	8.3	830	531
GW004049	8.3	1100	704

Name	pH as pH units	Conductivity as SPC µS/cm	TDS mg/L
GW004281	8.5	870	557
GW004344	8.3	890	570
GW004663	8.4	940	602
GW011115	8.4	730	467
GW011334	8.5	820	525
GW012246	8.4	790	506
GW019483	8.4	700	448
GW021766	8.6	1100	704
GW004046	8.3	780	499
GW004690	8.3	720	461
GW008253	8.4	1000	640
GW010070	8.4	900	576
GW014998	8.4	940	602
GW012047	8.3	1200	768
GW004152	8.1	1700	1088
GW004700	8.0	3300	2112
GW019111	8.2	1700	1088
GW003436	8.7	910	582
GW003734	8.4	1000	640
GW004371	8.4	920	589
GW004426	8.4	860	550
GW004370	8.4	810	518
GW003408	8.5	860	550
GW004502	8.5	1300	832
GW004445	8.5	1000	640
GW003860	8.4	1200	768
GW004751	8.5	1000	640
GW004519	8.5	740	474
GW003139	8.3	1200	768
GW003290	8.3	1200	768
GW004441	7.9	1000	640
GW004591	7.9	950	608
GW008442	8.3	1400	896
GW012499	8.4	1200	768
GW018764	7.1	890	570
GW008052	8.6	1200	768
GW014588	8.2	960	614
GW014722	8.5	1200	768
GW015757	8.2	1100	704
GW018041	8.3	1100	704
GW021144	8.2	970	621
GW021190	8.2	1000	640
GW021220	8.1	910	582

Name	pH as pH units	Conductivity as SPC µS/cm	TDS mg/L
GW003419	8.3	1200	768
GW004000	8.4	1400	896
GW004043	8.2	1100	704
GW004214	8.3	1000	640
GW004492	7.9	850	544
GW004675	8.1	1200	768
GW004757	8.3	1100	704
GW007181	8.3	1400	896
GW012094	8.3	760	486
GW013140	8.1	750	480
GW014675	8.4	930	595
GW022754	8.2	1000	640
GW004014	8.1	740	474
GW004580	8.4	1300	832
GW010523	8.2	830	531
GW010905	8.0	2000	1280
GW011271	8.3	820	525
GW003529	7.9	1600	1024
GW003529	7.9	1600	1024
GW003695	8.0	1400	896
GW004718	7.2	16000	10240
GW004741	8.2	870	557
GW004779	7.2	14000	8960
GW012852	8.3	1100	704
GW014537	8.1	2400	1536
GW014488	8.4	1200	768
GW014764	8.4	1000	640
GW029101	8.0	1500	960
GW004039	8.5	1100	704
GW004039	8.5	1100	704
GW004042	8.6	1100	704
GW004076	8.6	1100	704
GW004107	8.6	990	634
GW004290	8.4	1100	704
GW004642	8.4	1000	640
GW008162	8.6	1200	768
GW008404	8.6	1000	640
GW012298	8.6	1200	768
GW039439	8.4	1300	832
GW004034	8.4	960	614
GW004541	8.2	910	582
GW039313	8.4	920	589
GW039313	8.4	920	589

Table 5. Major ions and metals data for springs, bores, and rainfall in the south-eastern GAB study area.

	Major ions (mg/L)												Metals (µg/L, dissolved)													
Name	Calcium	Potassium	Sodium	Magnesium	Total hardness	Hydroxide Alkalinity	Bicarbonate Alkalinity	Carbonate Alkalinity	Total Alkalinity	Sulphate	Chloride	Ionic Balance (%)	Aluminium	Arsenic	Cadmium	Chromium	Copper	Iron	Lithium	Lead	Manganese	Mercury	Nickel	Silver	Strontium	Zinc
Springs and surface water samples																										
Tego[a]	3	46	9	397	7.1	-	-	-	-	-	-	-	-	-	-	-	-	-	-	-	-	-	-	-	-	-
Tego[a]	5	12	7	510	5.3		-	-	-	-	-	-	-	-	-	-	-	-	-	-	-	-	-	-	-	-
Tego[a]	6	6	8.7	720	2.2	23	-	-	1437	-	-	-	-	-	-	-	-	-	-	-	-	-	-	-	-	-
Gooroomero	4	14	180	2.1	19	5	170	5	170	1	150	4	20	1	0.1	1	1	1200	9	1	83	0.05	1	1	27	10
Old Gerara	2	12	89	1.2	9	5	94	5	94	7	95	-4	100	4	0.1	1	1	59	3	1	5	0.05	1	1	17	2
Thooro Mud	3	4	230	0.5	6.3	5	410	72	490	1	88	-10	60	1	0.1	1	1	53	15	1	5	0.05	1	1	26	1
Colless	4	10	180	5.5	32	5	280	5	280	8	66	7	10	1	0.1	1	1	240	7	1	9	0.05	1	1	110	1
MotherNosey	8	13	210	5.3	41	5	480	5	480	1	92	-8	50	2	0.1	1	1	21	10	1	12	0.05	1	1	250	3
MotherNosey	5	8	190	3.2	27	5	440	5	440	1	82	-10	20	1	0.1	1	1	14	10	1	7	0.05	1	1	160	1
MotherNosey	18	12	130	6.1	71	5	410	28	430	1	25	-11	40	2	0.1	1	2	10	15	1	5	0.05	27	1	520	2
Native Dog	7	3	19	1.1	22	5	77	5	77	1	3	-11	5100	2	0.1	6	4	3400	6	2	30	0.05	2	1	77	9
Youngerina	61	7	54	17	220	5	350	9	360	1	15	-4	620	4	0.1	1	3	310	11	1	61	0.05	60	1	1000	9
Coonbilly	20	5	100	5.1	70	5	270	5	270	1	20	-2	2000	5	0.1	1	3	1200	6	1	130	0.05	3	1	240	8
Lila	1	6	4.4	0.5	3	5	15	5	15	1	3	-4	10	1	0.1	1	3	120	2	1	8	0.05	1	1	10	4
Lila	1	4	2.4	0.5	3	5	14	5	14	1	1	-14	1200	1	0.1	1	6	540	2	1	5	0.05	2	1	12	23
Thully	5	4	50	1.1	16	5	99	5	99	3	25	-3	680	3	0.1	1	4	370	2	1	5	0.05	2	1	44	1
Thully	8	4	36	2	28	5	140	5	140	2	13	-19	1500	3	0.1	1	12	670	3	1	8	0.05	3	1	71	21
Thully	14	10	390	8.3	70	5	210	5	210	47	500	-1	20000	8	0.1	35	37	17000	28	9	250	0.05	23	1	190	66
Cumborah	9	10	63	17	92	5	83	5	83	26	80	4	10	1	0.1	1	1	22	3	1	6	0.05	2	1	210	2
Cumborah(CONTROL)	9	10	63	17	92	-	-	-	-	-	-	-	-	-	-	-	-	-	-	-	-	-	-	-	-	-
Cumborah	10	15	64	22	110	5	61	5	61	36	100	6	10	1	0.1	1	1	10	3	1	5	0.05	2	1	250	11
Youltoo	3	5	11	1.1	11	5	36	5	36	12	5	-14	1800	1	0.1	1	6	810	2	1	8	0.05	1	1	24	4
Peery	8	7	360	2.2	28	5	720	5	720	1	170	-8	100	1	0.1	1	1	65	78	1	5	0.05	1	1	300	3
Peery (CONTROL)	8	5	370	1.4	24	5	720	5	720	1	110	-2	10	1	0.1	1	1	10	69	1	5	0.05	1	1	320	2
Peery	8	6	540	1.9	29	5	720	5	720	1	150	13	10	1	0.1	1	2	29	65	1	6	0.05	1	1	310	2
Peery (CONTROL)	8	6	540	1.9	28	5	690	14	700	1	150	14	10	1	0.1	1	1	21	64	1	7	0.05	1	1	290	1
Peery	24	16	1200	11	110	<5	740	<5	740	<1	1400	0	<10	1	<0.1	<1	<1	170	360	<1	<5	<0.05	<1	<1	2300	1
Scrubber	4	10	180	5.5	32	<5	280	<5	280	8	66	7	10	1	0.1	1	8	490	3	1	38	0.05	4	1	11	3
Coolabah	1	8	30	0.7	6	5	60	5	60	4	20	-6	10	1	0.1	1	8	490	3	1	38	0.05	4	1	11	3
Wapweelah	3	2	220	0.5	8	5	450	24	480	1	57	-7	10	1	0.1	1	1	220	14	1	12	0.05	1	1	79	3
Bingewilpa	24	16	1200	11	110	5	730	5	730	1	1400	-1	10	1	0.1	1	1	170	360	1	5	0.05	1	1	2300	1
Muleyo	8	4	390	1.9	29	5	560	5	560	1	200	2	10	1	0.1	1	1	300	29	1	5	0.05	1	1	230	1
Tharnowanni	13	7	120	4.9	52	5	180	16	190	25	32	9	10	14	0.1	1	5	10	1	1	5	0.05	2	1	150	1

	Major ions (mg/L)												Metals (µg/L, dissolved)													
Name	Calcium	Potassium	Sodium	Magnesium	Total hardness	Hydroxide Alkalinity	Bicarbonate Alkalinity	Carbonate Alkalinity	Total Alkalinity	Sulphate	Chloride	Ionic Balance (%)	Aluminium	Arsenic	Cadmium	Chromium	Copper	Iron	Lithium	Lead	Manganese	Mercury	Nickel	Silver	Strontium	Zinc
Runoff	7	7	3.5	4.1	35	5	53	5	53	1	1	-1	40	1	0.1	1	1	250	3	1	17	0.05	1	1	86	2
Rainfall	12	3	3	1.3	35	5	32	5	32	4	2	7	10	1	0.1	1	2	10	1	1	36	0.05	1	1	80	31
Seawater	390	440	12000	1400	6700	5	120	5	120	2500	19000		10	1	0.1	1	1	10	200	1	5	0.05	1	1	7400	1
											Bores															
16783A	2	2	210	0.5	4	5	390	25	420	1	67	-6	20	1	0.1	1	1	16	13	1	5	0.05	1	1	41	2
GW004339	11	4	210	1.6	34	5	290	5	290	1	190	-5	10	1	0.1	1	1	130	19	1	57	0.05	1	1	150	4
GW003823	4	2	170	0.5	9	5	330	5	330	1	66	-6	20	1	0.1	1	1	81	10	1	6	0.05	1	1	39	1
GW004666	5	3	300	1.8	21	5	480	5	480	4	63	9	10	1	0.1	1	1	29	28	1	5	0.05	1	1	150	2
GW010786	4	2	280	1.2	15	5	460	5	460	2	59	7	10	2	0.1	1	1	120	15	1	8	0.05	1	1	110	1
GW011260	5	2	290	0.5	12	5	450	7	460	1	56	8	10	3	0.1	1	1	37	11	1	6	0.05	1	1	79	16
GW040866	71	15	220	45	360	5	270	5	270	140	330	-2	10	1	0.1	1	1	9500	4	1	320	0.05	1	1	810	8
GW010756	7	2	210	0.5	17	5	300	5	310	1	67	9	10	1	0.1	1	1	240	16	1	6	0.05	1	1	120	1
GW004047	2	2	210	0.7	9	5	320	30	350	1	87	0	10	1	0.1	1	1	31	11	1	5	0.05	1	1	56	1
GW012285	4	2	240	0.5	10	5	370	5	370	1	56	7	10	2	0.1	1	1	69	13	1	7	0.05	1	1	130	1
GW004705	5	3	230	2.2	21	5	300	33	340	1	110	3	10	1	0.1	1	1	61	6	1	14	0.05	1	1	77	1
GW008253	6	3	330	0.5	15	5	370	5	370	1	220	4	10	1	0.1	1	1	530	10	1	11	0.05	1	1	110	3
GW004659	2	2	190	0.5	6	5	330	5	330	1	59	1	10	1	0.1	1	1	220	5	1	5	0.05	1	1	47	2
GW012246	5	2	210	0.5	12	5	360	5	360	1	63	2	10	1	0.1	1	1	78	8	1	6	0.05	1	1	98	1
GW004591	4	2	200	0.5	11	5	430	12	440	1	63	-9	10	1	0.1	1	1	97	15	1	9	0.05	1	1	81	1
GW004267	8	4	380	1.9	28	5	560	5	560	1	200	1	10	1	0.1	1	1	180	28	1	5	0.05	1	1	230	2
GW004262	4	1	340	0.5	10	5	490	23	510	1	110	5	10	1	0.1	1	1	73	15	1	5	0.05	1	1	73	4
GW004262	4	1	340	0.5	10	5	490	23	510	1	110	6	0	0	0	0	0	0	0	0	0	0	0	0	0	0
GW004602	2	2	330	0.5	4	5	510	40	550	1	65	7	10	1	0.1	1	1	15	11	1	5	0.05	1	1	62	1
GW004619	5	4	270	0.8	14	5	470	19	490	26	29	4	10	2	0.1	1	1	60	30	1	5	0.05	1	1	96	4
GW004677	2	2	330	0.5	5	5	540	35	580	1	58	5	10	1	0.1	1	1	21	10	1	6	0.05	1	1	58	1
GW008339	4	3	280	0.5	10	5	480	16	500	20	33	5	10	1	0.1	1	1	41	31	1	5	0.05	1	1	110	2
GW012483	4	4	280	0.8	14	5	480	22	510	25	30	5	10	2	0.1	1	1	260	27	1	5	0.05	1	1	130	2
GW025018	2	2	320	0.5	5	5	550	33	580	1	67	2	10	1	0.1	1	1	59	12	1	5	0.05	1	1	57	2
GW039438	2	3	380	0.5	5	5	650	36	680	1	53	5	10	1	0.1	1	1	45	39	1	5	0.05	1	1	100	11
GW001648	3	2	290	0.5	7	5	570	21	590	1	23	1	10	5	0.1	1	1	51	11	1	5	0.05	2	1	150	45
GW004469	10	9	160	2	33	5	380	5	380	4	17	-2	10	2	0.1	1	1	270	57	1	6	0.05	1	1	200	3
GW008045	9	8	120	2	32	5	320	5	320	1	9	-3	10	1	0.1	1	1	110	39	1	5	0.05	1	1	200	1
GW012135	2	2	290	0.5	6	5	520	27	550	1	60	0	10	1	0.1	1	1	57	20	1	5	0.05	1	1	120	5
GW021037	3	3	280	0.5	7	5	510	23	530	1	53	1	10	1	0.1	1	4	43	24	1	5	0.06	1	1	130	37
GW064371	3	2	290	0.5	7	5	510	24	540	1	61	2	10	1	0.1	1	1	80	19	1	5	0.05	1	1	150	3
GW004117	5	2	260	1	16	5	460	22	480	1	67	1	10	1	0.1	1	1	64	39	1	8	0.05	1	1	110	1
GW004118	7	2	310	2.8	28	5	470	22	490	1	130	2	10	1	0.1	1	1	170	16	1	5	0.05	1	1	180	4

	Major ions (mg/L)												Metals (µg/L, dissolved)													
Name	Calcium	Potassium	Sodium	Magnesium	Total hardness	Hydroxide Alkalinity	Bicarbonate Alkalinity	Carbonate Alkalinity	Total Alkalinity	Sulphate	Chloride	Ionic Balance (%)	Aluminium	Arsenic	Cadmium	Chromium	Copper	Iron	Lithium	Lead	Manganese	Mercury	Nickel	Silver	Strontium	Zinc
GW004173	5	2	250	0.7	16	5	440	24	460	1	66	1	10	1	0.1	1	1	95	26	1	6	0.05	1	1	87	2
GW004205	2	1	290	0.5	6	5	510	36	550	1	60	1	10	1	0.1	1	1	48	9	1	5	0.05	1	1	90	1
GW004205 (control)	3	1	290	0.5	6	5	510	36	540	1	61	1	10	1	0.1	1	1	48	9	1	5	0.05	1	1	91	1
GW010433	5	2	260	0.5	14	5	470	25	490	1	66	0	10	3	0.1	1	1	61	38	1	11	0.05	1	1	84	1
GW004300	4	2	250	0.5	10	5	430	33	460	1	60	1	10	1	0.1	1	1	31	11	1	6	0.05	1	1	94	1
GW004733	3	1	290	0.5	7	5	480	42	520	1	64	2	10	1	0.1	1	2	53	9	1	5	0.05	1	1	51	2
GW004753	3	3	340	1	12	5	590	29	620	1	57	3	10	1	0.1	1	1	37	13	1	5	0.05	1	1	150	1
GW008035	3	2	340	0.5	8	5	520	36	560	1	110	3	10	1	0.1	1	1	290	14	1	7	0.05	1	1	110	19
GW021322	3	3	370	0.5	9	5	640	35	670	1	59	4	10	1	0.1	1	1	79	35	1	5	0.05	1	1	150	1
GW021322 (control)	3	3	370	0.5	10	5	640	34	670	1	58	4	10	1	0.1	1	1	76	37	1	5	0.05	1	1	150	1
GW014672	6	2	230	0.6	16	5	430	17	450	1	64	-2	10	1	0.1	1	1	100	27	1	5	0.05	1	1	77	2
GW039377	3	2	220	0.5	7	5	390	31	420	1	61	-2	10	1	0.1	1	1	42	11	1	5	0.05	1	1	65	1
GW039445	4	2	200	0.5	9	5	340	32	370	1	59	-2	10	1	0.1	1	1	21	16	1	7	0.05	1	1	54	1
GW003761	3	2	280	0.5	7	5	510	31	540	1	61	0	10	1	0.1	1	1	50	21	1	5	0.05	1	1	69	1
GW027500	4	2	280	0.5	9	5	500	20	520	1	58	1	10	2	0.1	1	1	89	12	1	6	0.05	1	1	71	2
GW027500	4	2	280	0.5	9	5	520	20	540	1	58	0	0	0	0	0	0	0	0	0	0	0	0	0	0	0
GW010441	23	4	580	12	110	5	520	9	530	57	480	4	10	1	0.1	1	1	35	25	1	38	0.05	1	1	500	1
GW012310	4	2	290	0.5	9	5	500	33	540	1	65	1	10	1	0.1	1	1	59	19	1	5	0.05	1	1	73	1
GW021414	2	2	330	0.5	4	5	590	41	630	1	57	1	10	1	0.1	1	1	17	18	1	5	0.05	1	1	43	1
GW038300	3	2	320	0.5	7	5	590	28	620	1	55	0	10	2	0.1	1	1	150	24	1	5	0.05	1	1	63	1
GW014627	4	2	300	0.5	9	5	520	32	550	1	64	2	10	1	0.1	1	1	49	16	1	5	0.05	1	1	100	1
GW004367	2	2	290	0.5	4	5	520	36	560	1	59	0	10	1	0.1	1	1	26	16	1	6	0.05	1	1	45	1
GW001346	3	2	270	0.7	10	5	530	27	560	1	62	-3	10	2	0.1	1	1	77	15	1	5	0.05	1	1	150	3
GW001551	4	2	270	0.9	13	5	530	16	540	1	59	-3	10	1	0.1	1	1	63	11	1	5	0.05	1	1	150	1
GW004125	1	1	230	0.5	3	5	430	21	450	1	63	-3	10	1	0.1	1	1	23	13	1	5	0.05	1	1	45	1
GW004165	53	27	55	9.5	170	5	340	5	340	1	17	-5	10	1	0.1	1	1	3900	29	1	29	0.05	1	1	280	2
GW004311	3	2	280	0.6	9	5	540	27	560	1	59	-3	10	1	0.1	1	1	32	6	1	5	0.05	1	1	120	2
GW004374	5	4	300	2.7	23	5	660	21	680	1	49	-5	10	7	0.1	1	1	65	20	1	5	0.05	1	1	350	3
GW008351	3	2	270	0.5	9	5	540	24	570	1	56	-4	10	1	0.1	1	1	48	19	1	5	0.05	1	1	130	1
GW010608	10	10	240	2.5	35	5	540	5	540	17	26	-3	10	1	0.1	1	1	110	39	1	5	0.05	1	1	340	3
GW012177	2	2	290	0.6	8	5	580	31	610	1	56	-4	10	2	0.1	1	1	32	13	1	5	0.05	1	1	100	6
GW012259	3	2	260	0.5	8	5	500	26	530	1	61	-3	10	1	0.1	1	1	460	14	1	7	0.05	1	1	95	1
GW039435	4	3	330	0.6	12	5	680	24	710	1	56	-4	10	1	0.1	1	1	10	32	1	5	0.05	1	1	190	15
GW039504	58	28	55	8	180	5	340	5	340	8	10	-4	10	1	0.1	1	1	520	36	1	9	0.05	1	1	300	1
GW039584	1	1	290	0.5	3	5	580	46	630	1	55	-5	20	1	0.1	1	1	17	11	1	5	0.05	1	1	56	1
GW273148	5	3	280	2.4	23	5	540	32	570	1	89	-4	10	1	0.1	1	1	24	35	1	5	0.05	1	1	220	3
GW003333	170	19	2300	10	470	5	140	5	140	1	3800	1	10	1	0.1	1	1	990	590	1	280	0.05	2	1	10000	230

	Major ions (mg/L)												Metals (µg/L, dissolved)													
Name	Calcium	Potassium	Sodium	Magnesium	Total hardness	Hydroxide Alkalinity	Bicarbonate Alkalinity	Carbonate Alkalinity	Total Alkalinity	Sulphate	Chloride	Ionic Balance (%)	Aluminium	Arsenic	Cadmium	Chromium	Copper	Iron	Lithium	Lead	Manganese	Mercury	Nickel	Silver	Strontium	Zinc
GW003627	3	6	430	0.5	8	5	760	5	760	1	100	2	10	1	0.1	1	1	25	36	1	5	0.05	1	1	220	1
GW004035	3	2	290	0.5	6	5	500	28	530	1	58	2	10	1	0.1	1	1	26	8	1	5	0.05	1	1	110	1
GW004311	3	2	300	0.6	9	5	530	28	550	1	59	2	10	1	0.1	1	1	28	6	1	5	0.05	1	1	130	2
GW004505	3	7	300	0.5	8	5	510	5	510	1	73	4	10	1	0.1	1	1	24	25	1	13	0.05	1	1	150	1
GW004506	4	7	350	0.5	10	5	640	5	640	1	81	1	10	1	0.1	1	1	26	26	1	9	0.05	3	1	170	5
GW004634	18	15	1100	7	75	5	1000	5	1000	1	1000	1	10	2	0.1	1	1	140	720	1	5	0.05	1	1	2300	1
GW030963	17	21	930	2.2	50	5	1200	5	1200	1	540	4	10	1	0.1	1	1	30	370	1	6	0.05	1	1	1200	1
GW030963 (control)	17	21	930	2.2	50	5	1200	5	1200	1	540	4	10	1	0.1	1	1	30	370	1	7	0.05	1	1	1200	1
GW039505	9	18	740	1.5	28	5	1200	5	1200	1	210	4	10	1	0.1	1	1	140	320	1	9	0.1	1	1	580	6
GW273269	2	2	300	0.5	6	5	500	31	530	1	57	4	10	1	0.1	1	1	110	5	1	5	0.05	1	1	88	1
GW004536	4	2	230	0.5	10	5	480	5	480	1	60	-4	10	2	0.1	1	1	250	15	1	6	0.05	1	1	76	2
GW007251	95	12	1300	31	360	5	150	5	150	1	2300	-1	10	1	0.1	1	1	620	200	1	120	0.05	1	1	2100	24
GW014564	5	2	240	0.5	12	5	520	5	520	1	60	-7	10	1	0.1	1	1	62	18	1	7	0.05	1	1	83	2
GW014992	12	4	340	4.2	48	5	550	5	550	1	200	-2	10	3	0.1	1	1	130	62	1	10	0.05	1	1	350	6
GW020109	2	1	260	0.5	4	5	550	29	580	1	58	-7	10	1	0.1	1	1	35	11	1	5	0.05	1	1	50	1
GW965066	2	2	350	0.5	4	5	720	31	750	1	120	-8	10	1	0.1	1	1	18	15	1	5	0.05	1	1	110	2
GW004215	2	2	230	0.5	5	5	470	24	500	1	47	-6	10	1	0.1	1	1	37	13	1	5	0.05	1	1	76	1
GW004303	2	2	230	0.5	6	5	490	21	510	1	48	-7	10	1	0.1	1	1	120	13	1	5	0.05	1	1	71	1
GW004432	4	4	250	0.5	10	5	550	5	550	1	63	-7	10	1	0.1	1	1	18	22	1	8	0.05	1	1	160	1
GW004558	2	2	200	0.5	4	5	400	27	430	3	55	-6	10	1	0.1	1	1	58	10	1	8	0.05	1	1	51	3
GW041048	2	3	210	0.5	6	5	400	23	420	7	60	-6	10	1	0.1	1	1	65	11	1	10	0.05	1	1	88	1
GW273060	2	3	230	0.5	5	5	470	28	500	1	55	-6	10	1	0.1	1	1	72	12	1	11	0.05	1	1	72	1
GW273061	2	3	230	0.5	5	5	470	26	500	1	48	-4	10	1	0.1	1	1	52	12	1	9	0.05	1	1	75	1
GW273270	3	4	270	0.5	8	5	590	5	590	1	54	-6	10	1	0.1	1	1	90	23	1	5	0.05	1	1	140	1
GW004119	4	1	240	0.5	10	5	430	29	460	1	56	1	10	4	0.1	1	1	30	19	1	5	0.05	1	1	72	1
GW004295	4	2	260	0.5	12	5	500	5	500	1	53	0	10	3	0.1	1	1	86	23	1	5	0.05	1	1	120	1
GW004719	4	2	290	0.5	13	5	520	5	520	1	86	0	10	1	0.1	1	1	250	17	1	5	0.05	1	1	110	3
GW010491	5	2	260	0.5	13	5	470	25	500	1	57	0	10	11	0.1	1	1	130	22	1	6	0.05	1	1	80	3
GW010491 (duplicate)	5	2	260	0.5	13	5	470	26	490	1	57	0	10	11	0.1	1	1	130	23	1	6	0.05	1	1	81	1
GW011136	6	2	260	1.1	19	5	470	26	500	1	59	1	10	1	0.1	1	1	240	30	1	10	0.05	1	1	100	1
GW012121	3	2	300	0.5	6	5	570	38	600	1	58	-2	10	1	0.1	1	1	50	24	1	5	0.05	1	1	75	1
GW021603	3	2	300	0.5	6	5	580	40	620	1	66	-3	10	1	0.1	1	1	59	18	1	5	0.05	1	1	95	1
GW030868	3	2	240	0.5	9	5	450	33	480	1	56	-3	10	1	0.1	1	1	31	15	1	6	0.05	1	1	78	1
GW004659	2	2	180	0.5	5	5	310	25	330	1	53	1	10	1	0.1	1	1	76	5	1	5	0.05	1	1	49	1
GW007210	3	2	200	0.5	7	5	320	25	350	1	59	2	10	1	0.1	1	1	130	9	1	5	0.05	1	1	64	1
GW008053	3	2	190	0.5	7	5	320	23	340	1	57	2	10	1	0.1	1	1	34	10	1	5	0.05	1	1	72	1

	Major ions (mg/L)												Metals (µg/L, dissolved)													
Name	Calcium	Potassium	Sodium	Magnesium	Total hardness	Hydroxide Alkalinity	Bicarbonate Alkalinity	Carbonate Alkalinity	Total Alkalinity	Sulphate	Chloride	Ionic Balance (%)	Aluminium	Arsenic	Cadmium	Chromium	Copper	Iron	Lithium	Lead	Manganese	Mercury	Nickel	Silver	Strontium	Zinc
GW008449	3	2	210	0.5	7	5	360	29	390	1	53	1	10	1	0.1	1	1	45	13	1	8	0.05	1	1	93	1
GW011266	4	2	230	0.5	10	5	400	30	430	1	52	1	10	1	0.1	1	1	89	15	1	7	0.05	1	1	95	1
GW004252	5	2	260	0.5	13	5	470	27	490	1	120	-6	10	1	0.1	1	1	77	16	1	5	0.05	1	1	130	2
GW025066	5	2	260	0.5	13	5	460	29	490	1	81	-1	10	1	0.1	1	1	270	25	1	7	0.05	1	1	130	1
GW004048	5	2	210	0.5	11	5	390	5	390	1	59	-1	10	2	0.1	1	1	81	10	1	8	0.05	1	1	100	1
GW004048	5	2	210	0.5	11	5	380	5	380	1	58	0	10	2	0.1	1	1	78	10	1	8	0.05	1	1	100	1
GW004049	6	2	260	2.5	26	5	360	5	360	3	150	1	10	1	0.1	1	1	150	15	1	8	0.05	1	1	180	1
GW004281	3	2	220	0.5	9	5	360	27	380	1	68	0	10	1	0.1	1	1	94	8	1	7	0.05	1	1	72	1
GW004344	5	2	210	0.7	16	5	330	5	330	4	97	1	10	1	0.1	1	1	180	7	1	11	0.05	1	1	140	1
GW004663	4	2	230	0.5	9	5	370	22	390	1	87	0	10	1	0.1	1	1	120	16	1	5	0.05	1	1	100	1
GW011115	3	2	180	0.5	6	5	290	18	310	1	68	-1	10	1	0.1	1	1	78	5	1	5	0.05	1	1	53	1
GW011334	4	2	210	0.5	9	5	360	29	390	1	53	1	10	1	0.1	1	1	230	13	1	12	0.05	1	1	100	5
GW012246	5	2	200	0.5	12	5	350	19	370	1	58	0	10	1	0.1	1	1	79	9	1	6	0.05	1	1	100	1
GW019483	3	2	170	0.5	7	5	300	21	320	1	60	-3	10	1	0.1	1	1	110	3	1	7	0.05	1	1	50	1
GW021766	2	2	270	1	10	5	410	34	440	1	120	-1	10	1	0.1	1	1	130	14	1	5	0.05	1	1	75	2
GW004046	4	2	230	0.6	13	5	390	5	390	1	69	2	10	1	0.1	1	1	80	8	1	7	0.05	1	1	95	1
GW004690	6	1	210	0.5	14	5	300	5	300	1	65	8	10	1	0.1	1	1	110	6	1	6	0.05	1	1	44	1
GW008253	4	2	300	0.5	10	5	320	10	330	1	140	11	10	1	0.1	1	1	470	8	1	8	0.05	1	1	69	1
GW010070	5	2	270	0.5	13	5	400	12	420	1	64	9	10	1	0.1	1	1	86	14	1	10	0.05	1	1	98	1
GW014998	4	2	280	0.5	9	5	320	9	330	1	120	11	10	1	0.1	1	1	67	11	1	6	0.05	1	1	91	1
GW012047	5	3	340	0.7	16	5	420	5	420	1	130	10	10	6	0.1	1	1	110	85	1	6	0.05	1	1	72	1
GW004152	8	4	480	1.6	28	5	560	5	560	1	200	12	10	1	0.1	1	1	120	29	1	6	0.05	1	1	210	1
GW004700	20	7	860	13	100	5	550	5	550	1	690	13	10	1	0.1	1	1	170	56	1	5	0.05	1	1	670	1
GW019111	9	3	460	1.1	26	5	500	5	500	1	230	11	10	1	0.1	1	1	160	22	1	5	0.05	1	1	250	1
GW003436	2	2	280	0.5	5	5	390	30	420	1	62	10	10	1	0.1	1	1	170	9	1	5	0.05	1	1	65	1
GW003734	4	2	290	0.5	10	5	470	11	480	1	55	8	10	2	0.1	1	1	48	17	1	6	0.05	1	1	76	1
GW004371	4	2	270	0.5	10	5	410	15	430	1	51	9	10	1	0.1	1	1	100	14	1	5	0.05	1	1	97	1
GW004426	6	2	250	0.5	15	5	330	14	340	1	76	11	10	1	0.1	1	1	110	8	1	5	0.05	1	1	91	1
GW004370	4	2	240	0.5	10	5	340	13	350	1	60	11	10	1	0.1	1	1	110	8	1	7	0.05	1	1	76	1
GW003408	5	1	250	0.5	13	5	340	14	360	1	77	10	10	1	0.1	1	1	91	9	1	8	0.05	1	1	70	1
GW004502	3	3	380	3.3	21	5	460	17	480	1	140	11	10	1	0.1	1	1	97	13	1	5	0.05	1	1	45	1
GW004445	6	2	300	1	18	5	360	15	380	1	120	11	10	1	0.1	1	1	270	15	1	5	0.05	1	1	110	1
GW003860	8	2	330	1.2	26	5	440	13	460	1	110	10	10	1	0.1	1	1	160	22	1	13	0.05	1	1	170	1
GW004751	4	2	320	0.5	10	5	490	17	510	1	54	10	10	2	0.1	1	1	10	9	1	6	0.05	1	1	88	1
GW004519	3	1	220	0.5	7	5	290	14	310	1	60	11	10	1	0.1	1	1	32	4	1	5	0.05	1	1	41	1
GW003139	3	2	360	0.5	6	5	560	5	560	1	85	8	10	1	0.1	1	1	54	21	1	5	0.05	1	1	120	1
GW003290	2	2	350	0.5	6	5	570	19	590	1	58	7	10	1	0.1	1	1	17	17	1	5	0.05	1	1	100	1

	Major ions (mg/L)												Metals (µg/L, dissolved)													
Name	Calcium	Potassium	Sodium	Magnesium	Total hardness	Hydroxide Alkalinity	Bicarbonate Alkalinity	Carbonate Alkalinity	Total Alkalinity	Sulphate	Chloride	Ionic Balance (%)	Aluminium	Arsenic	Cadmium	Chromium	Copper	Iron	Lithium	Lead	Manganese	Mercury	Nickel	Silver	Strontium	Zinc
GW004441	4	3	310	0.8	12	5	550	5	550	1	35	7	10	1	0.1	1	1	110	45	1	5	0.05	1	1	160	3
GW004591	5	2	280	0.5	11	5	430	5	430	1	63	8	10	1	0.1	1	1	81	16	1	8	0.05	1	1	100	1
GW008442	3	2	390	0.5	8	5	530	19	550	1	130	9	10	1	0.1	1	1	42	18	1	5	0.05	1	1	94	1
GW012499	2	2	370	0.5	5	5	600	20	620	3	59	7	10	1	0.1	1	1	69	16	1	5	0.05	1	1	110	1
GW018764	29	22	200	8.4	110	5	460	5	460	18	22	5	10	2	0.1	1	1	1100	31	1	15	0.05	1	1	220	4
GW008052	3	1	370	0.5	7	5	510	31	540	2	160	3	10	1	0.1	1	1	220	12	1	7	0.05	1	1	75	1
GW008052	0	0	0	0	0	0	0	0	0	0	0	0	10	1	0.1	1	1	220	12	1	7	[NT]	1	1	76	1
GW014588	4	2	280	0.5	10	5	430	5	430	2	110	3	10	1	0.1	1	1	10	8	1	6	0.05	1	1	86	1
GW014722	2	2	360	0.5	6	5	530	25	550	1	110	5	10	1	0.1	1	1	70	18	1	5	0.05	1	1	74	1
GW015757	4	2	310	0.5	11	5	480	5	480	1	110	4	10	1	0.1	1	1	60	23	1	5	0.05	1	1	79	2
GW018041	3	2	340	0.5	8	5	540	5	540	1	110	4	10	1	0.1	1	1	90	16	1	6	0.05	1	1	99	1
GW021144	3	2	290	0.5	7	5	450	5	450	1	100	3	10	2	0.1	1	1	27	8	1	11	0.05	1	1	83	1
GW021190	4	2	310	0.5	10	5	470	5	470	1	110	4	10	1	0.1	1	1	230	15	1	8	0.05	1	1	100	1
GW021220	4	4	270	0.7	12	5	460	5	460	20	52	5	10	2	0.1	1	1	110	51	1	5	0.05	1	1	95	1
GW003419	3	2	370	0.5	7	5	530	16	550	1	120	6	10	1	0.1	1	1	49	22	1	5	0.05	1	1	120	1
GW004000	2	2	470	0.5	5	5	700	22	720	1	110	8	10	1	0.1	1	1	64	17	1	5	0.05	1	1	83	1
GW004043	5	2	320	0.7	15	5	490	5	490	1	130	4	10	2	0.1	1	1	170	15	1	5	0.05	1	1	88	1
GW004214	4	2	310	0.5	9	5	470	5	470	1	100	5	10	2	0.1	1	1	96	14	1	5	0.05	1	1	66	1
GW004492	7	6	250	1.3	22	5	420	5	420	17	45	6	10	1	0.1	1	1	67	60	1	5	0.05	1	1	140	1
GW004675	10	2	350	1.3	31	5	430	5	430	1	260	-1	10	3	0.1	1	1	100	21	1	21	0.05	1	1	270	1
GW004757	4	2	320	0.5	9	5	490	16	500	1	120	3	10	2	0.1	1	1	53	40	1	6	0.05	1	1	68	2
GW007181	7	2	400	1.1	23	5	480	14	490	5	310	-2	10	4	0.1	1	1	110	17	1	13	0.05	1	1	180	1
GW012094	2	2	220	0.5	4	5	330	5	330	1	53	10	10	2	0.1	1	1	130	9	1	10	0.05	1	1	49	1
GW013140	3	2	220	0.5	8	5	320	5	320	1	56	10	10	1	0.1	1	1	49	9	1	8	0.05	1	1	81	1
GW014675	3	1	280	0.5	8	5	400	12	410	1	53	12	10	1	0.1	1	1	46	14	1	5	0.05	1	1	69	1
GW022754	3	2	310	0.5	8	5	480	5	480	1	49	10	10	2	0.1	1	1	33	13	1	8	0.05	1	1	90	11
GW004014	3	2	220	0.5	7	5	310	5	310	1	59	12	10	1	0.1	1	1	43	8	1	10	0.05	1	1	74	1
GW004580	9	2	380	0.6	24	5	490	12	500	1	120	13	10	1	0.1	1	1	69	23	1	12	0.05	1	1	140	3
GW010523	4	2	240	0.5	10	5	340	5	340	1	66	10	10	1	0.1	1	1	140	6	1	7	0.05	1	1	59	1
GW010905	45	4	450	15	180	5	280	5	280	3	400	15	10	1	0.1	1	1	210	30	1	36	0.05	1	1	1200	1
GW011271	3	2	250	0.5	7	5	380	5	380	1	56	9	10	1	0.1	1	1	46	11	1	7	0.05	1	1	70	1
GW003529	5	6	540	0.5	12	5	780	5	780	1	94	14	10	1	0.1	1	1	34	40	1	5	0.05	1	1	210	1
GW003529	5	6	550	0.5	12	5	760	5	760	1	94	15	10	1	0.1	1	1	34	40	1	5	0.05	1	1	200	1
GW003695	9	3	420	3.9	39	5	460	5	460	1	170	16	10	2	0.1	1	1	210	30	1	9	0.05	1	1	300	13
GW004718	460	23	4000	140	1700	5	72	5	72	1	4600	23	10	1	0.1	1	1	1100	220	1	740	0.05	1	1	12000	1
GW004741	6	2	270	1.4	19	5	350	5	350	1	80	14	10	1	0.1	1	1	59	9	1	5	0.05	1	1	100	8
GW004779	390	16	3500	74	1300	5	74	5	74	1	3900	23	10	1	0.1	1	1	1200	220	1	550	0.05	1	1	8100	1

	Major ions (mg/L)												Metals (µg/L, dissolved)													
Name	Calcium	Potassium	Sodium	Magnesium	Total hardness	Hydroxide Alkalinity	Bicarbonate Alkalinity	Carbonate Alkalinity	Total Alkalinity	Sulphate	Chloride	Ionic Balance (%)	Aluminium	Arsenic	Cadmium	Chromium	Copper	Iron	Lithium	Lead	Manganese	Mercury	Nickel	Silver	Strontium	Zinc
GW012852	4	2	340	0.5	10	5	470	5	470	1	78	13	10	1	0.1	1	1	60	19	1	7	0.05	1	1	110	1
GW014537	26	4	670	9	100	5	310	5	310	3	510	20	10	1	0.1	1	1	460	27	1	23	0.05	1	1	520	1
GW014488	3	1	390	0.5	7	5	570	13	580	1	52	13	10	3	0.1	1	1	37	36	1	5	0.05	1	1	70	1
GW014764	4	1	320	0.5	9	5	430	13	450	1	68	13	10	1	0.1	1	1	21	17	1	5	0.05	1	1	87	1
GW029101	9	4	460	0.5	24	5	520	5	520	1	160	16	10	1	0.1	1	1	240	23	1	5	0.05	1	1	200	3
GW004039	3	1	370	0.5	7	5	530	20	550	1	51	14	10	1	0.1	1	1	32	8	1	5	0.05	1	1	52	1
GW004039	3	1	370	0.5	7	5	530	19	550	1	51	13	10	1	0.1	1	1	31	8	1	5	0.05	1	1	51	1
GW004042	2	1	370	0.5	5	5	510	22	530	1	53	14	10	1	0.1	1	1	28	9	1	5	0.05	1	1	41	1
GW004076	2	1	370	0.5	6	5	520	26	550	1	53	13	10	1	0.1	1	1	30	12	1	5	0.05	1	1	50	3
GW004107	2	2	330	0.5	5	5	470	22	490	1	45	14	10	3	0.1	1	1	58	12	1	5	0.05	1	1	57	1
GW004290	2	2	360	0.5	6	5	530	16	550	1	40	13	10	1	0.1	1	1	20	17	1	5	0.05	1	1	79	1
GW004642	3	2	340	0.5	7	5	470	13	480	1	51	14	10	1	0.1	1	1	22	14	1	5	0.05	1	1	95	1
GW008162	3	1	400	0.5	7	5	540	27	570	1	61	14	10	1	0.1	1	1	74	15	1	5	0.05	1	1	42	1
GW008404	2	1	350	0.5	4	5	480	26	510	1	52	14	10	1	0.1	1	1	36	9	1	5	0.05	1	1	31	1
GW012298	3	1	390	0.5	6	5	530	24	550	1	72	14	10	1	0.1	1	1	28	13	1	5	0.05	1	1	68	1
GW039439	3	3	460	0.5	11	5	700	12	710	1	43	14	10	1	0.1	1	1	63	34	1	5	0.05	1	1	150	1
GW004034	2	2	320	0.5	4	5	440	16	450	6	56	13	10	1	0.1	1	1	42	10	1	5	0.05	1	1	49	1
GW004541	3	2	300	0.5	7	5	440	5	440	1	53	13	10	2	0.1	1	1	52	10	1	13	0.05	1	1	89	1
GW039313	3	3	310	0.5	6	5	380	15	400	21	63	14	10	1	0.1	1	1	270	10	1	19	0.05	1	1	93	1
GW039313	3	3	310	0.5	6	5	380	15	400	21	63	14	10	1	0.1	1	1	270	10	1	19	0.05	1	1	93	1

Table 6. Variation of strontium isotope ratios with strontium concentration in spring samples indicates the mixing of two endmembers with distinct Sr isotope ratios.

Name	$^{87}Sr/^{86}Sr$	Sr (mg/L)	1/[Sr]	Mixing ratio Hooray sandstone:rainwater
Gooroomero	0.7082	0.03	37.04	0.3
Nulty	0.7089	0.11	9.09	0.2
Boongunyarra	0.7078	0.16	6.25	0.4
Boongunyarra	0.7078	0.52	1.92	0.4
Colless	0.7089	0.11	9.09	0.2
Native Dog	0.7081	0.08	12.99	0.4
Youngerina	0.7078	1.00	1.00	0.4
Lila	0.7082	0.01	100.00	0.3
Thully	0.7078	0.04	22.73	0.4
Thully	0.7080	0.19	5.26	0.4
Cumborah	0.7081	0.21	4.76	0.4
Cumborah	0.7081	0.25	4.00	0.4
Youltoo	0.7101	0.02	41.67	0.1
Peery	0.7093	0.31	3.23	0.2
Peery	0.7092	0.32	3.13	0.2
Peery	0.7092	0.32	3.13	0.2
Tharnowanni	0.7080	0.15	6.67	0.4
Bingewilpa	0.7075	2.30	0.43	0.4
Gooroomero	0.7084	0.03	37.04	0.3
Mulyeo	0.7084	0.20	5.00	0.3
GW004591	0.7049	0.08	12.35	0.8
GW004267	0.7084	0.23	4.35	0.3
GW096004	0.7084	0.23	4.35	0.3
GW004361	0.7075	2.30	0.43	0.4
GW004282	0.7051	0.07	15.15	0.8
Hooray sandstone aquifer[5]	0.7036	-	-	-
Rainfall	0.7106	$2.5x10^{-4}$	3932.58	-
Muscovite[1]	0.7733	79.36	0.01	-
Plagioclase[1]	0.7122	440.70	0.00	-
Seawater[4]	0.7092	8.50	0.12	-

Strontium data table notes: ^{87}Sr uncertainty is ± 0.0000075 at 2σ.

Table references: [1] (Bailey, James W. Hornbeck,: Charles T. Driscoll, 1996) Table 1a Rock and Soil Isotopic Data. [2] (Gray, 1978). [3] average rainfall results from (Bailey, James W. Hornbeck,: Charles T. Driscoll, 1996) Table lb. Water Isotopic Data. [4] seawater from (Taylor et al., 2015), [5] adopted from whole rock sandstone geochemical analysis from Surat Basin by (Baublys et al., 2019).

Table 7. Stable water isotope data for springs, bores, and rainfall in the south-eastern GAB study area.

Name	Spring vent ID	Date sampled	Latitude	Longitude	δ^2H (‰)	$\delta^{18/16}O$ (‰)
Tego[a]	196.3	3/03/2015	-28.850	146.792	-36.9	-5.28
Tego[a]	196.1	3/03/2015	-28.850	146.791	-16.1	0.24
Towry[a]	197.2	3/03/2015	-28.971	146.925	-30.5	-3.99
Towry[a]	197.1	3/03/2015	-28.972	146.926	-29.2	-4.05
Toulby[a]	996	3/03/2015	-29.019	146.930	-38.1	-5.47
Gooroomero	967.2	24/10/2018	-29.091	146.649	-12.2	-0.07
Gerara	965	13/03/2018	-29.268	146.383	-11.1	0.67
Gerara[a]	965	30/04/2015	-29.268	146.383	17.8	7.44
Thooro	976.24	16/07/2019	-29.399	145.322	-32.6	-4.74
Nulty[a]	968	30/04/2015	-29.418	146.115	18.6	3.25
Colless	969.1	23/10/2018	-29.465	146.282	-37.7	-5.95
Boongunyarra	963	11/03/2018	-29.454	145.101	-31.2	-4.05
Boongunyarra	963	16/10/2018	-29.454	145.101	-35.7	-5.25
Boongunyarra	963	17/07/2019	-29.454	145.101	23.5	5.86
Scrubber[a]	970	30/04/2015	-29.510	146.147	-37.5	-5.52
Native Dog	960.1	22/07/2019	-29.524	145.834	4.5	0.12
Youngerina	973	19/07/2019	-29.544	145.122	28.3	7.33
Coonbilly	974.17	9/03/2018	-29.533	145.257	-22.2	-1.14
Lila	1006.3	25/10/2018	-29.563	146.069	0.0	2.13
Lila	1006.4	24/07/2019	-29.564	146.067	-4.1	-1.32
Thully	961.1	22/10/2018	-29.716	146.284	2.8	1.47
Thully	961.1	25/07/2019	-29.717	146.284	39.0	8.27
Cumborah	992	10/10/2018	-29.741	147.764	-22.6	-3.91
Cumborah	992.3	10/10/2018	-29.741	147.765	-22.0	-4.06
Youltoo	1001	9/07/2019	-30.577	143.101	31.0	5.99
Peery	1000.200	7/03/2018	-30.733	143.575	-40.4	-6.53
Peery	1000.200	13/07/2019	-30.733	143.575	-37.8	-6.18
Peery	1000.200	11/10/2018	-30.733	143.575	-39.1	-6.39
Coolabah	994.1	6/03/2018	-30.833	146.950	-32.4	-2.82
Tharnowanni	-	10/10/2018	-29.150	-145.234	59.1	13.28
Coolabah	994.1	6/03/2018	-30.833	146.950	-32.4	-2.82
Rainfall-runoff	-	11/03/2018	-29.561	145.167	-22.5	-1.15
Bingewilpa	1270	12/07/2019	-29.563	146.069	-41.4	-6.67
Rainfall	-	16/10/2018	-29.243	145.140	-18.5	-0.61
Muyleo	1005	7/11/2019	-30.631	144.422	-39.2	-6.46
Muyleo	1005	7/11/2019	-30.632	144.422	-38.9	-6.36
GW004361	-	12/07/2019	-30.028	142.662	-41.4	-6.67
GW004259	-	13/03/2018	-29.232	146.322	-39.8	-6.26
16783A	-	15/03/2018	-28.983	147.954	-40.4	-6.47
GW096004	-	11/07/2019	-30.632	144.422	-39.2	-6.46
GW004339	-	12/03/2018	-29.571	145.262	-38.7	-6.03
GW004666	-	03/08/2018	146.282	146.282	-40.0	-6.41

Name	Spring vent ID	Date sampled	Latitude	Longitude	δ²H (‰)	δ18/16O (‰)
GW010786	-	03/08/2018	-29.462	145.759	-40.2	-6.52
GW011260	-	03/08/2018	-29.451	145.838	-40.3	-6.55
GW040866	-	21/03/2018	-30.769	143.420	-36.0	-5.05
GW010756	-	05/04/2018	-29.447	145.116	-40.3	-6.54
GW004047	-	28/03/2018	-29.219	144.756	-39.9	-6.47
GW012285	-	20/04/2018	-29.098	145.283	-40.4	-6.57
GW004705	-	27/03/2018	-29.156	144.699	-40.3	-6.22
GW008253	-	27/03/2018	-29.164	144.725	-39.0	-6.07
GW004659	-	27/03/2018	-29.273	145.351	-39.5	-6.12
GW004591	-	30/07/2019	-29.287	145.431	-38.9	-6.32
GW004267	-	26/07/2019	-30.632	144.422	-38.9	-6.36
GW004282[b]	-	17/05/2019	-29.753	144.962	-39.2	-6.51
GW004641[b]	-	18/05/2019	-29.346	145.000	-39.6	-6.38
GW004081[b]	-	3/05/2019	-30.613	144.435	-39.3	-6.56
GW007268[b]	-	14/05/2019	-30.230	144.485	-36.9	-6.12

Table 8. ^{14}C activity (as pMC) and ^{14}C-modelled groundwater travel times.

Sample	Type	^{14}C DIC pMC	Conventional Radiocarbon Age	Tamers	Ingerson and Pearson	Fontes and Garnier	Revised F&G v2	$\delta^{13}C$ mixing formula	^{14}C DIC final age
Springs and rainfall-runoff									
Runoff	Wetland	103.30	Modern	0	0	0	0	0	Modern
Boongunyarra	Spring	35.08	8415	3241	0	0	0	0	Modern
Boongunyarra	Spring	15.89	14770	9559	3942	3619	5024	6181	5000
Boongunyarra	Spring	93.51	540	0	0	0	0	0	Modern
Coonbilly	Spring	102.25	Modern	0	0	0	0	0	Modern
Peery	Spring	2.51	29620	24810	13722	12746	15335	17304	15000
Peery	Spring	4.20	25470	20438	10978	10249	12491	14100	12000
Peery	Spring	2.57	29430	24914	13009	11886	14656	17000	15000
Gerera	Bore	0.46	43310	38841	28695	27868	30214	31996	>30000
Gerera	Spring	103.05	Modern	0	0	0	0	0	Modern
Coolabah	Spring	92.34	640	0	0	0	0	0	Modern
Cumborah	Spring	103.04	Modern	0	0	0	0	0	Modern
Cumborah	Open well	102.85	Modern	0	0	0	0	0	Modern
Thully	Spring	99.79	Modern	0	0	0	0	0	Modern
Thully	Spring	102.30	Modern	0	0	0	0	0	Modern
Colless	Spring	25.17	11080	6564	394	25	1710	2586	2000
Gooroomero	Spring	102.43	Modern	0	0	0	0	0	Modern
Lila	Spring	99.34	55	0	0	0	0	0	Modern
Tharnowinni	Spring	100.95	Modern	0	0	0	0	0	Modern
Bingawilpa	Spring	0.27	47500	43418	29220	27577	31425	33711	>30000
Yoorltoo	Spring	93.48	540	0	0	0	0	0	Modern
Muleyo	Spring	0.26	47800	43854	35900	35356	37110	38564	>30000
Muleyo	Spring	0.21	49700	45372	37154	36580	38451	39938	>30000
Thooro	Spring	14.02	15780	10582	5291	4994	6407	7460	6000
Youngerina	Spring	103.10	Modern	0	0	0	0	0	Modern
Native Dog	Spring	100.33	Modern	0	0	0	0	0	Modern
Wapweelah	Bore	0.71	39790	35253	30947	30721	31940	32956	>30000

Sample	Type	^{14}C DIC pMC	Conventional Radiocarbon Age	Tamers	Ingerson and Pearson	Fontes and Garnier	Revised F&G v2	$\delta^{13}C$ mixing formula	^{14}C DIC final age
Bores									
GW004591	Bore	0.32	46200	41867	36225	35899	37306	38465	>30000
GW004081	Bore	0.23	49000	44684	37396	36921	36395	39952	>30000
GW004282	Bore	0.30	46600	42087	38228	38031	39464	40168	>30000
GW004641	Bore	1.25	35210	30533	27527	27383	28505	29332	29000
GW007268	Bore	0.87	38140	33899	28578	28279	29578	30705	>30000
GW011260	Bore	0.17	51460	47000	41191	40839	42286	43481	>30000
GW004666	Bore	0.22	49240	45000	39823	39538	40868	41971	>30000
GW012285	Bore	0.16	51640	47971	42333	42008	43341	44504	>30000
GW010756	Bore	0.32	46060	41841	37645	37427	38630	39636	>30000
GW004047	Bore	0.22	49010	44908	41269	41087	42221	43177	>30000
GW004659	Bore	0.16	51550	47541	43483	43274	44461	45457	>30000
GW010786	Bore	0.19	50140	46188	41275	41006	42302	43381	>30000
GW004339	Bore	1.62	33130	28831	24558	24334	25483	26497	26000
GW004705	Bore	0.43	43860	39382	35729	35546	36681	37637	>30000
GW008253	Bore	0.44	43630	39285	34680	34433	35680	36726	>30000
16783A	Bore	0.43	43790	39382	35093	34869	36085	37102	>30000
GW003823	Bore	0.75	39330	34881	30712	30496	31685	32685	>30000
GW040866	Bore	24.92	11165	6593	5419	5369	6153	6899	6000
GW003823	Bore	0.73	39480	35145	31354	31162	32298	33262	>30000

Table 9. ^{36}Cl Isotope data for springs, bores, and rainfall in the south-eastern GAB study area.

Name	Latitude (decimal degrees)	Longitude (decimal degrees)	36Cl Isotope – Cor CL36/CL	36Cl Isotope - Sigma	36Cl Isotope – sigma (%)	36Cl Isotope - Cor.F (%)
16783A	-28.98	147.95	4.4E-14	1.9E-15	4.3	2.0
Gooroomero	-29.09	146.65	1.9E-13	7.5E-15	4.0	1.3
GW004259	-29.23	146.32	1.3E-14	7.7E-16	6.0	9.3
Old Gerara	-29.27	146.38	5.5E-13	2.2E-14	4.1	1.7
Nulty	-29.47	146.28	1.1E-13	4.5E-15	4.0	0.7
Boongunyarra	-29.45	145.10	6.9E-14	3.9E-15	5.7	4.2
Boongunyarra	-29.45	145.10	6.5E-14	2.8E-15	4.3	1.4
Coonbilly	-29.53	145.26	1.3E-13	5.9E-15	4.5	2.5
Lila	-29.56	146.07	1.9E-13	1.7E-14	8.9	21.2
Thully	-29.72	146.28	1.5E-13	6.0E-15	3.9	0.3
Cumborah	-29.74	147.76	3.8E-13	1.6E-14	4.3	0.3
Cumborah	-29.74	147.76	4.0E-13	1.6E-14	4.0	0.4
Peery West	-30.73	143.58	2.8E-14	5.9E-15	21.5	21.0
Peery West	-30.73	143.58	2.5E-14	1.3E-15	5.2	3.8
Coolabah	-30.83	146.95	2.2E-13	1.1E-14	5.2	3.2
GW004339	-29.57	145.26	4.9E-14	2.6E-15	5.3	4.4
GW003823	-29.57	145.21	4.4E-14	1.8E-15	4.1	1.6
GW004666	-29.74	146.28	2.6E-14	1.1E-15	4.1	2.2
GW010786	-29.46	145.76	3.9E-14	1.7E-15	4.3	2.8

Name	Latitude (decimal degrees)	Longitude (decimal degrees)	36Cl Isotope – Cor CL36/CL	36Cl Isotope - Sigma	36Cl Isotope – sigma (%)	36Cl Isotope - Cor.F (%)
GW011260	-29.45	145.84	3.2E-14	4.6E-15	14.4	14.3
GW040866	-30.77	143.42	1.6E-13	8.2E-15	5.3	3.5
GW010756	-29.45	145.12	4.7E-14	4.8E-15	10.3	11.2
GW004047	-29.22	144.76	4.5E-14	5.5E-15	12.3	13.7
GW012285	-29.10	145.28	4.4E-14	2.2E-15	4.9	1.5
GW004705	-29.16	144.70	3.3E-14	2.2E-15	6.7	5.8
GW008253	-29.16	144.73	1.5E-14	1.8E-15	11.3	10.8
Wapweelah (GW004659)	-29.27	145.35	5.2E-14	4.3E-15	8.3	7.1

Additional graphs

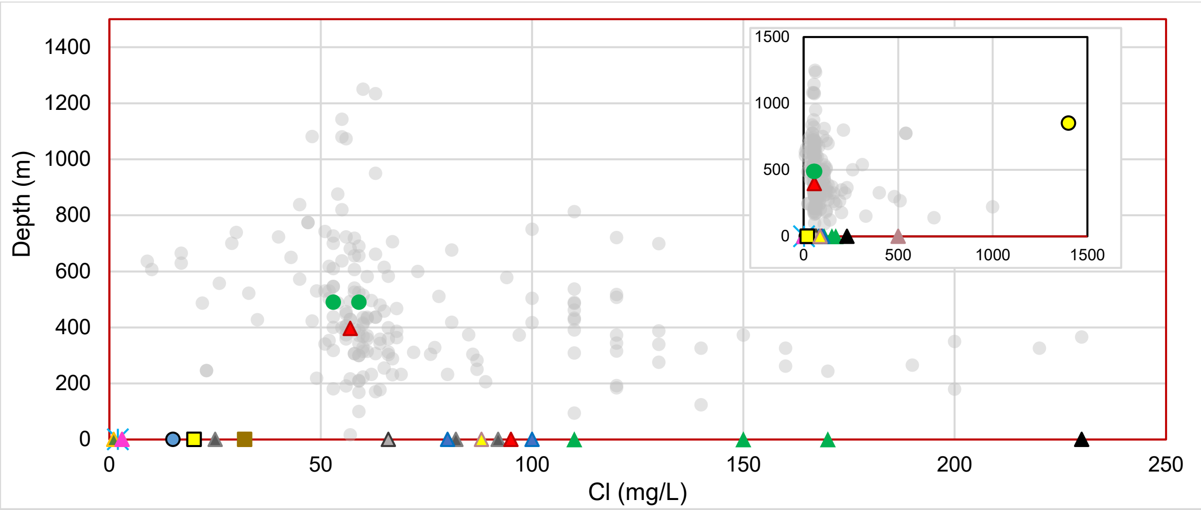

Figure 30. Depth versus chloride for springs expression (ground surface = 0m) and bores (depth to screened section).

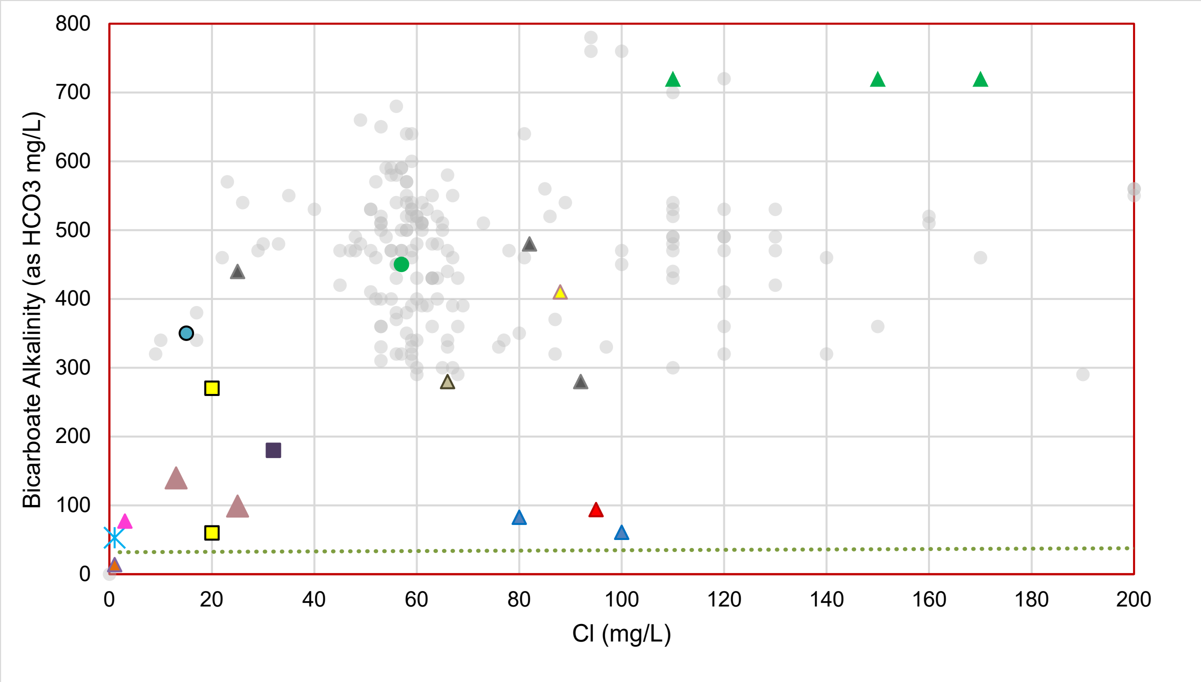

Figure 31. Bicarbonate alkalinity versus chloride for springs and bores.

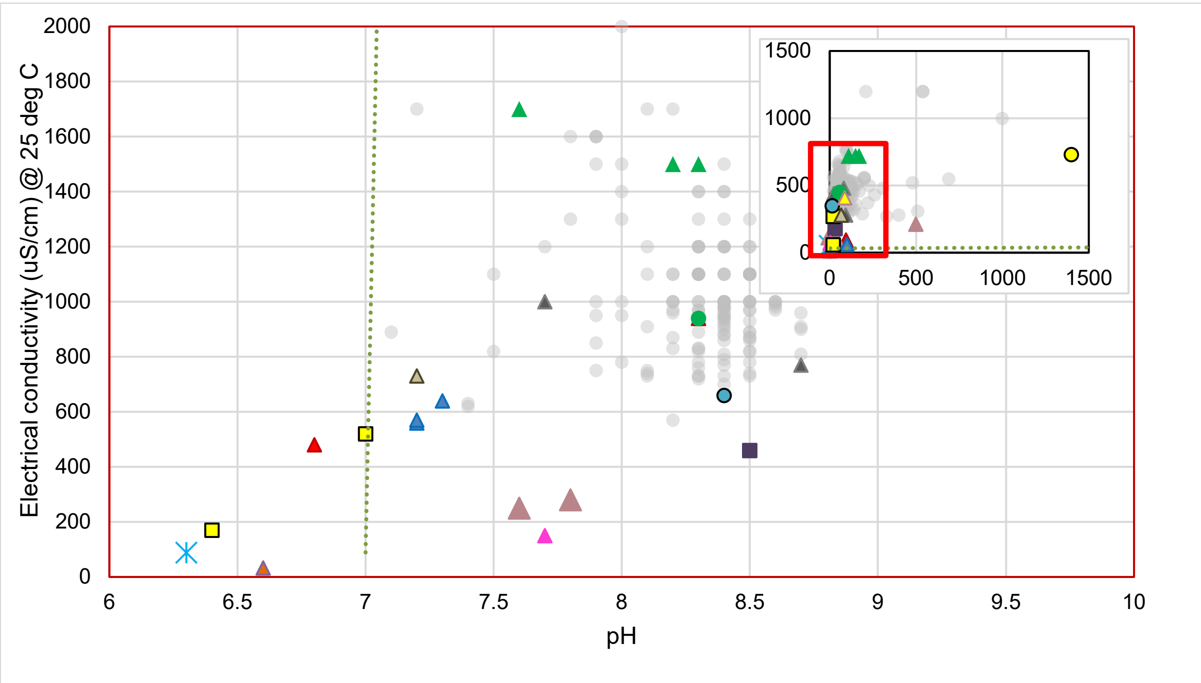

Figure 32. Electrical conductivity versus pH for springs and bores.

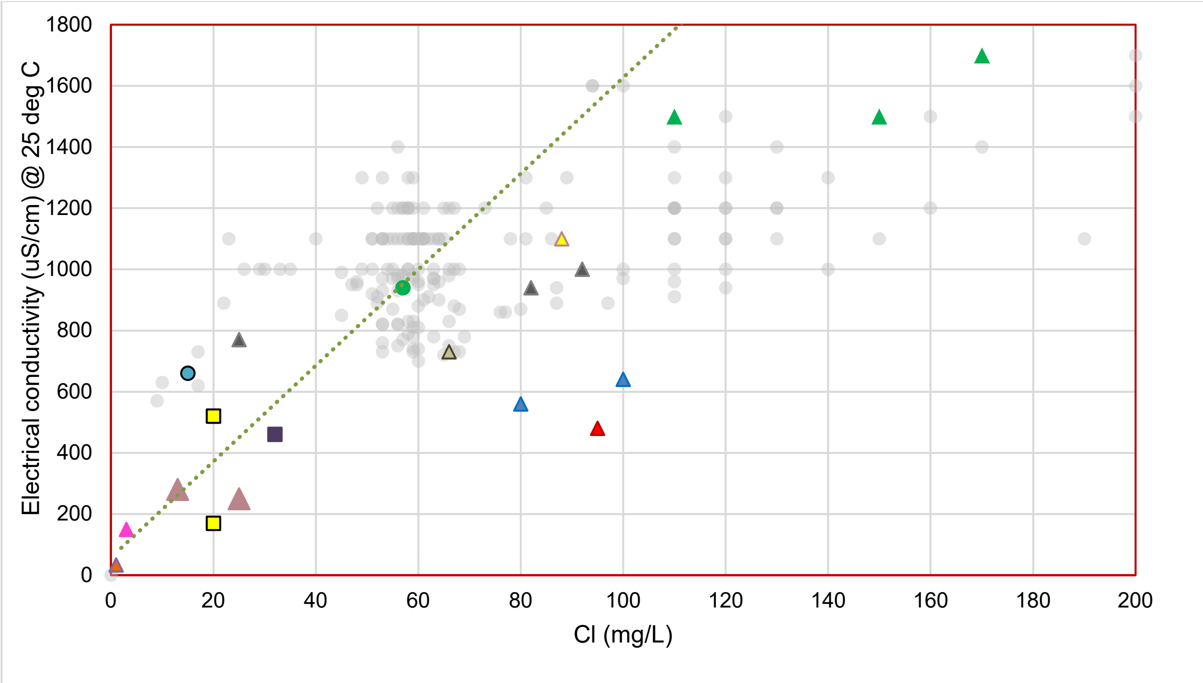

Figure 33. Electrical conductivity versus chloride for springs and bores.

Appendix C – Potentiometric head measurements

Table 10. Groundwater bore head levels for C-H sandstone aquifer used in the potentiometric surface map.

Work number	Measurement date	Potentiometric head (mAHD)
GW004159	3/06/2019	91.38
GW004149	3/06/2019	91.25
GW004512	30/05/2019	109.41
GW004337	24/05/2019	109.02
GW004219	18/05/2019	141.84
GW004008	15/05/2019	100.94
GW004146	14/05/2019	96.17
GW004145	14/05/2019	94.20
GW004666	1/08/2018	130.50
GW803757	7/06/2018	137.72
GW004005	6/06/2018	112.30
GW039561	6/06/2018	103.18
GW004366	5/06/2018	102.80
GW004613	5/06/2018	110.90
GW273194	17/05/2018	101.02
GW014713	16/05/2018	51.76
GW039455	15/05/2018	94.20
GW004541	8/05/2018	162.00
GW004014	28/04/2018	145.41
GW004043	20/04/2018	114.89
GW004214	20/04/2018	136.49
GW273027	19/04/2018	122.23
GW041075	18/04/2018	115.78
GW004442	17/04/2018	140.72
GW004073	16/04/2018	152.10
GW004591	9/04/2018	136.40
GW004519	6/04/2018	104.40
GW004558	6/04/2018	163.70
GW004183	5/04/2018	137.80
GW041078	4/04/2018	158.19
GW004690	28/03/2018	145.13
GW004046	27/03/2018	120.71
GW004049	26/03/2018	124.91
GW004295	23/03/2018	125.73
GW004048	23/03/2018	136.80
GW004047	22/03/2018	122.05
GW004659	20/03/2018	135.57
GW004035	8/03/2018	127.97
GW004300	1/03/2018	118.99
GW004666	28/02/2018	111.41
GW004043	28/02/2018	95.83
GW004472	28/02/2018	102.41
GW004598	28/02/2018	87.80
GW040932	27/02/2018	125.36
GW008354	27/02/2018	102.37
GW004431	8/02/2018	131.00
GW004107	7/02/2018	175.10
GW014992	14/11/1995	131.09
GW039560	13/11/1995	134.24
GW004254	12/11/1995	143.64
GW004289	11/11/1995	125.61
GW004506	11/11/1995	103.75
GW004103	9/11/1995	103.34
GW004407	8/11/1995	49.11
GW011192	7/11/1995	81.19
GW019373	2/11/1995	83.26
GW004396	1/11/1995	92.68
GW010800	1/11/1995	79.74
GW004395	31/10/1995	91.46
GW012047	31/10/1995	109.34
GW004472	30/10/1995	108.82
GW004342	13/10/1995	241.63
GW004535	13/10/1995	220.98
GW004340	12/10/1995	224.69
GW004578	11/10/1995	218.68
GW004672	20/09/1995	181.25
GW004043	19/09/1995	134.6
GW004362	18/09/1995	141.75
GW008372	15/09/1995	143.16
GW012451	13/09/1995	177.35
GW800546	12/09/1995	153.04
GW004085	11/09/1995	186.39
GW004687	30/07/1995	239.23
GW004040	27/07/1995	129.22
GW004120	27/07/1995	227.31
GW001654	23/07/1995	171.79
GW004442	21/07/1995	171.02
GW001570	20/07/1995	187.55
GW004280	19/07/1995	144.23
GW004073	18/07/1995	169.39

Work number	Measurement date	Potentiometric head (mAHD)
GW004091	18/07/1995	167.69
GW004460	17/07/1995	194.67
GW004503	6/07/1995	248.53
GW004080	5/07/1995	247.96
GW004127	5/07/1995	230.69
GW015926	5/07/1995	231.90
GW001326	4/07/1995	225.99
GW022902	2/07/1995	222.28
GW024784	2/07/1995	223.17
GW007554	1/07/1995	235.90
GW019801	1/07/1995	231.02
GW019900	1/07/1995	239.42
GW804172	1/07/1995	139.61
GW006574	29/06/1995	229.94
GW004777	3/06/1995	218.99
GW004034	1/06/1995	215.04
GW000656	30/05/1995	240.95
GW018995	30/05/1995	243.53
GW044593	30/05/1995	244.45
GW049209	30/05/1995	238.59
GW017247	29/05/1995	238.46
GW004024	27/05/1995	208.11
GW004185	26/05/1995	202.15
GW004106	25/05/1995	179.78
GW004378	25/05/1995	175.78
GW004088	24/05/1995	194.12
GW004204	1/02/1995	214.99
GW004676	27/11/1994	143.58
GW004015	25/11/1994	158.93
GW008232	24/11/1994	232.05
GW004685	22/06/1994	210.4
GW039504	8/05/1994	182.87
GW004469	6/05/1994	145.41
GW004104	15/11/1993	125.94
GW004175	7/09/1993	223.97
GW004549	26/10/1992	107.02
GW004515	23/10/1992	99.78
GW014232	8/11/1991	106.55
GW030963	3/11/1991	95.91
GW003398	31/10/1991	83.82
GW004611	22/01/1991	204.58
GW021842	8/11/1990	156.03
GW004251	7/11/1990	151.87

Work number	Measurement date	Potentiometric head (mAHD)
GW012341	7/11/1990	148.46
GW014317	7/11/1990	156.19
GW004110	6/11/1990	140.29
GW014588	6/11/1990	160.45
GW058924	5/11/1990	175.54
GW039445	4/11/1990	226.78
GW004613	3/11/1990	141.4
GW014764	3/11/1990	169.47
GW004366	2/11/1990	151.42
GW021144	2/11/1990	146.78
GW004004	1/11/1990	174.88
GW004005	1/11/1990	146.04
GW010371	1/11/1990	155.63
GW012068	1/11/1990	185.51
GW012013	31/10/1990	146.16
GW014488	31/10/1990	157.87
GW004190	30/10/1990	186.01
GW004223	29/10/1990	162.68
GW004400	29/10/1990	182.26
GW004658	28/09/1990	169.35
GW004307	26/09/1990	137.31
GW021603	25/09/1990	189.91
GW012480	24/09/1990	147.04
GW050527	24/09/1990	130.33
GW014672	22/09/1990	139.35
GW014520	21/09/1990	151.79
GW014713	21/09/1990	199.49
GW004579	20/09/1990	169.4
GW020109	20/09/1990	136.34
GW012121	19/09/1990	182.94
GW017679	19/09/1990	127.92
GW038300	18/09/1990	169.74
GW003858	17/09/1990	135.45
GW039325	16/09/1990	146.8
GW008470	15/09/1990	130.22
GW012298	15/09/1990	136.61
GW004128	14/09/1990	149.84
GW008195	14/09/1990	149.34
GW004032	11/09/1990	217.76
GW004244	11/09/1990	170.73
GW004021	10/09/1990	228.67
GW064371	30/08/1990	148.54
GW012091	27/08/1990	164.28

Work number	Measurement date	Potentiometric head (mAHD)
GW017686	27/08/1990	160.26
GW003954	26/08/1990	156.26
GW008413	25/08/1990	159.58
GW039304	22/08/1990	158.05
GW030906	21/08/1990	170.15
GW004502	1/08/1990	124.89
GW004445	31/07/1990	130.34
GW008475	29/07/1990	136.85
GW011115	29/07/1990	120.53
GW008410	26/07/1990	119.76
GW004214	24/07/1990	141.81
GW004107	10/07/1990	193.21
GW004322	14/06/1990	199.85
GW001233	31/03/1990	161.25
GW051470	30/03/1990	169.6
GW039438	27/03/1990	145.06
GW014632	14/03/1990	142.16
GW024786	13/03/1990	219.51
GW008467	11/03/1990	138.5
GW008070	10/03/1990	138.82
GW039435	8/03/1990	156.81
GW004265	7/03/1990	187.96
GW008226	7/03/1990	196.82
GW008341	6/03/1990	202.9
GW004326	5/03/1990	198.22
GW004323	28/02/1990	195.12
GW004558	28/02/1990	200.36
GW008455	14/02/1990	134.37
GW021322	13/02/1990	135.23
GW008103	12/02/1990	135.17
GW039442	12/02/1990	135.2
GW004205	10/02/1990	131.14
GW008351	9/02/1990	133.57
GW012177	9/02/1990	142.64
GW001551	8/02/1990	144.98
GW039434	5/02/1990	161.81
GW025173	1/02/1990	131.92
GW012259	31/01/1990	132.45
GW039439	29/01/1990	139.19
GW021148	13/12/1989	140.77
GW004331	12/12/1989	183.28
GW004751	12/12/1989	144.95
GW010483	12/12/1989	135.78

Work number	Measurement date	Potentiometric head (mAHD)
GW010786	11/12/1989	134.71
GW004384	10/12/1989	144.07
GW003708	9/12/1989	113.63
GW012215	8/12/1989	189.62
GW004121	7/12/1989	209.40
GW004183	7/12/1989	164.26
GW004283	7/12/1989	113.26
GW004666	7/12/1989	120.09
GW004345	6/12/1989	218.56
GW007263	6/12/1989	125.35
GW004413	5/12/1989	193.56
GW004477	5/12/1989	196.89
GW025066	5/12/1989	167.67
GW004263	4/12/1989	185.77
GW039436	4/12/1989	193.72
GW004545	16/11/1989	136.8
GW004041	15/11/1989	130.22
GW012198	12/11/1989	134.65
GW008045	11/11/1989	157.05
GW008207	11/11/1989	155.29
GW021037	8/11/1989	195.62
GW004692	7/11/1989	168.49
GW012448	19/10/1989	166.82
GW012335	17/10/1989	166.35
GW004213	16/10/1989	139.85
GW018041	15/10/1989	138.64
GW004181	13/10/1989	144.09
GW011260	12/10/1989	155.77
GW004555	11/10/1989	105.98
GW010696	11/10/1989	108.32
GW004186	27/09/1989	141.10
GW004405	21/09/1989	175.77
GW010608	20/09/1989	175.87
GW012094	20/09/1989	143.66
GW021046	19/09/1989	149.71
GW004278	18/09/1989	163.02
GW008482	18/09/1989	146.14
GW004074	17/09/1989	149.12
GW004593	17/09/1989	144.29
GW008382	17/09/1989	151.52
GW004171	16/09/1989	168.38
GW004134	15/09/1989	171.74
GW004725	15/09/1989	142.35

Work number	Measurement date	Potentiometric head (mAHD)
GW010075	15/09/1989	139.30
GW004054	14/09/1989	160.39
GW011266	14/09/1989	167.41
GW008317	13/09/1989	151.65
GW014561	13/09/1989	141.56
GW004063	12/09/1989	186.63
GW004399	12/09/1989	179.45
GW008406	12/09/1989	139.24
GW008449	12/09/1989	147.61
GW016861	12/09/1989	138.66
GW004471	24/08/1989	163.62
GW004564	24/08/1989	167.97
GW004432	23/08/1989	166.72
GW005594	22/08/1989	176.87
GW004556	22/02/1989	166.64
GW004431	3/08/1988	165.32
GW025429	25/07/1988	166.32
GW061681	3/03/1988	219.90
GW004188	2/03/1988	214.61
GW008096	2/03/1988	211.01
GW014808	9/02/1988	149.96
GW025423	9/02/1988	167.94
GW025370	8/02/1988	160.91
GW008339	7/02/1988	159.58
GW027744	5/02/1988	169.83
GW030889	4/02/1988	168.42
GW004519	25/11/1987	113.34
GW012197	24/11/1987	107.76
GW003862	22/11/1987	115.57
GW029101	21/11/1987	96.93
GW014627	27/10/1987	137.05
GW012419	26/10/1987	143.87
GW016020	23/10/1987	141.88
GW004499	20/10/1987	139.66
GW025018	20/10/1987	132.26
GW007181	19/10/1987	144.89
GW004537	18/10/1987	146.55
GW014675	18/10/1987	151.5
GW003436	17/10/1987	147.04
GW039377	17/10/1987	133.73
GW014739	15/10/1987	181.53
GW018053	26/08/1987	123.89
GW003780	25/08/1987	131.73

Work number	Measurement date	Potentiometric head (mAHD)
GW021766	28/07/1987	108.90
GW004424	26/07/1987	164.08
GW004452	26/07/1987	155.03
GW010582	21/07/1987	83.43
GW003529	14/07/1987	106.62
GW004649	2/07/1987	193.9
GW034677	29/06/1987	172.22
GW004490	21/06/1987	97.54
GW004462	20/06/1987	99.97
GW003564	19/05/1987	129.23
GW003636	18/05/1987	129.38
GW012246	15/05/1987	137.36
GW004736	11/05/1987	110.74
GW003908	10/05/1987	118.16
GW027398	9/04/1987	147.42
GW027499	9/04/1987	180.84
GW008388	8/04/1987	128.76
GW004609	7/04/1987	163.40
GW012272	6/04/1987	171.67
GW014571	6/04/1987	132.52
GW021190	4/04/1987	148.73
GW010433	3/04/1987	124.35
GW003859	2/04/1987	141.50
GW012430	31/03/1987	156.30
GW030921	31/03/1987	130.95
GW014564	30/03/1987	160.34
GW027500	27/03/1987	168.78
GW012310	26/03/1987	147.24
GW012490	25/03/1987	189.43
GW021448	25/03/1987	127.72
GW004314	23/03/1987	128.30
GW021105	23/03/1987	131.36
GW021414	23/03/1987	147.83
GW008404	4/03/1987	127.66
GW008267	3/03/1987	141.36
GW004441	28/02/1987	141.03
GW008275	23/02/1987	155.34
GW008158	22/02/1987	149.14
GW008213	20/02/1987	171.27
GW008451	20/02/1987	143.33
GW018220	18/02/1987	175.30
GW019300	17/02/1987	171.10
GW003717	14/12/1986	136.29

Work number	Measurement date	Potentiometric head (mAHD)
GW004757	14/12/1986	136.08
GW004117	13/12/1986	140.43
GW004300	12/12/1986	144.94
GW015757	12/12/1986	147.53
GW004258	10/12/1986	146.50
GW008354	10/12/1986	139.16
GW004257	8/12/1986	146.33
GW025256	7/12/1986	148.60
GW003638	4/12/1986	130.79
GW014773	11/11/1986	131.03
GW021207	11/11/1986	145.93
GW008540	10/11/1986	142.33
GW004296	3/11/1986	144.50
GW009938	3/11/1986	158.70
GW003770	1/11/1986	143.38
GW004448	1/11/1986	131.30
GW032500	1/11/1986	142.30
GW004665	30/10/1986	130.70
GW004439	29/10/1986	107.25
GW008125	26/09/1986	131.58
GW030944	23/09/1986	107.70
GW012157	20/09/1986	138.8
GW012483	19/09/1986	149.74
GW008395	18/09/1986	128.32
GW004132	16/09/1986	210.55
GW008486	27/08/1986	160.13
GW004648	21/08/1986	171.16
GW011311	16/07/1986	89.73
GW030554	28/05/1986	143.34
GW004150	23/05/1986	85.94
GW014998	19/05/1986	120.94
GW013140	18/05/1986	135.09
GW011271	17/05/1986	134.34
GW004158	5/05/1986	180.48
GW004016	28/04/1986	155.93
GW012428	4/04/1986	163.27
GW021391	1/03/1986	130.69
GW004076	28/02/1986	128.75
GW008162	27/02/1986	139.18
GW004224	4/02/1986	152.8
GW004608	26/11/1985	156.63
GW030868	22/11/1985	180.33
GW012314	21/11/1985	174.51

Work number	Measurement date	Potentiometric head (mAHD)
GW021039	18/11/1985	159.93
GW021378	17/11/1985	198.90
GW004453	15/11/1985	152.70
GW021220	15/11/1985	139.27
GW014722	13/11/1985	139.45
GW030820	9/11/1985	136.37
GW030614	7/11/1985	149.34
GW021483	13/10/1985	139.97
GW007705	12/10/1985	173.43
GW004341	11/10/1985	157.92
GW012426	9/10/1985	166.41
GW004309	11/09/1985	141.89
GW004770	10/09/1985	124.98
GW014329	9/09/1985	80.91
GW004248	7/09/1985	105.00
GW004337	5/09/1985	106.75
GW031221	4/09/1985	94.42
GW032090	4/09/1985	86.12
GW054009	20/07/1985	157.55
GW003805	19/07/1985	156.90
GW012499	19/07/1985	169.68
GW025210	17/07/1985	148.55
GW012156	20/05/1985	150.87
GW004118	17/05/1985	131.25
GW004173	17/05/1985	142.50
GW014513	13/05/1985	156.29
GW022754	30/04/1985	140.94
GW004295	29/04/1985	137.98
GW012274	28/04/1985	139.19
GW004049	25/04/1985	119.63
GW021167	25/04/1985	125.69
GW004684	23/04/1985	115.67
GW004008	17/04/1985	92.56

Appendix D – PHREEQC output

Table 11. PHREEQC (Parkhurst & Appelo, 2013) saturation indices results

Sample name	Al(OH)3(a)	Alunite	Anglesite	Anhydrite	Aragonite	Calcite	Cd(OH)2	CdSO4	Celestite	Cerrusite	CO2(g)	Dolomite	Fe(OH)3(a)	FeS(ppt)	Gibbsite	Goethite	Gypsum	H2(g)	H2S(g)	Halite	Hausmannite	Hematite	Jarosite-K	Mackinawite	Manganite	Melanterite	O2(g)	Otavite	Pb(OH)2	Pyrite	Pyrochroite	Pyrolusite	Rhodochrosite	Siderite	Smithsonite	Sphalerite	Strontianite	Sulphur	Zn(OH)2(e)
Hooray aquifer (GW004591)	-3	-15	-9	-5	0	0	-6	-15	-2	-3	-3	0	2	-76	0	8	-5	-25	-2	-80	-6	-10	18	-11	-76	-4	-12	-35	-1	-3	-124	-6	-8	-1	-3	-4	-69	2	-61
GW004361	-2	-10	-9	-5	0	0	-8	-16	-1	-2	-2	0	2	-67	1	8	-5	-23	-2	-71	-4	-17	18	-8	-66	-6	-10	-39	-3	-4	-108	-8	-12	-1	-1	-4	-61	2	-54
Peery	-3	-13	-9	-5	0	0	-7	-15	-1	-3	-2	0	1	-74	0	7	-5	-24	-2	-77	-6	-13	16	-12	-73	-5	-12	-36	-1	-4	-120	-7	-9	-1	-3	-4	-66	2	-59
Peery	1	5	-6	-5	-3	-3	-10	-14	-2	-3	-2	-6	0	-55	4	6	-5	-21	-2	-58	-8	-22	13	-8	-54	-8	-7	-43	-4	-4	-85	-9	-15	-2	-1	-5	-49	-2	-43
Peery	-1	0	-6	-5	-3	-2	-10	-14	-2	-3	-2	-5	-1	-55	2	5	-4	-21	-2	-58	-10	-24	12	-11	-54	-9	-8	-44	-4	-5	-85	-9	-16	-3	-2	-5	-49	-1	-43
Peery	-3	-13	-9	-5	0	0	-7	-15	-1	-3	-2	0	1	-74	0	7	-5	-24	-2	-77	-6	-13	16	-12	-73	-5	-12	-36	-1	-4	-120	-7	-9	-1	-3	-4	-66	2	-59
Coolabah	1	5	-6	-5	-3	-3	-10	-14	-2	-3	-2	-6	0	-55	4	6	-5	-21	-2	-58	-8	-22	13	-8	-54	-8	-7	-43	-4	-4	-85	-9	-15	-2	-1	-5	-49	-2	-43
Boongunyarra	-1	-7	-8	-5	0	0	-8	-15	-1	-2	-2	0	1	-68	1	7	-5	-23	-2	-72	-6	-14	16	-10	-68	-5	-11	-38	-2	-4	-110	-7	-11	-1	-2	-3	-61	2	-54
Boongunyarra	-2	-12	-9	-5	0	0	-6	-15	-2	-2	-3	0	1	-75	0	7	-5	-25	-2	-78	-6	-11	16	-12	-74	-4	-13	-36	-1	-3	-121	-6	-9	-1	-3	-4	-67	2	-59
Boongunyarra	-3	-14	-9	-5	1	1	-6	-15	-1	-3	-3	2	1	-80	0	7	-4	-25	-2	-82	-7	-9	16	-14	-79	-3	-14	-34	-1	-3	-129	-6	-8	-1	-4	-4	-71	3	-63
Runoff	-1	0	-6	-5	-3	-2	-10	-14	-2	-3	-2	-5	-1	-55	2	5	-4	-21	-2	-58	-10	-24	12	-11	-54	-9	-8	-44	-4	-5	-85	-9	-16	-3	-2	-5	-49	-1	-43
Rainfall	-1	-4	-6	-4	-2	-2	-9	-14	-1	-3	-2	-4	0	-61	1	6	-4	-22	-2	-64	-10	-17	13	-11	-60	-7	-9	-41	-4	-3	-97	-8	-13	-2	-3	-3	-53	0	-48
Cumborah	-1	-4	-6	-4	-2	-2	-9	-14	-1	-3	-2	-4	0	-61	1	6	-4	-22	-2	-64	-10	-17	13	-11	-60	-7	-9	-41	-4	-3	-97	-8	-13	-2	-3	-3	-53	0	-48
Cumborah	-2	-4	-6	-3	-2	-1	-8	-13	0	-2	-2	-2	1	-63	1	6	-3	-23	-2	-66	-7	-18	15	-7	-62	-7	-9	-40	-3	-3	-100	-8	-12	-2	-2	-3	-55	0	-50
Native Dog	-2	-4	-6	-3	-2	-1	-9	-13	0	-2	-2	-2	1	-62	1	7	-3	-22	-2	-66	-7	-18	15	-7	-61	-7	-8	-40	-3	-4	-98	-8	-13	-2	-2	-4	-55	0	-49
Bingewilpa	1	-2	-7	-5	-1	-1	-7	-14	-2	-2	-3	-3	4	-66	3	9	-4	-23	-2	-72	-9	-12	21	-3	-65	-5	-8	-38	-3	-2	-107	-6	-10	-1	0	-3	-60	0	-54
Muleyo	-2	-10	-9	-5	0	0	-8	-16	-1	-2	-2	0	2	-67	1	8	-5	-23	-2	-71	-4	-17	18	-8	-66	-6	-10	-39	-3	-4	-108	-8	-12	-1	-1	-4	-61	2	-54
Youngerina	-2	-11	-9	-5	0	0	-7	-15	-2	-2	-2	0	3	-69	0	8	-5	-24	-2	-74	-6	-14	19	-7	-69	-5	-10	-37	-2	-4	-113	-7	-10	-1	-1	-4	-63	2	-56
Colless	-1	-9	-9	-4	1	1	-6	-15	-1	-2	-3	2	3	-75	2	8	-4	-25	-2	-79	-8	-7	19	-9	-74	-3	-12	-35	-2	-3	-122	-5	-7	0	-2	-3	-67	3	-60
Youltoo	-2	-5	-7	-4	-1	-1	-9	-14	-1	-2	-2	-2	2	-61	1	7	-4	-22	-2	-66	-7	-18	17	-5	-61	-7	-8	-40	-3	-4	-98	-8	-13	-2	0	-4	-56	1	-50
Wapweela	1	5	-5	-4	-3	-3	-9	-13	-1	-3	-2	-6	1	-57	4	7	-4	-22	-2	-62	-9	-21	16	-5	-56	-8	-7	-42	-4	-4	-90	-9	-14	-3	-1	-4	-52	-1	-46
Muelyo	-3	-14	-9	-5	0	0	-6	-15	-2	-2	-3	-1	2	-74	0	8	-5	-25	-2	-78	-7	-11	18	-9	-73	-4	-11	-36	-2	-3	-120	-6	-9	-1	-2	-3	-66	1	-59
Muleyo	-2	-11	-9	-5	0	0	-7	-15	-2	-2	-2	0	3	-69	0	8	-5	-24	-2	-74	-6	-14	19	-7	-69	-5	-10	-37	-2	-4	-113	-7	-10	-1	-1	-4	-63	2	-56
Thully	0	1	-6	-5	-3	-2	-9	-14	-2	-3	-2	-5	0	-59	2	6	-4	-22	-2	-62	-7	-22	14	-8	-58	-8	-8	-42	-4	-4	-92	-9	-14	-2	-2	-4	-52	-1	-46
Old Gerera	0	-3	-7	-4	-1	-1	-8	-14	-1	-2	-3	-3	3	-65	3	8	-4	-23	-2	-70	-7	-15	19	-5	-65	-6	-9	-39	-3	-3	-106	-7	-11	-2	-1	-4	-59	0	-53
Thooro Mud	0	1	-6	-5	-3	-2	-9	-14	-2	-3	-2	-5	0	-59	2	6	-4	-22	-2	-62	-7	-22	14	-8	-58	-8	-8	-42	-4	-4	-92	-9	-14	-2	-2	-4	-52	-1	-46
Coonbilly	-3	-16	-10	-5	0	1	-5	-15	-2	-3	-4	1	2	-84	0	7	-5	-26	-2	-87	-6	-7	17	-14	-84	-2	-15	-32	-1	-3	-138	-5	-6	-1	-4	-4	-76	2	-66
Lila	1	1	-7	-4	-1	-1	-9	-15	-1	-2	-2	-2	2	-60	4	8	-4	-22	-2	-65	-7	-16	17	-6	-59	-6	-8	-41	-3	-4	-96	-7	-12	-1	0	-3	-54	1	-49
Lila	-1	-3	-6	-6	-4	-4	-10	-14	-2	-3	-2	-7	0	-57	2	6	-5	-21	-2	-61	-9	-22	13	-10	-57	-8	-9	-43	-4	-4	-90	-9	-15	-3	-2	-5	-51	-2	-45

Appendix E – PCA data set

Table 12. Principal component analysis input code to MATLAB R2021b (The MathWorks Inc, 2021)

```
% Principle component analysis adapted from 'lake water provided by Herczag'
% use embedded functions.

% load in the data
clear all;

data0=xlsread('Copy of Jess_springs - trace added.xlsx', '220225_majorv2',
'E2:AW314');
% 1ID, 2Ca, 3K, 4Na, 5Mg, 6Hardness, 7OH, 8HCO3, 9CO3, 10Alkalinity, 11SO4,
% 12 Cl, δ 2H, δ 18/16O
% Data in mg/l
data=[data0(:,2:6), data0(:,8:9), data0(:,11:12), data0(:,15:16), data0(:,21:22),
data0(:,24:24), data0(:,28:29), data0(:,44:45)];

% convert the unit from mg/l to mmol/l
data(:,1)=data(:,1)/40.0;  % calcium
data(:,4)=data(:,4)/24.3;  % Mg
data(:,3)=data(:,3)/23.0;  % Na
data(:,2)=data(:,2)/39.1;  % K
data(:,5)=data(:,5)/61;  % HCO3
data(:,6)=data(:,6)/60;  % CO3
data(:,8)=data(:,8)/35.5;  % Cl
data(:,7)=data(:,7)/96;  % SO4
%data(:,9)=data(:,9);% δ 2H
%data(:,10)=data(:,10); % δ 18/16O


v_id1=['Ca';'Mg';'Na';'Kk';'HC';'Cc';'Ss';'Cl';'IB';'Al';'Fe';'Li';'Pb';'Mn';'Sr';'Zn
';'pH';'EC'];
%v_id2=['HC';'Cl';'Br';'S6';'Ca';'Kk';'Mg';'Na';'HH';'OO'];
%JT note added in δH (Hi - hydrogen isotope) and δ 18/16O (Oi - oxygen isotope)

%major=data;    % major ions, spring rows with for graph labels
v_id3=['01'; '02';'03'; '04'; '05'; '06'; '07'; '08'; ...
    '09'; '10'; '11'; '12'; '13'; '14'; '15'; '16'; ...
    '17'; '18'; '19'; '20'; '21'; '22'; '23'; '24'; '25'; '26'];
thedata=data;
[n,p]=size(thedata);   % dimension of the data
%corm=cov(thedata);   % correlation matrix
%corm=cov(major(:,5:12));

[Z,MU,SIGMA] = zscore(thedata); %standardize the data

[coeff, score, latent, tsquared] = pca(Z);

xlswrite('Results.xlsx',score, 'm_ion_scores','B2');
xlswrite('Results.xlsx',latent, 'm_ion_eigenvalues','B2');

save 'score.txt' score -ascii

xsc_corr=corrcoef([thedata,score]);  % calculate the correlation coefficient between
data and the score in the PC space
loading=xsc_corr(1:p,p+1:p+4);      % extract the loading of PCs

xlswrite('Results.xlsx',loading, 'm_ion_loadings','C2');
xlswrite('Results.xlsx',v_id1, 'm_ion_loadings','A2');
```

```
% plot the scores
figure (14)
plot(score(1:26,1), score(1:26,2), '+k');
text(score(1:26,1), score(1:26,2), v_id3, 'fontsize', 10,
'Color','red','verticalalignment','bottom');
hold on;
plot(score(27:n,1), score(27:n,2), '+k');
xlabel('PC1');
ylabel('PC2');
hold off;

figure (24)
plot(score(1:26,1), score(1:26,2), '+k');
text(score(1:26,1), score(1:26,2), v_id3, 'fontsize', 10,
'Color','red','verticalalignment','bottom');
hold on;
plot(score(27:n,1), score(27:n,2), '+k');
axis([-5 10 -4 6])
xlabel('PC1');
ylabel('PC2');
hold off;

figure (13)
plot(score(1:26,1), score(1:26,3), '+k');
text(score(1:26,1), score(1:26,3), v_id3, 'fontsize', 10,
'Color','red','verticalalignment','bottom');
hold on;
plot(score(27:n,1), score(27:n,3), '+k');
xlabel('PC1');
ylabel('PC3');
hold off;


figure (12)
plot(score(1:26,2), score(1:26,3), '+k');
text(score(1:26,2), score(1:26,3), v_id3, 'fontsize', 10, 'Color','red',
'verticalalignment','bottom');
hold on;
plot(score(27:n,2), score(27:n,3), '+k');
xlabel('PC2');
ylabel('PC3');
hold off;

figure (11)
plot(score(1:26,3), score(1:26,4), '+k');
text(score(1:26,3), score(1:26,4), v_id3, 'fontsize', 10,'Color','red',
'verticalalignment','bottom');
hold on;
plot(score(27:n,3), score(27:n,4), '+k');
xlabel('PC3');
ylabel('PC4');
hold off;


% plot the loadings
figure (15)
plot(loading(:,1), loading(:,2), '+k');
text(loading(:,1), loading(:,2), v_id1, 'fontsize', 10,
'Color','red','verticalalignment','bottom');
xlabel('PC1');
ylabel('PC2');
```

```
axis([-1 1 -1 1]);

% plot the loadings
figure (16)
plot(loading(:,3), loading(:,4), '+k');
text(loading(:,3), loading(:,4), v_id1, 'fontsize', 10,'Color','red',
'verticalalignment','bottom');
xlabel('PC3');
ylabel('PC4');
axis([-1 1 -1 1]);
```

Table 13. PCA eigenvalues and variance for the 18 variables tested.

Factors	Eigenvalues	Variance (%)
Ca	8.562826	0.475713
Mg	1.843827	0.102435
Na	1.538089	0.085449
K	1.301462	0.072303
HCO_3	1.187091	0.065949
$CaCo_3$	0.784306	0.043576
SO_4	0.759563	0.042198
Cl	0.529359	0.029409
IB	0.472516	0.026251
Al	0.351707	0.019539

Factors	Eigenvalues	Variance (%)
Fe	0.278047	0.015447
Li	0.210374	0.011687
Pb	0.108136	0.006008
Mn	0.038463	0.002137
Sr	0.027095	0.001505
Zn	0.005484	0.000305
pH	0.001491	8.28E-05
EC	0.00011	6.09E-06
Totals	18	100%

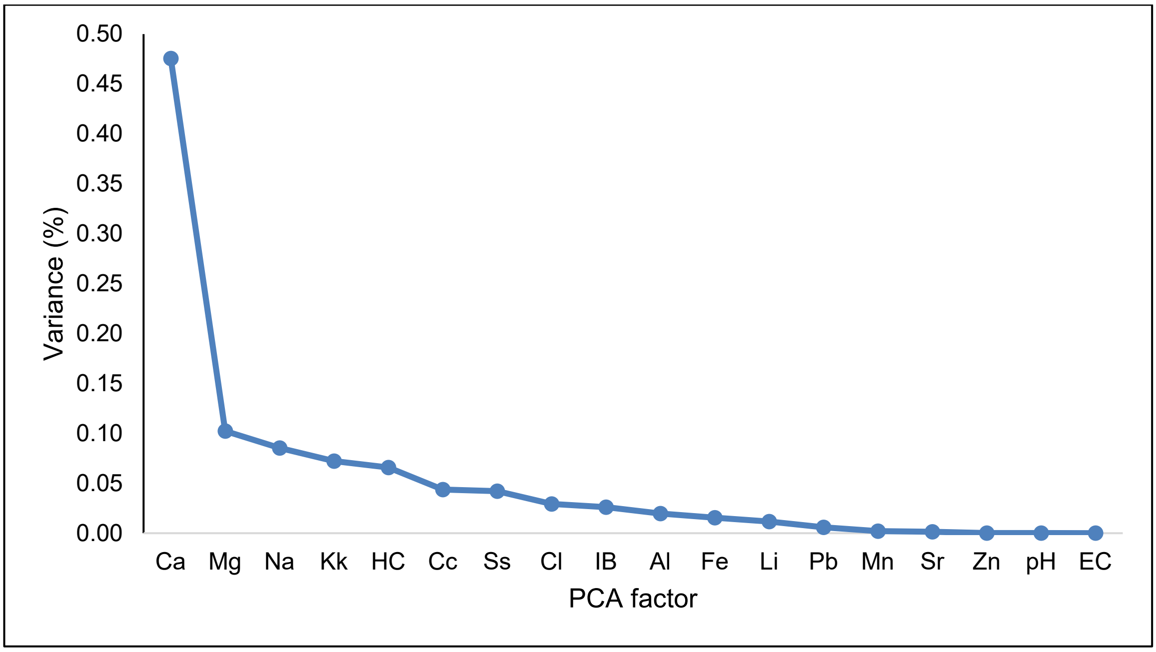

Figure 34. Plot of variance (%) of PCA factors